The Hong Kong Polytechnic University
Department of Applied Biology and Chemical Technology

A Study of Electrodeposition and Electroless Ternary Alloys

by

Lee Chi Yung

A thesis submitted in partial fulfillment of the requirements for the Degree of Master of Philosophy

March 2004

CERTIFICATE OF ORIGINALITY

I hereby declare that this thesis is my own work and that, to the best of my knowledge and belief, it reproduces no material perviously published or written nor material wheh has been accepted for the award of any other degree or diploma, except where due acknowledgement has been made in the text

_____(Signed)

Lee Chi Yung (Name of Student)

Abstract of thesis entitled ‘A Study of Electrodeposition and Electroless Ternary Alloys’

submitted by Lee Chi Yung

for the degree of Master of Philosophy

at the Hong Kong Polytechnic University in March 2004

Abstract

Electroplating and electroless plating processes are widely used in the surface-finishing industry. Nickel plating had been used in many surface treatment processes in the past 30 years. One of the most important applications is acting as a diffusion barrier in printed circuit board and gold plated ornaments to prevent the interdiffusion of the top layer of plated gold and the base metal. However, human perspiration can penetrate through the cracks of the gold overplate of ornaments and corrodes the nickel underneath. The leached nickel product can irritate the human skin. On 30 June 1994, the Council of European Union has adopted the directive 76/769/EEC that listed nickel compounds as one of the regulated chemicals. Ornament manufacturers seek for replacements for nickel, the replacement material is palladium; but the rapid rise in the cost of palladium has deterred the use of this metal as a barrier. Cobalt and its alloys can form a good barrier and are less toxic in terms of skin toxicity but the corrosion resistance is worse than nickel. The main objective of this project is to develop ternary electroplated cobalt alloys and electroless plated

cobalt alloys as a barrier having good corrosion resistant properties. We also determined the chemical and physical properties of the coating. The formulation for the plating solution and the plating conditions were optimized.

The Cobalt-Tungsten-Phosphorus (Co-W-P) and Cobalt-Tungsten (Co-W) alloys were successfully developed for use in electroless-plating and electroplating processes respectively. The formulation for producing electroless plated Co-W-P alloy with 8.0 wt. % W and 4.0 wt. % P were optimized. An Co-W electroplating bath was also developed and W content can be controlled in the range of 20-35wt. % W while P content is less than 1 wt. %.

The interdiffusion coefficients of copper/ barrier were determined. Micro profiling and Boltzmann-Matano methods were used to obtain the interdiffusion coefficients. It was found that the interdiffusion coefficients of cobalt and its alloys are lower than nickel alloys. The soldering property of the plated cobalt alloys is similar to nickel coating. These indicated the potential of cobalt alloys for replacing nickel and it alloys.

ACKNOWLEDGEMENTS

This research was carried out for four years at The Hong Kong Polytechnic University. Many people have given helps and guidance to the author during the course of this research work. The authors would like to thank Dr. C. H. Yeung (Department of Applied Biology and Chemical Technology) and Dr. H. C. Man (Department of Industrial and Systems Engineering), for their supervision guidance, encouragement, suggestions and information.

The author would also like to express his gratitude to Dr. W. Y. Ng for his encouragement to the author during his work at The Hong Kong Polytechnic University.

The author would like to thank Mr. Siu Cho Lung, my working partner, for his advises and suggestions at Research Group of Department of Industrial and Systems Engineering.

The author would like to thank all the staff members of the Chemical Technology section, department of ABCT, Physical, Metallurgy division and Materials Research Center at the Hong Kong Polytechnic University.

The financial support from the Research Committee of the Hong Kong Polytechnic University, which was essential for the author's graduate studies, is acknowledged.

Table of contents

List of Tables

List of Figures

CHAPTER 1 INTRODCUTION

1.1 Background

Corrosion occurs on metals surfaces and causes them to lose their luster and colour. The incorporation of corrosion resistance on surfaces of metal by different plating processes is therefore important in many manufacturing processes. Electroplating or electrodeposition, which may be simply described as the deposition of a metallic layer by the passage of an electric current through a solution containing the metal ion between two electrodes. While the other one, electroless plating process is the deposition of a metallic layer without electric current.

Nowadays, electroplating and electroless plating processes are widely used in the surface finishing industry. In the past 30 years, nickel plating had been widely used in many surface treatment processes. One of its most important applications is acting as diffusion barrier [45] in printed circuit board (PCB) and ornament. In this application, nickel is used to prevent the diffusion of the base metal, usually a copper alloy to the surface gold coating. The other purpose is to level the surface of the copper-base alloy and improve the brightness of ornament. Cobalt also possesses similar properties as nickel like leveling the surface of the base metal and acting as an intermediate layer to prevent the inter-diffusion of copper and gold [3].

Human perspiration can penetrate through cracks of the gold overplate of jewelry and corrode the nickel underneath. The leached nickel product can be irritating to human skin [1]. Since Directive 76/769/EEC of 30 June 1994 [2], which controls the use of nickel in objects

intended for prolonged contact with human skin [4], has been adopted by the Council of European Union, most manufacturers have replaced nickel with palladium [5]. However, the rapid rise in the cost of palladium in the past three years has deterred the use of this metal as a barrier. Cobalt and its binary and ternary alloys have been explored as palladium's possible replacement.

1.2 The history of nickel development and the potential element Cobalt

In 1844, Wurtz observed that nickel ion was reduced by hypophosphite anion, but he could get only a black powder. Breteau developed the method for bright nickel deposition in 1911. In1916, Ronx filed the first patent on electroless nickel plating and in the following years, Brenner and Riddell [36] published a paper that described the proper conditions for obtaining electroless deposition. [6]

Nowadays, many manufacturers are using the relatively cheap nickel plating for surface treatment in ornament industry [40,41]. In this application, nickel having anti-diffusion characteristic is used to prevent the diffusion of the base metal, copper to the surface gold coating and levels the surface of the base metal. Cobalt is next to nickel in the periodic table and has similar properties. However, most of the ornament is only plated with a very thin gold layer by the process known as flash gold plating. Human sweat can penetrate through the cracks of the gold overplate of jewelry and corrode the nickel underneath. The released nickel will irritate human skin [1] and because of the limitations set by the Council of European Union [2], most manufacturers have to replace nickel with palladium [5]. However, palladium is expensive and the rapid rise in the cost of palladium has encouraged the investigation on using cobalt and its binary and ternary as the possible replacement for palladium. In the printed circuit board industry, when the surface copper clad of PCB forms an oxide film on the surface, solderability will decrease. Gold overplate is used to increase the solderability and bondability. Cobalt, tungsten

and phosphorus ternary alloy is a potential replacement of gold to form a stable layer to keep the solderability and bondability.

1.3 The electroplating and electroplating coating of cobalt alloy

The deposition rate of electroless plating is much lower than electrodeposition plating but the throwing power of electrodeposition plating is dependent on the plating process. Hence, researches on using these two methods to produce a more effective copper barrier for both the decorative and electroplating industries are being undertaken. In the view of only few studies have been made on ternary alloys [8-15]. This project will enhance the understanding of the procedure of deposition of ternary alloys, their potential replacements of noble metal as cost-effective barriers, and improving the solderability for surface mount technology.

1.4 Current work on Cobalt alloy

There are many reports on Nickel alloys [12-15] such as nickel-tungsten, nickel-molybdenum with phosphorus or boron. On the contrary, very few studies done on cobalt ternary alloys can be found. Many different deposition methods, such as pulse electroplating and different complexing agents had been investigated. In this project we will use simple DC plating methods; Hull cell testing and different complexing agents will be used to optimize a good coating for use as a barrier.

The standard potential of cobalt is –0.28v, its potential is more negative than nickel [11], so the electroless deposition of cobalt is more difficult than nickel. Formation of cobalt alloys depends on induced-codeposition [47] and different kinds of complexing agents will affect the deposition rate and composition of coating.

1.5 Objective

The present research program aims at developing the application of cobalt binary and ternary alloys. The project will focus on:

(a) The technology of deposition of ternary alloys containing cobalt, tungsten, and phosphorus.

(b) The application of these alloys in coating of watch cases, spectacles, jewelry and the production of printed circuit board.

CHAPTER 2 LITERATURE AND THEORY REVIEW

2.1 The function of electroplating and electroless plating technology

Most of the commercial goods are finished with surface treatments. These treatments include laser treatment, heat treatment, painting, electroplating and electroless plating. Most of these treatments are of functional purposes. In this project, the objective of electroplating and electroless plating are to provide a coating that will protect the underlying metal from corrosion when exposed to atmospheric or other conditions for decorative purposes.

Hence, the electroplating and/or electroless plating are a necessary step in the production of metallic products. Although the plated layer cannot totally prevent corrosion, corrosion rate can be reduced and the lifetime of the object can be extend.

The main functions of electroplating are:

(a) Increasing the corrosion resistance and protecting the surface of metallic products and goods.

(b) Adding a special function on the surface, for example, increasing the hardness [55], conductivity, anti-corrosion, solderability and bondability.

(c) Decorating jewelry.

2.2 Theory of electroplating

Electrodeposition of metallic alloys on metallic surface or plastics requires different conditions from those that are usually employed for electrodeposition of a single metal. Current is supplied from an external power supply. In order to pass an electric current through a solution we have to insert two electrodes - an anode and a cathode- and it is the properties and behavior of these electrodes that we have to examine. When the electrode is placed in a bath solution with no current flowing and a voltage is applied from an external source, such as a battery, difference of potential is set up between the metal and the solution. When two different electrodes of different element are put into a solution, there will be a potential difference. This means that a partial separation of positive and negative charges occurs at the surface of separation between the metal and the solution in which it is placed.

The actual process by which a dissolved metal ion is converted into a solid crystalline deposit can be explained in terms of the modern theories of physics and chemistry. The variations of electroplating depend on the complexing agent. Different complexing agents can affect the mechanism and the content of the coating. The following very elementary description merely gives a picture of the process in terms of the accepted simple theories. Only the reaction at the cathode will be discussed. In general, the reactions at a soluble anode will be the reverse of those at the cathode. At cathode, the metal ions absorbed on cathode surface will receive electron from the power supplier [17],

$$M^{n+} + ne^- \rightarrow M_{(\text{on the surface})}.$$

In the solution of a metal salt such as cobalt sulfate, the salt is dissociated to a considerable extent to form positively charged cations, in this case, Co^{2+}, and negatively charged anions, $SO4^{2-}$. The water present is slightly dissociated to form hydrogen ions, H^+, and hydroxyl ions, OH^-. In electroplating of Co-W-P [42], the metals combine with complexing agents. Sulfuric acid present is dissociated into hydrogen ions, H^+, and sulfate ions, either HSO_4^- or SO_4^{2-}. Most of these ions are hydrated; i.e., they are combined with one or more molecules of water and all these reactions will occur during electroplating is processing.

The relationship between current and potential, when an electrode is made a part of an electrochemical cell through which current is flowing; its potential will differ from the equilibrium potential. If the equilibrium potential of the electrode (potential in the absence of current) is E and potential of the same electrode as a result of current flowing is E (I), then the difference η between these two potentials

$$\eta = E(I) - E$$

is called overpotential. The influence of mass transport on electrode kinetics depending on the current-potential relationship is valid for the case where the charge transfer, the dynamic equilibrium of electrode potential is the slow process (rate-determining step). This relationship has a limit where the rate of deposition reaction is limited by transport of M^{Z+} ions.

2.3 Theory of electroless plating

Brenner and Riddell developed electroless plating in 1946. When the process was first developed, there were only a few metals having autocatalytic reactions. Nowadays, metals including Ni, Co, Pd, Cu, Au and Ag have been successfully electroless plated to form alloys with other metals and non-metals with amorphous or crystallize structures. This method produces a thin metallic film on metals, plastics or ceramics at a moderate temperature, by just immersing the objects or substrates into an electrolyte solution (electroless plating bath). It is widely used for producing electronic parts [44] and the base layer of plastic electroplating. The electroless plating bath is a complex electrolyte solution containing metallic ions, reductants, complexing agents and other minor components, for example, stabilizers, wetting agents or brighteners.

These processes give coatings both corrosion resistance properties and hardness. Many workers from chemical or electrochemical viewpoint [16] have studied the basic mechanism of electroless plating. It is now widely accepted that electroless plating proceeds along the lines of an electrochemical mechanism as the simultaneous reaction of cathodic metal deposition and anodic oxidation of reductants according to the mixed-potential theory. Panuovic and Saito suggested an electrochemical model for the process of electroless metal deposition on the basis of the Wagner-Traud mixed-potential of corrosion process. According to the mixed-potential theory of electroless deposition, the overall reaction is given by

$$ML_m^{n+}{}_{solution} + Red_{solution}. \rightarrow M_{lattice} + Ox_{\ solution}.$$

The mixed potential theory, electroless plating can be explain by a combination of cathodic deposition of metal and the anodic oxidation of reductant at immersion potential E_{im}. The partial reactions are written as follows: the cathodic reaction

$$ML_m^{n+}{}_{solution} + ne^-_{\ (on\ surface)} \rightarrow M + mL,$$

And the anodic reaction is

$$Red_{\ solution} \rightarrow Ox_{\ solution} + ne^-$$

Where L indicates a ligand (complexing agent), $Red_{\ solution}$ is a reductant and $OX_{\ solution}$ as oxidant in solution bath and n is the number of electrons concerned. These two partial reactions occur at one electrode, the same metal-solution interphase. The equilibrium (rest) potential of the reducing agent, anodic reaction, must be more negative than the cathodic reaction of the metal electrode, so that the reducing agent Red can function as an electron donor and M^{n+} as an electron acceptor.

The electrochemical conditions for electroless deposition to take place are the oxidation potential of the reductant is less noble to the reversible potential of the metal to be deposited, the metal has enough catalytic activity for the anodic oxidation to take place at a reasonable rate. The first condition can be readily provided by simply thermodynamic consideration of reductants is, in some senses, a dominant factor in electroless deposition.

The oxidization of reducing agent provides the electrons for reducing the metal ion in the

bath. The reductants used in electroless plating have a special feature. Only a few reductants are used in an electroless process, e.g. hypophosphite. Electroless deposition usually accompanies hydrogen evolution, of which the rate is not directly related to that of metal deposition. Different reaction mechanisms have been proposed to account for the hydrogen evolution during electroless deposition:

(1) the proton discharge mechanism;

(2) the hydride mechanism;

(3) the atomic hydrogen mechanism,

$H_2PO_2^- + H_2O \rightarrow H_2PO_3^- + 2H$; $H_2PO_2^- + H \rightarrow P_{(in\ coating)} + OH^- + H_2O$;

(4) the hydride ion mechanism,

$H_2PO_2^- + O^{2-} \rightarrow HPO_3^{2-} + H^-$, $H^+ + H^-$

$\rightarrow H_2$, $2PO_2^{2-} + 6H^- + 4H_2O \rightarrow 2P + 3H_2 + 8OH^-$ and

(5) Electrochemical theory, $H_2PO_2^- + H_2O \rightarrow H_2PO_3^- + 2H^+ + 2e^-$(Anode); $2H^+ + 2e^- \rightarrow H_2$, $H_2PO_2^- + e^- \rightarrow P + 2OH^-$ (Cathode).

This method can form an amorphous layer when phosphorus was added. Induced codeposition [18, 19] also happens in the reaction, if we add other elements like tungsten to the bath solution and the coating will contain tungsten. However, induced codeposition is not certain because there are only very few reports at this moment.

In the comparisons between crystalline and amorphous alloy [26,43,51], amorphous

material have better corrosion resistance. There are many reports about amorphous alloy. Electrodeposited alloys usually have a better appearance than the parent metals, being smoother, brighter, and having finer grains. The grains of many electrodeposited alloys are too small to be seen with the microscope and their size must be estimated by means of X-rays diffraction. Some alloys, for example, the high phosphorus nickel alloys, seem to possess no crystal structure at all and are apparently amorphous. Their X-ray diffraction pattern yields no lines, but only a blur characteristic of glasses. These alloys may be considered as a metallic glass, like glass they are hard and brittle and break with a conchoidal fracture. Amorphous alloys are new to metallurgy. One of the methods for preparing the amorphous structure is by electroplating, the mechanism depends on hydrogen evolution [48] at the anode when metal deposit on it. There are many hydrogen bubbles and the structure is crystal structure in Chromium plating. The adding of P, B, C, Si, alloy elements, leads to amorphous structure easily because most of the electroless plating need to deposit with other elements like P, B to form an amorphous alloy.

2.4 Effect of additives [58,61,62]

There are two basic types of adsorption: chemisorption (an abreviation of chemical adsorption) and physisorption (an abreviation of physical adsorption). In chemisorption the chemical attractive forces of adsorption act between the surface and the adsorbate (usually these are covalent bonds).

Thus there is a chemical combination between the substrate and the adsorbate where electrons are shared and/or transferred. New electronic configuration may be formed through this sharing of electrons. In physisorption the physical forces of adsorption, Van de Waals or electrostatic forces, act between the surface and the adsorbate; there is no electron transfer and no electron sharing.

The adsorption energy for chemisorbed species is greater than that for physisorption species. Typical values for chemisorption are the range of 20 to 100 $kcalmol^{-1}$ and for physisorption, it is around $5kcalmol^{-1}$

2.5 Growth Mechanism

There are two basic mechanisms for formation of a coherent deposit, layer growth and three-dimensional (3D) crystallite growth.

In the layer growth mechanism a crystal enlarges by spreading of discrete layers (steps), ions after another across the surface. In this case a growth layer is a structure components of a coherent deposit. Steps and growth layers, are the structural components for the construction of a variety of growth forms in the electrodeposition of metals. There are three steps for distinguish, monatomic steps, polyatomic microsteps, and polyatomic macrosteps. In general, there is a tendency for a large number of thin steps to bunch into a system of a few thick steps. Many monatomic steps can unite to form a polyatomic step.

In the 3-D growth mechanism the structural components are 3 D crystallites, and a coherent deposit is built up as a result of coalescence of these crystallites. The growth sequence of electrodeposition via nucleation-coalescence consists four stages:

1. Formation of isolated nuclei and their growth to three-dimensional crystallites
2. Coalescence of three-dimensional crystallites
3. Formation of linked network
4. Formation of a continuous deposit

The development of columnar microstructure is perpendicular to the substrate surface. This mircostructure is composed of relatively fine grain near the substrate but then changes to a

columnar mircostructure with much coarser grains at greater distances from the substrate. The development of the columnar microstructure may be interpreted as the result of growth competition among adjacent grains. The low-surface-energy grains grow faster than the high energy ones. This rapid growth of the low-surface-energy grains at the expense of the high-energy grains results in an increase in mean grain size with increased thickness of deposit and the transition from a fine grain size near the substrate to a coarse, columnar grain size.

The development of growth forms on overpotential stems from the potential dependence of the nucleation and growth processes competition between nucleation and growth processes is strongly influenced by potential of the cathode.

2.6 Leveling

Leveling is defined as the progressive reduction of the surface roughness during deposition. Surface roughness may be the result of mechanical polishing. In this case scratches on the cathode represent the initial roughness and the result of cathodic leveling is a smooth (flat) deposit or a deposit of reduced roughness. During this type of leveling more metal is deposited in recessed areas than on peak (bumps). This leveling is of great value in the metal finishing industry. Leveling can be achieved in solution either in the absence of addition agents or in the presence of leveling agents. Thus there are two types of leveling processes:

1. Geometric leveling corresponding to leveling in the absence of specific agents and

2. True or electrochemical leveling corresponding to leveling in the presence of leveling agents.

Dukovic, Tobias, Madore and Landolt developed theoretical model of leveling during electrodeposition in both the absence and presence of additives. Both models indicate that a significant leveling of semicircular and triangular grooves by uniform current distribution (geometric leveling) is achieved when the thickness of deposit is at least equal to the depth of the grooves. Leveling in the presence of leveling agents (true leveling) is achieved at much lower deposit thickness.

Theories of leveling by additives are based on

1. The correlation between an increase in the polarization produced by the leveling agents, Leidheisier and preferential adsorption of a leveling agent on the high point (peaks of the

substrate or flat surface and by this inhibition) slowing down of deposition at these points.

2.7 Electrodeposition of alloys

Alloy deposition is as old an art and science as the electrodeposition of individual metals (e.g., brass, which is an alloy of copper and zinc, deposition was invented circa1840). As may be excepted, alloy deposition is subject to the same principles as single-metal plating. Indeed progress in both types of plating has depended on similar advances in electrodeposition science and technology. The subject of alloy electroplating is being dealt with by an ever-increasing number of scientific and technical publications. The reason for this is the vastness of the number of possible alloy combinations and the concomitant possible practical applications.

Properties of alloy deposits superior to those of single-metal electroplates are common place and are widely described in the literature. In other words, it is recognized that alloy deposition often provides deposits with properties not obtained by employing electrodeposition of single metals. It is further the case that, relative to the single component metals involved, alloy deposits can have different properties in certain composition ranges. They can be denser, harder, more corrosion resistant, more protective of underlying basis metal, tougher and stronger, more wear resistant, different in magnetic properties, more suitable for subsequent electroplate overlays and conversion chemical treatments, and superior in antifriction application.

Electrodeposited binary alloys may or may not be the same in phase structure as those formed metallurgically. By way of illustration, we note that in the case of brass (Cu-Zn alloy), X-ray examination reveals that, apart from the superstructure of β-brass, virtually, the same phases

occur in the alloys deposited electrolytically as those form in the melt. Phase limits of electrodeposited alloys closely agree with those in the bulk form. Somewhat oppose is the case of the Ag-Pb alloy. In the cast alloy form it contains “large” silver crystals with lead present in the grain boundaries as dendrites. In the electrodeposited form the alloy contains exceedingly fine grains exhibiting no segregation of lead.

Induced codeposition is characterized by the deposition of alloys containing metals, such as molybdenum, tungsten or phosphorus, which cannot be deposited alone. However, these metals readily codeposited with the iron group metals. Metals which stimulate deposition are called reluctant metals and the effect of the plating variables on the composition of the alloys of induced codeposition are more vagarious and unpredictable than the effects on the composition of alloys of any other types of codeposition. The last two types of codeposition, since on the basis of elementary considerations, codeposition of these types would not be expected.

2.8 Tungsten Coating

A high melting point metal can be a good barrier at high temperature. Tungsten and Molybdenum both have this characteristic. The reduction potential of tungsten is higher than the hydrogen reduction potential, and tungsten does not dissolve anodically readily in an acid solution, nor does tungsten deposit cathodically because the electrode and solution do not react and reactions at the surface of this electrodes is irreversible reaction. It was found that adding some kinds of complexing agents can reduce the reduction potential of tungstate ion but the value is still more positive than hydrogen. Hence, only hydrogen evolves at the anode.

Currently, pure tungsten cannot be electrodeposited from aqueous solution, but it can be codeposited easily with nickel, cobalt or ion forming an alloy. The tungsten content depends on relative concentrations, mass transport of tungsten, cobalt or component in the solution bath and all these will be limited to the deposition rate of tungsten in the coating content. [20]

The induced codeposition [18,19] of tungsten with cobalt has been reported and will be used as alloy formation for barrier coating in this project.

2.9 Cobalt-Tungsten [7, 59]

In the past ten year, nickel was used as barrier by the jewelry industry. Nickel ion was found to irritate human skin [56] when it was corroded by human sweat [1,57]. Nickel and cobalt are in the same periodic group and they have similar chemical properties, hence, we will try to use cobalt to replace nickel. Comparing Nickel with Cobalt, the corrosion resistance of nickel is better than cobalt but nickel ion irritates human skin, as the result, cobalt will substitute nickel for barrier in jewelry [21] watches industry. Concerning the corrosion resistance of cobalt, its alloy with W, Mo, and Cr will be developed in this study. For increasing the corrosion resistance, Cr is the most efficient alloy element. The alloy element resistance power is in the order Cr>Mo>W>Co [22]. In electroplating, Mo and W cannot deposit directly on the surface, they need induced codeposition[23]. Hence, a cobalt-tungsten alloy electroplating process will be presented. The deposition of amorphous alloys of tungsten is accompanied by anodic decomposition of ammonium citrate electrolyte [24].

There are many reports on Cobalt-tungsten and Nickel-tungsten coatings [25]. They were using many different depositing methods, such as pulse electroplating and different complexing agents [26]. In this project, we will use simple DC plating method, Hull cell, and complexing agent for optimizing a good coating for use as a barrier.

2.10 Cobalt-Tungsten-Phosphorus

In the past ten years, there were many researches on producing amorphous coating through electroplating or electroless plating. The main elements of amorphous coating were iron group metal (Fe, Ni, Co), non-metal (P,B,S) and high melting point metal (Mo, W). Nickel base amorphous coating was developed by many researchers but there were only a few researches on cobalt base amorphous coating. There were reports on coating containing over 8 wt%. phosphorus [27]or over 40 wt% of tungsten [28], cobalt coating containing 22.5 atom% of tungsten [29], and nickel coating containing over 44wt% of tungsten [30]. All these coatings were amorphous. The amorphous alloy coating will become in interest of industrial use for its application. [31, 32] Some of these alloys are known to act as protective layer and resist corrosion, others have unusually soft magnetic characteristics, which make them an interesting material for production of storage devices. Two methods of producing an amorphous alloy layer on the substrate, electroplating of Co-W-P [33] and electroless plating of Co-W-P [34], will be studied. Electroplating is using external electric supply and the electroless plating is by oxidation of an reducing agent, to reduce the metal ion to the metal. In this project, we will concentrate on these two plating methods for Co-W-P coating. There are few reports on the electroless plating of Co-W-P. Previously, the deposition rate for electroless plating is too low for industrial process, so, we will need to change the formulation of electroless plating bath to quicken the process [35].

2.11 Nickel and its alloy coating

The electroless plating of a metal from an aqueous solution of the said metal salt has an electrochemical mechanism bath. Oxidation and reduction reaction (Redox reaction) involves the electrons transfer between reacting chemicals.

Reagents like hypophosphite ions, $H_2PO_2^-$, in the electroless plating reaction, will be undergo oxidation and provide electrons to reduction reaction in the metal ions.

In general, electroless plating is characterized by the selective reduction of metal ions only at the surface of a catalytic substrate immersed into an aqueous solution of said metal ions, with continuous deposition on the substrate through the catalytic action of the deposit itself.

Alloy plating can provide properties that are not attainable with single metal coatings or by layered metals. Properties enhanced by alloy include harder coating, finer grain structure, more uniform component dispersion and unique structures.

Furthermore, structures can be obtained with alloy plating that is not obtainable by any other means. For example, Nickel coating, the hardness is not higher than nickel containing tungsten coating.

2.12 Improvement of alloy coating

In electroless plating, the quality and quantity are important. There are two views we need to consider, the deposition rate of the reaction and the physical and chemical properties of the coating.

About the deposition rate, there are additives for enhancement. In our coming research, if chemical additive like sodium hypophosphite is added, the reaction composition was changed and the deposition rate will also be varied. It is difficult to determine the deposition without the experiment. And there are many variables that we cannot work on each and every one. We need to consider the orthogonal experiment design.

After using this method, we can save more time for finding the best formulation of the solution bath. In CHAPTER 3, the development of formulation will be discussed in more detail. The higher deposition rate has been found and the coming step will be determining the quality of the coating. The coating needs to be checked on its the physical and chemical properties. From the experiments, the result obtained would be in support of the project aim, that is improving the content of solution bath.

2.13 Electroplating Hull cell experiment

Hull cell was used for the wide range test for electroplating and the late R.O.Hull developed it. It was described in the American Electroplaters and Surface Finishers Society's Proceeding in 1939 and has probably contributed more to the advancement of electroplating than any other tool. The Hull Cell employed usefully for the testing of plating solutions. One of its great advantages is the fact that it is possible to assess the deposit characteristics at varying current densities all on one test panel.

The Hull cell consists of a container of Perspex or other construction having a trapezoidal plan. The cathode is fixed at an angle to the anode, and both occupy the full cross section of the cell. It is important to note that the shape and dimensions of the cell play the most important part in determining the cell current distribution.

The anode in the cell is corrugated in shape. This provides additional surface area that lowers the anode current densities without producing excessive anode polarization. In 276 ml Hull cell, the panel is 4 inches(100mm) long x 2.75 inches(75mm) in depth or width. The current density increases as the distance from the anode decreases.

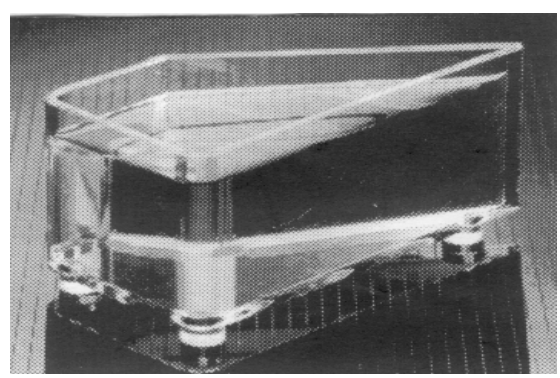

The current density at any vertical plane on the cathode may be found,

$$i_{(L)} = I_{appl}(5.10 - 5.24\log L)$$

$i_{(L)}$ = Current density at a distance L (A/dm^2)

I_{appl} = Total cell current employed (A)

L = Length along the panel from High Current Density End (cm)

The Hull cell test is valuable for troubleshooting for electroplating. It can help the electroplaters in preventive maintenance, process development and process modification. In troubleshooting, the aim is to discover the cause of poor deposits and to find the best method to correct the problem. In view of the very wide range of current densities that exist on a Hull Cell panel, many problems can be spotted before they appear on the work, and the proper preventive maintenance operations performed before rejects appear. The Hull Cell is widely used in research to develop new plating processes. In the development of a new bath solution, the electroplaters have to find out the suitable optimum current density range in other operating conditions. If they need to plate in each current density for each condition, they need to spend a lot of time. When they use the Hull cell, they can obtain a wide range of current densities for one condition in a single Hull cell experiment. The Hull Cell can be used to evaluate properties, such as brightness, burning range, leveling, ductility, covering power, throwing power and efficiency of the plating bath for a range of current density.

2.14 Determination of Interdiffusion Coefficients by the Boltzmann-Matano Method [50,60]

In general jewelry, a thin gold layer was coated on copper base object and there is inter-diffusion between the two layers. To prevent the inter-diffusion of gold and the base metal, a barrier layer is deposited on the surface of the base metal before the deposition of the gold layer. Study of diffusion of gold in the barrier layer will enable us to determine the effectiveness of the barrier layer. The problems associated with diffusion in a concentration gradient can be handled by the Boltzmann-Matano method. Interdiffusion of different Cu/electrodeposit couples are studied by determination of the concentration-distance profile after heat treatment at different temperatures. Heat treatment on these two layers increases the rate of diffusion. The EDAX microprobe method is used for monitoring the amount of metal in the barrier coating. A chemical interdiffusion coefficient D is introduced which varies along the concentration gradient in the diffusion zone of the Cu/electrodeposit couple. The determination of metal diffusion coefficient is according to the Fick's laws. Hence, chemical diffusivities are calculated from the concentration versus distance data at different copper concentration. Arrhenius plots (log diffusivity versus reciprocal temperature) can be constructed.

In this research, we will study the concentration of Cu and the electroplating barrier. For the inter-diffusion of two metals A and B in intimate contact as interdiffusion proceeds, metal will develop a profile of fractional atomic concentration $c_A(x).D_{AB}(x)$ describes the progress of Metal

A atoms at a particular depth x measured form the original interface, where the host matrix is a mixture of metal A and B atoms in the proportion $c_A(x):c_B(x)$. Exchange of two metal A atoms does not contribute to observed diffusion flux of species A. However, in a random vacancy diffusion process, the probability of a successful replacement of a B atom with one type A will be proportional to $c_B(X)$. Thus, the effective transport of species A from the interface, due to combined migration of metal A and B atoms, is described by $D_{AB}(x)$, where

$D_{AB}(x) = D_A c_B(x) + D_B c_A(x)$

D_A and D_B can be deduced by measuring D_{AB} at several known concentrations (cA, cB) and then solve for D_A and D_B, for which the variation in D_{AB} with varying concentration can be handled by a method first proposed by Boltzmann. Fick's second law for one dimensional diffusion is generalized to allow explicitly for the variation in D by writing in the form below

$$\frac{\partial c}{\partial t} = \frac{\partial}{\partial x}\left(D \frac{\partial c}{\partial x} \right) = D \frac{\partial^2 c}{\partial x^2} + \frac{\partial D(c)}{\partial c}\left(\frac{\partial c}{\partial x} \right)^2$$

Assume a solution of the form

$c = c\,(xt^{-1/2})$

and define $y = xt^{-1/2}$. Now by differentiation we obtain

$$\frac{\partial c}{\partial t} = \frac{dc}{dy}\frac{\partial y}{\partial t} = -\frac{1}{2}\frac{x}{t^{3/2}}\frac{dc}{dy} = -\frac{y}{2t}\frac{dc}{dy}$$

$$\frac{\partial c}{\partial x} = \frac{dc}{dy}\frac{\partial y}{\partial x} = t^{-1/2}\frac{dc}{dy}$$

$$\frac{\partial^2 c}{\partial x^2} = \frac{1}{t}\frac{\partial^2 c}{\partial y^2}$$

$$\frac{\partial D}{\partial x} = t^{-1/2}\frac{dD}{dy}$$

After the Substitution,

$$\frac{\partial c}{\partial t} = \frac{D}{t}\frac{\partial^2 c}{\partial y^2} + \frac{1}{t}\frac{dD}{dy}\frac{dc}{dy} = -\frac{y}{2t}\frac{dc}{dy}$$

or in another form

$$\frac{d\left(D\dfrac{dc}{dy}\right)}{dy} = -\frac{y}{2}\frac{dc}{dy}$$

After solving the D and substituting for y,

$$\tilde{D} = -\frac{1}{2}\frac{dy}{dc}\int_{c_o}^{c} y dc = \frac{1}{2t}\frac{dx}{dc}\int_{c_o}^{c} x dc$$

The interdiffusion coefficient, $\tilde{D}$, reflects the average of the overall movement of all constituents diffusing in a concentration gradient.

Imagine two homogeneous semi-infinite cylinders of different chemical composition, which are intimately joined at mutual planar interface. For such a configuration it becomes obvious that x = $\pm\infty$, dc/dx =0 and hence, equation is undetermined as a result of the fact that c = 0 or c = c_0 for each the arbitrary number of constituents.

As the result,

$$\frac{1}{2}\int_{c_0}^{c^1} y dc = \tilde{D}\frac{dc}{dy} = -\frac{1}{2}\int_{c_0}^{c^1} x dc$$

However, x must run from -∞ to +∞ for equation to be valid, and x = 0 must define a surface such

that the depletion of a particular constituent to the left of it must exactly equal the accumulation on the right. This is simply the requirement of the existence of a conservation of mass surface, which is called the Matano interface. As the result of this condition, we now write for t equal to a constant

$$\int_{c_0}^{c_1} x dc - \int_{c^1}^{c_1} x dc = 0 \quad \text{or} \quad \int_{c_0}^{c_1} x dc = \int_{c^1}^{c_1} x dc$$

When the diffusion coefficient is independent of composition, $c_1 = c_0 2$ and the Matano interface after corrections for change in molar volumes corresponds to the original interface. This is seldom if ever the case, although this condition is closed approached when the two members of the diffusion couple are nearly the same composition. In the actual practice, different elements diffuse with different velocities and furthermore are dependent upon composition. Values of D are computed graphically; e.g., dc/dx is determined by drawing the tangent to the experimental measured diffusion profile at c'_1, the composition of interest, and the integration performed graphically:

$$D_{c=c'_1} = \frac{1}{2t} \frac{dx}{dc}\bigg|_{c=c'_1} \int_{c'}^{c_1} x dc$$

This method may be extended to other concentrations if one component is far more mobile than the rest.

$$D_{c=c'_1} = -\frac{1}{2t} \frac{dx}{dc}\bigg|_{c=c'_1} \int_{0}^{c_1} x dc$$

By the repetition of the process at a series of temperatures, Arrhenius plots for D_{AB}, D_A and D_B may be obtained, leading to experimental values for activation energies Q_{AB}, Q_A and Q_B.

2.15 X-ray diffraction

Being a good barrier coating, corrosion resistance is important. Comparing amorphous with crystalline structure, amorphous structure has better corrosion resistance than crystallize structure, so it is important to determine the structure in this research. In 1912, M.T.T. von Laue observed diffraction when X-ray was transmitted through a crystal. This technique is used to detect the crystal structure, lattice parameter and grain size.

X-ray is an electromagnetic wave with wavelength in the range of 0.001 to 10 nm. It is usually produced by the collision of high velocity electron onto anode.

It is generally observed that the interdiffusion property between two different metal layers behaves differently upon heat treatment at different specific temperature range. This is due to the structural changes and intermetallic phase formation of the electrodeposition upon heat treatment, which affect the interdiffusion behavior for the copper/electroplating couple. Formation of lattice vacancies and change of grain boundary density result to higher interdiffusion coefficients.

X-ray diffraction techniques are used to identify the phase present in samples and to provide information on the grain size, texture and lattice parameter.

High-energy (20kV) electron beam is directed into a water-cooled target for generation of x-rays. As the electrons are decelerated in the target, most of the electron beam energy lost in collisions that set the atoms in motion and produce heat, which must be dissipated through the cooling water. The decelerated electron caught in the electric fields of the atom produces X-rays of a

continuum of all energies between zero and the excitation potential, and is termed as white radiation. Some target electrons are knocked out of their orbital, for which these electron transition are quantified and have specific wavelengths. Therefore, x-rays exiting the target have a few strong characteristic concentrations of specific wavelengths superimposed on the white radiation. Copper is used as the target because the Kα characteristic radiation is useful wavelength, 0.15406nm, and the target is easily cooled for high efficiency. For copper radiation, a nickel foil absorbs most of the white radiation and the other characteristic peaks, transmitting essentially pure Kα radiation. In this case, flat graphite crystal monochomator is used since it monochromates the x-ray beam better than nickel foil filter. The crystal monochromator also suppresses the effects of sample fluorescence. A proportional detector filled with Xe gas is used for detection of x-rays as it is particularly good for detecting radiation that has the wavelength of Cu or longer.

Characteristics of a sample can be determined from the collection angles at which diffracted x-ray beams are detected. The lattice of the sample reflects the size and sharp of the unit cells and their periodic arrangement in soace. The lattice is fundamental to the geometry of any diffraction experiment. Interference of the scattered x-rays in most directions results in cancellation and absence of detectable beams. However, in a few selected directions, reinforcement of all the scattered rays occurs, and a strong beam results. These are the diffracted beams because the crystal is periodic in three dimensions, and the resulting diffracted rays define family of cones in

space. The three-dimensional lattice of scattering centers restricts a diffraction experiment severely, and diffraction can only occur when the incident beam makes precisely the correct angle relative to the crystal.

2.16 DC polarization measurement

The corrosion resistance of the electroplated layer is a key factor for the usefulness of the layer. The coatings should be investigated for their suitability as diffusion barriers [52] and the corrosion resistance of the metal coatings should be evaluated. Electrochemical methods are useful for determining the corrosion rate of metal within a short period. Linear polarization is using low current-potential applications around the corrosion potential values. It is the most widely used the electrochemical method. This technique is one of the most used techniques for studying metal corrosion. The potential would be scanned linearly around corrosion potential (E corr) as a function of time and the current monitored as the potential changes. When the potential is plotted as a function of the log of the current, portions of both of the anodic and cathodic regions may be linear and follow a Tafel behaviors. In cases, it is possible to extrapolates these linear regions to where they should intersect, at the corrosion potential (Ecorr), and obtain a value for the corrosion current (Icorr)[20].

2.17 Solderability review

Soldering is an important technique in most of the electronic product [44]. Since soldering technology occupies an intermediate position in several science aspects such as mechanics, electronic engineering, chemistry and metallurgy, it involves many different people in this technique. Electronic assembly is composed of components that are soldered onto a printed circuit board. Soldering happens between two metal surfaces (component termination and a connecting pad on printed circuit board track) jointed by metallic bonds created by molten solder between them. The solder supports the solder joints when it solidifies, and the solder allows electrical contact between metals in the joints. Successful soldering depends largely on the wetting of the surfaces with molten solder.

Soldering is different from adhesive joining. Adhesive bond by mechanical attraction has to do with mechanical surface properties of the material relative to the adhesive. In the case of soldering, there is also a chemical reaction in addition to physical reaction.

Electroless nickel [37] was well developed in past 30 years and it had been widely used in many surface treatment processes, such as printed circuit board industry. One of its most important applications is as diffusion barrier in Printed Circuit Board (PCB). It can be used in plastic plating such as the production of Printed Circuit Board. Electroless plating of Nickel coating have fast deposition rate. It can increase the productivity process in industries. When electroless-plating nickel is used to be a barrier, it has a good performance in anti-diffusion.

However, the nickel layer deposit on the base will be easily oxidize and corrode by atmosphere. The oxidized surface will reduce the wetting ability of solder and bondability between the base material and solder. As the result, in industrial production, the electroplaters always plate a very thin gold layer, flash gold, to maintain the solderability. Another method is adding flux activators to increase the wetting ability and solderability and trying to replace the flash gold plating process. However, these methods increase the production cost and waste time on production procedures.

Wetting of Surface

Wetting is an essential prerequisite for soldering. Wetting means that a specific interaction takes place between the liquid solder and the solder surface of the part to be soldered. When a solid metallic piece is immersed in a bath of liquid/ molten solder, there is contact between the piece and the liquid solder, but this does not automatically imply wetting as a barrier may be present. Wetting is possible only if the solder can come into immediate contact with the metallic surface of the solid metal part and sufficient attraction is ensured. If oxide layer is present on the base metal and the soldering obtained is as one work at low temperature, it is called cold joints. The electrical conductance of these colder joints is rather poor because the current has to pass through the more or less insulating oxide film. Adhesion is also poor on solidification, the solder droplet can easily separate when subjected to mechanical load.

If the base metal is clean and molten solder is dropped onto the clean plate, the solder atoms are

able to come closer to the atom of the base metal. Both of them can be attracted and will form an alloy at the interface.

The surface tension has the dimensions of energy per unit area (J/m^2). A system strives to a minimum value of its free energy and hence a minimum surface area.

A floating droplet therefore assumes the shape of a sphere because this shape has the minimum surface at a given volume. This tendency to reduce the surface area implies that there exists a pressure different, ΔP, between two sides of a curved surface.

$\Delta P = \gamma_1 (1/R_1 + 1/R_2)$

There is another simple method to determine the surface tension. It is observed that the contact angle between solder droplet spreads on the plate and the base plate, if it is less than 45^o,the surface tension will be lower and the coverage of solder will be increased.

An effective reaction of a flux with the oxide on a solid surface causes an increase on the surface tension γs by the removal of oxide. The effect of removal of the oxide film from molten solder is not so clear but it is favorable for wetting.

In our project, we found that electroless Co-W-P plating is having solderability better than nickel plating. A coated sample placed for 3 months can still be wetted by tin-lead solder. The advantage of this coating is reducing the procedure of producing printed circuit board. On the other hand, it can also reduce the production cost of PCB. Therefore, it is important to determine the solderability of coating.

CHAPTER 3 EXPERIEMTNAL PROCEDURE

3.1 Pretreatment Procedure

3.1.1 Electroless plating- 4 cm x 4 cm brass plates were electrocleaned in alkaline soak cleaner for 1 minute, then activated in 10 % aqueous solution of H_2SO_4 for 30 seconds. D. I. water would used for rinsing after each step.

3.1.2 Electroplating- a 10cm x 7cm copper plated steel panel was used for 250 ml Hull Cell test, following the pretreatment procedure 3.1.1,

3.2 Electroless plating (auto-catalytic plating)

The plating solution contained cobalt (II) sulphate, sodium tungstate [15], sodium hypophosphite, sodium citrate, succinic acid, lactic acid and 1-Phenylthiourea.

The plating temperature was 90°C. Before the plating, the brass plates were immersed into $PdCl_2$ (0.1g/L) solution with few drops of hydrochloride acid to start up the reaction.

3.3 Electroplating

Platinizied titanium was used as the anode place in the Hull Cell for electroplating test. Temperature of the solution was controlled during the experiment. The anode was connected to the positive outlet and the cleaned panel will be connected to the negative outlet of the power supply. The total current was kept at 2 A for 5 minutes in each test. The bath contained cobalt (II) sulphate, sodium tungstate, sodium hypophosphite and citrate acid.

3.4 Energy Dispersive X-ray fluorescence

All the alloy compositions were determined by Energy Dispersive Xray fluorescence. The element identification was analysed by means of wavelength dispersive spectra.

The setup data about Two EDAX instrument.	MRC	A. P.
Probe Current	300 pA	0.4 mA
W. D. (Sample distance)	25 mm	25 mm
EHT. (Voltage)	15.00 - 20.00 kV	15.00 - 20.00 kV
Magnitude	200 X	600 X

3.5 Interdiffusion studies

This project was divided into two sections, the Copper /barrier system and the Copper /barrier/Nickel system.

3.5.1 Copper/Barrier System

The coated sample plate would be cut into pieces of 4 cm x 4 cm large and heat treated in quartz tube under vacuum condition at temperature range at 400°C to 800°C. The samples were treated for a time interval range from 3/4 to 168 hours. After the heat treatment, the samples were micro-sectioned and polished with fine sandpaper and alumina powder.

Then, the samples would be analyzed by Energy Dispersive X-ray Spectroscopy. This was employed to obtain the chemical composition value using the Link ISIS program in which ZAF corrections were made for atomic number, absorption and fluorescence effects. Concentration-versus-distance profile was obtained.

The chemical interdiffusion coefficients were calculated using Boltzmann-Matano method. Concentration-distance data points with different diffusion times were fitted into a polynomial curve using computer software Tablecurve produced by AISN Software. Then the position of the Matano interface and the evaluation of the Matano solution at different concentrations were calculated numerically. Diffusion annealing schedule for Cu/Barrier diffusion couples was listed in Table3.1.

Table 3.1 Heat Treatment schedule for Copper/Barrier Diffusion Couples

Sample Designation	Heating Temperature(°C)	Heated time(hr)
Cu/Ni 1	400	168
Cu/Ni 2	500	72
Cu/Ni 3	600	24
Cu/Ni 4	700	5
Cu/Ni 5	800	3/4
Cu/Co-W-P(ELP) 1	400	168
Cu/Co-W-P(ELP) 2	500	72
Cu/Co-W-P(ELP) 3	600	24
Cu/Co-W-P(ELP) 4	700	5
Cu/Co-W-P(ELP) 5	800	3/4
Cu/Co-W(EP) 1	400	168
Cu/Co-W(EP) 2	500	72
Cu/Co-W(EP) 3	600	24
Cu/Co-W(EP) 4	700	5
Cu/Co-W(EP) 5	800	3/4

3.5.2 Copper/Cobalt- tungsten- Phosphorus (Barrier)/ Ni System

The samples would undergo take the same procedure, condition and pretreatment. Electroplated copper plates would be coated with 20μm bright nickel before the heat treatment. This diffusion experiment was conducted on samples at temperature ranging from 400°C to 800°C. Concentration-distance profiles were obtained by EDS and the results were compared to the Cu/Ni system.

3.6 DC polarization

Cobalt tungsten Phosphorus coating will be measured on its corrosion property by DC polarization method. A 1 cm^2 coated copper plate would be used for testing and placed in the cell. The testing cell included a platinum counter electrode and a saturated KCL/AgCl reference electrode. The reference electrode was housed in a Luggin cell with fixed Teflon Luggin capillary protruding from the bottom of the cell. The Teflon gasket exposed a 1 cm^2 area of the working electrode to the cell solution. The Luggin capillary was positioned at the proximity to the center of the working electrode.

DC polarization studies were carried out using EG & G PARC Model 273 Potentiostat. The potential scans were taken place within ±smile250mV of E_{corr} for each specimen with a scan rate of 0.166mV/s. Different samples would reach different results of Tafel plots and potential versus current polarization plots.

3.7 Polargraphic analyzer MODEL 394 with DC ramp connected to Electrode MODEL 303A SEDM hanging Mercury electrode

A. Calibration curve of Cobalt

1. All the glasswares were immersed in diluted HNO_3 for a day

2. All the glasswares were rinsed by distilled water

3. The 0, 2.0, 4.0, 6.0, 8.0 ppm of cobalt sulfate standard solutions were prepared in 50 ml Volumetric-flasks.

4. The sample plates were immersed into artificial sweat for a week to prepare the sample solution.

   (Artificial sweat: NaCL~5 %, Urea~0.1%,Lactic acid (85%)~0.1%

   Ammonia water was adjust pH at 6.5)

5. The 1.0 ml standard solution and 4.0 ml distilled water were pipetted in the container

6. The hanging mercury electrode MODEL 303A setup was used as below condition:

   Drop size: Large

   Mode: H DME

7. The polargraphic analysis MODEL 394 condition was set as below:

Scan rate:	5mV/sec.
Scan range:	1.2V
Scan direction:	Positive
Initial potential:	-1.2V
Pulse height:	25 mV
Operation Mode:	Differential pulse
Drop time:	1 second

Purge time: 240 seconds
Deposition time: 105 seconds
Equilibrium time: 15 seconds.

8. Step 3 with other standard concentration was repeated to make the calibration curve.

9. The concentration and peak height relation was plotted.

10. Step 4 using the sample solution was repeated. (If the peak was over the calibration curve, dilute the sample solution for analysis)

3.8 Determination of Internal stress by Spiral Contract-meter

A. Procedure of measuring internal stress

1. The helix was weighted and the weight recorded as “G”

2. The helix was mounted onto the meter body.

   (The helix was rotated for 2 rounds and then released, to observe whether there was a change in reading.)

3. The helix was cleaned by immersing it in detergent, PC-449 (60-70°C) for 3 minutes.

4. The helix was rinsed with 2 bottles of deionized water.

5. The helix was immersed in 10% HCL (at room temperature) for 1 minute.

6. The helix was rinsed with a bottle of deionized water.

7. The plating tank was filled with nickel strike.

8. The helix was immersed in nickel strike, and then the circuit was connected.

   Nickel strike plating

Current	2.5A
Temperature	50-60°C
Time	20-30 seconds

   The composition of nickel strike solution

Chemicals	Amount
Nickel chloride	240 g/L
Boric acid	30 g/L
Hydrochloric acid	120 ml/L

9. The helix was removed from the plating tank and rinsed with a bottle of deionized water.

10. The plating tank was replaced with the electroless plating solution, and then the circuit was connected for 30 seconds.

11. The meter was adjusted to zero and the reading was recorded at 1 minute time interval in the first 15 minutes. Then, the reading was recorded every 5 minutes time interval in follows 30 minutes.

12. The helix was removed and rinsed with deionized water, and immersed in ethanol for 5-10 seconds. It was then dried and weighed. The data were recorded in the spiral contraction meter and the internal stress δ_E was calculated.

B. Calculation of internal stress

$\delta_E = \mathbf{k} \times 2/(\mathbf{B} \times \mathbf{S}) \times \alpha/\mathbf{D} \times (1+\mathbf{D}/\mathbf{S})$

δ_E = Internal stress (kg/mm^2) **k** = spiral constant (mmg/degree)

α = torsional angle (degree) **D**= Electrodeposit thickness (mm or μ)

B = Spiral plate width (mm) **S** = Spiral plate thickness (mm)

C. Setup of Spiral Contractmeter

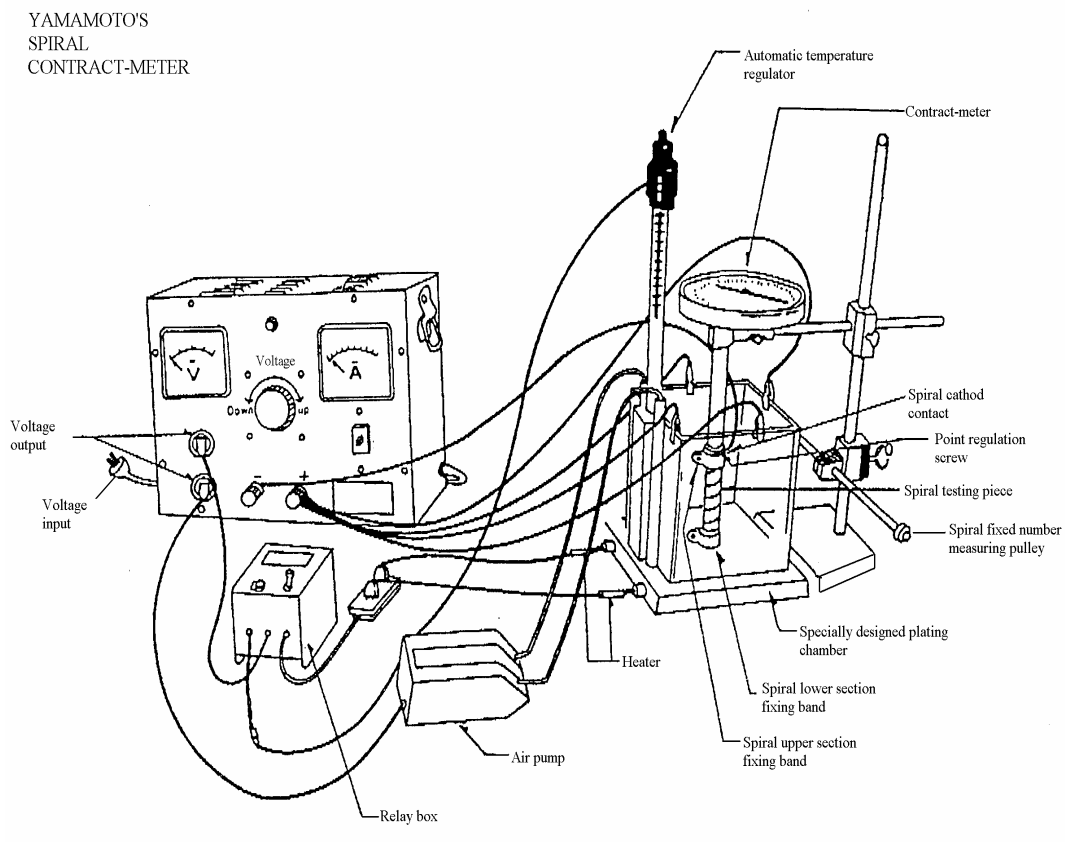

Fig 3.2 Setup of Spiral Contractmeter

3.9 Wetting measurement- coverage percentage

1. Melt the tin- lead in melt-oven at different temperature from 200 to 400˚C.

2. Prepare 3 sample plates,

   2.1 A sample exposed in atmosphere for 3 months
   2.2 A sample exposed in atmosphere for 3 months and flux resin before step 3
   2.3 A Sample prepare in fresh plate
   For step 3 at each temperature, copper plates sized 1 cm X 4 cm. (Pre-treatment) were used

3. Immerse the copper plate into the molten solder,

4. The tin-lead solder would adhere on the surface of the coated plates.

5. The solderability would be measured by counting the area that was coated by tin-lead solder.

   (The percentage of coverage)

CHAPTER 4 RESULT AND DISCUSSION

4.1 Investigation of Electroless plating of Co-W-P alloy

The formulation for the electroless deposition of Co-W-P includes many different functional chemicals. The starting experimental formulation for electroless plating of Co-W-P included. Cobalt (II) sulfate (35g/L), Sodium tungstate [15] (33g/L), Sodium hypophosphite (45g/L) and different amount of Succinic acid, Malic acid and Lactic acid which were the accelerator in the bath. 1-phenylthiourea was added to act as a stabilizer [38].

The following variations were performed to maximize the deposition rate [39]

4.1.1 Variation in Succinic acid concentration

Variation of succinic acid concentration with deposition rate, the procedure could be referred Chapter 3.2, electroless plating.

The effect of succinic acid content on deposition rate was illustrated in Fig 4.1. It was found that the optimum deposition ate 7.6 mb/cm^2/h could be attained at the succinic acid concentration of about 40g/L at 95^oC

In the concentration range of 56-80g/L, a constant deposition rate of 6.25 mg/cm^2/h was recorded. Succinic acid suppressed the deposition of the Co-W-P alloy in this concentration range. The deposition rate was measured as described in chapter 3.2.

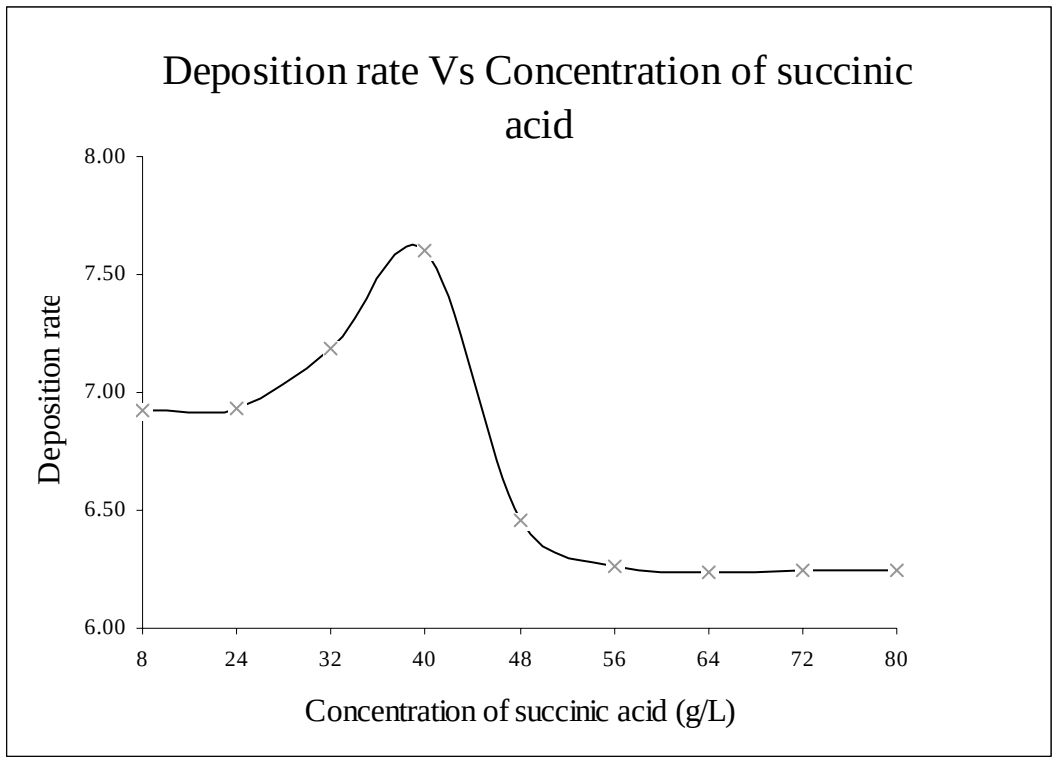

Fig 4.1 The deposition rate against concentration of succinic acid.

4.1.2 Variation in Malic acid concentration

It was found that a malic acid concentration of 32 g/L would result to an optimum deposition rate at 7.39 mg/cm^2/h. Figure 4.2 showed the plot of deposition rate against concentration of malic acid.

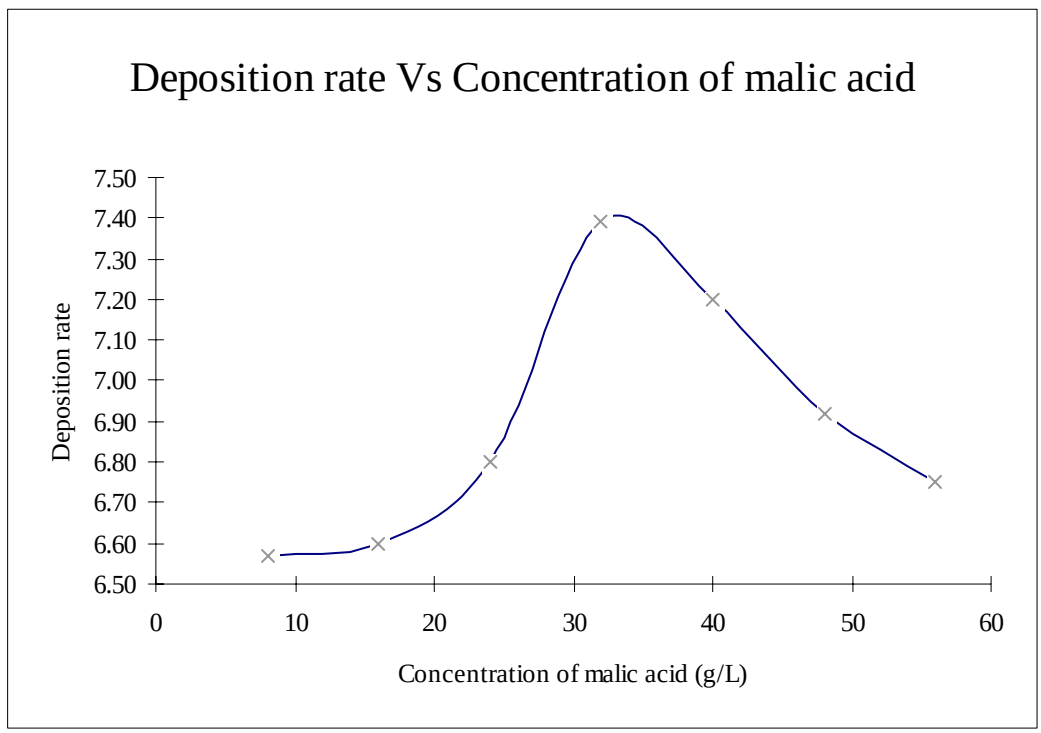

Fig 4.2 Deposition rate of Co-W-P alloy against concentration of malic acid

4.1.3 Variation in electroless plating bath content sodium hydroxide Vs Ammonia, sodium citrate Vs Sodium Tartrate

Two electroless plating baths were prepared with sodium citrate. The pH of the first bath was adjusted to 10 with ammonia, whereas the second bath was adjusted to pH 10 with sodium hydroxide. After electroless plating, precipitate appeared in the second bath. Deposition rate recorded in the first bath (1.12 mg/cm^2/h) was faster than that in the second one (0.84mg/cm^2/h). It can be explained by the reaction between cobalt ions and sodium hydroxide, forming precipitate cobalt (II) hydroxide ($Co(OH)_2$). The precipitate decreased the concentration of available cobalt and hence reduced the deposition rate. In the ammonia solution, complex of cobalt ion with ammonia prevented the precipitation of $Co(OH)_2$.

A third and a fourth bathes containing sodium tartrate instead of sodium citrate were prepared. Ammonia and sodium hydroxide were added respectively to adjust the pH to 10. The initial precipitation redissolved after the addition of alkalis. The deposition rate of was 0.16 mg/cm^2/h in the third bath and 0.08 mg/cm^2/h in the fourth.

From the results, it can be seen that the complexing ability of ammonia played an important role. Ammonia can dissolve the precipitate salted out by sodium tartrate while sodium hydroxide cannot. If the concentration of reactant decreased, the reaction rate also decreases. Therefore, sodium citrate and ammonia were chosen form the electroless plating bath that would form $[Co(NH_3)_xCit_y]^-$. Sodium tartrate and sodium hydroxide would not be used in later experiments.

4.1.4 Variation in Lactic acid concentration

Lactic acid concentration was found to affect the deposition rate. The highest deposition rate is 10.6 mg/cm^2/h at 56 ml/L of lactic acid. In this bath, the concentrations of succinic acid was 40 g/L, malic acid was 32 g/L and 1-Phenylthiourea was 1.0 mg/L. Figure 4.3 shows the change of deposition rate against concentration of lactic acid in the bath.

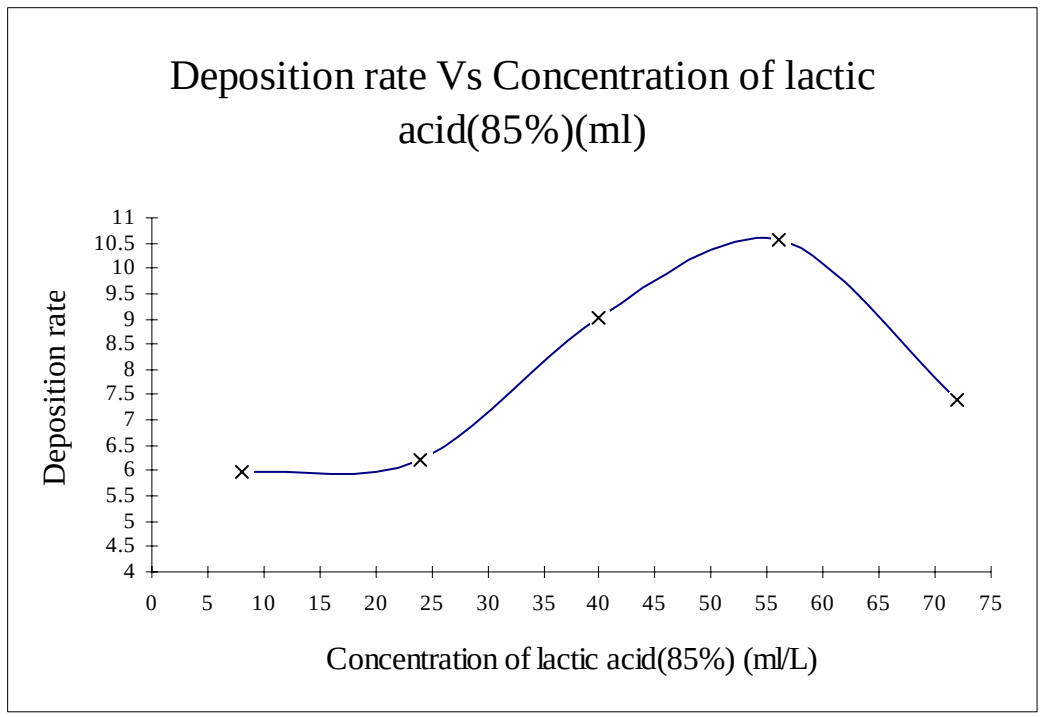

Figure 4.3 Deposition rate against concentration of lactic acid.

The accelerator 1-Phenylthiourea not only increased the deposition rate but also served as a brightener . Sodium citrate was a stabilizer to prevent cobalt ions to from forming precipitate like $Co(OH)_2$ or $Co(HPO_3)$.

4.1.5 Variation of 1-Phenylthiourea concentration

It was found that the most suitable concentration of 1-phenylthiourea is 1.0 mg/L. The deposition rate of Co-W-P alloy is 6.49mg/cm^2/h at this concentration. Figure 4.4 shows the variation of deposition rate against concentration of 1-Phenylthiourea

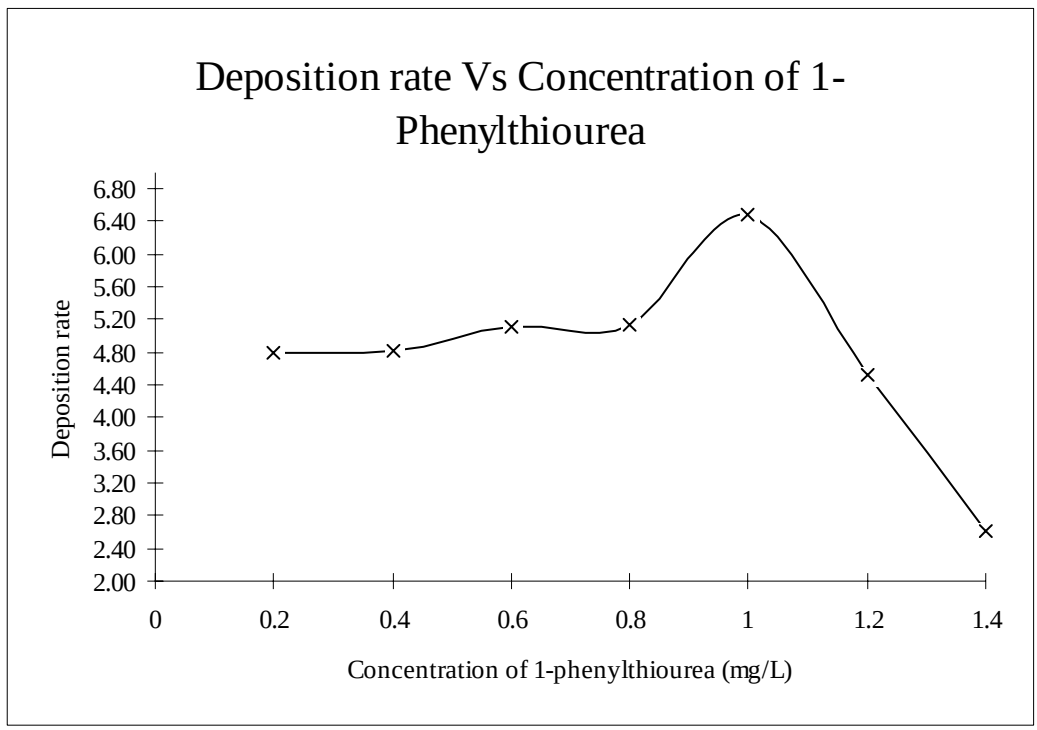

Figure 4.4. Deposition rate against concentration of 1-Phenylthiourea

The deposition rate decreased after reaching the maximum at 1.0 mg/L. Most probably, the accelerator inhibited the reaction that its concentration was too high. If the concentration of 1-phenylthiourea was lowered to less than 1.0 mg/L, the deposition rate remained constant. Thus, the concentration of 1-Phenylthiourea fell within a narrow range for optimum performance of the reaction.

4.1.6 The variation of N-Acethylthiourea

Apart from the accelerators mentioned above, a further adduct, N-acteylthiourea was added 0.5 mg/L and 1.0 mg/L of N-acethylthiourea were added to 2 different baths respectively. There was no bubble evolved and only a very thin coating was formed on the test-plate. Our observations indicated that N-acetylthiourea does not enhance the electroless plating process of Co-W-P alloy.

4.1.7 Buffer salt in the bath.

Ammonia sulfate was added to bath solution containing sodium hydroxide and it acted a media for a solution bath. The result was shown below:

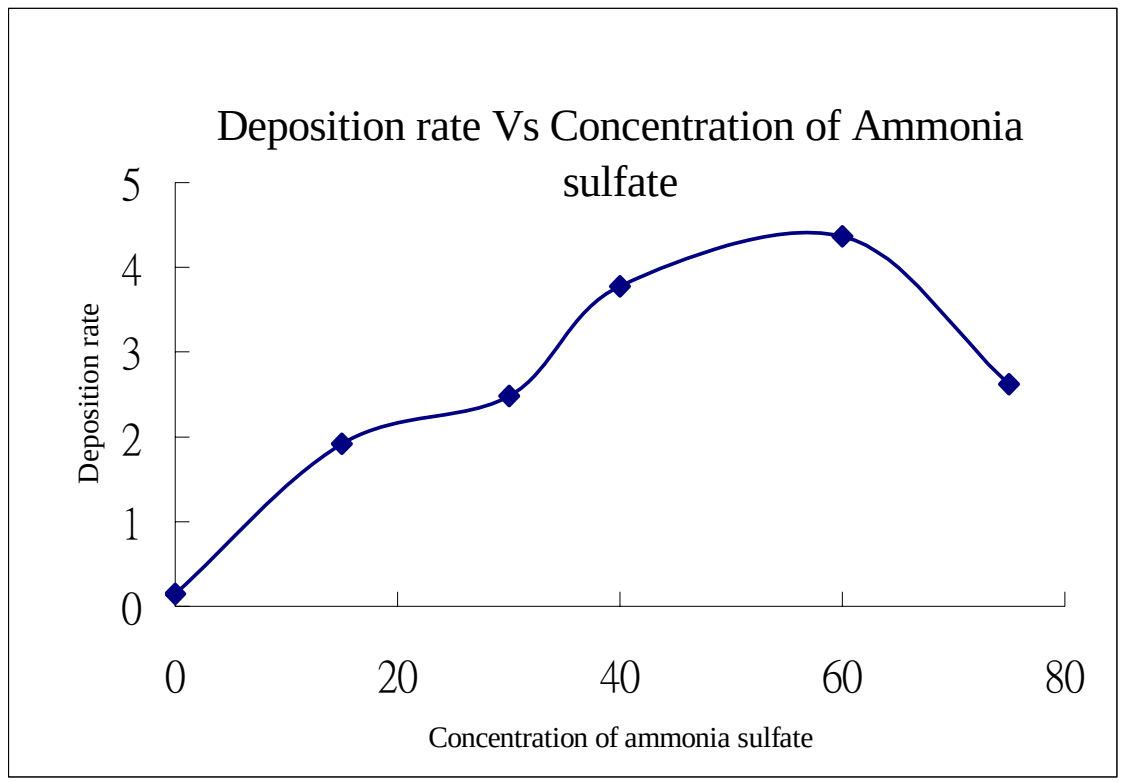

Fig 4.5 Deposition rate against concentration of ammonia sulfate

The ammonium salt acted as a buffer and provided ammonium ion. However, from the result, the deposition rate was not faster than the ammonia formulation after adding the buffer salt to the bath. As a result, ammonium sulfate/ sodium hydroxide formulation would not be used in later part of this research.

From the result of tests performed, the optimal formulation of electroless deposition Co-W-P was, as shown in Table 4.1

Ingredient	Concentration, (g/L)
Cobalt sulfate	35
Sodium tungstate	33
Sodium hypophosphite	45
Succinic acid	40
Malic acid	32
Lactic acid(85%)	56ml/L
Sodium citrate	65
Ammonia	Adjust pH to 10
1-Phenylthiourea	$1x\ 10^{-3}$ g/L
Temperature	95^0C
The Deposition rate	10.6 mg/cm^2/h.

Table 4.1 the optimal formulation of electroless deposition Co-W-P

The deposition rate for this formulation was found to be 10.6 mg/cm^2/h at a bath temperature of 95^{o}C.[54]

4.1.8 Further modification for industrial application

In industrial application, the coating surface needs to be smooth and bright. It should also be produced in low cost. In section 4.1.1-4.1.7, the aim is to optimize the deposition rate. In this section, we concentrate on the appearance of the coating.

4.1.8.1 Malic acid

When 15.0 g/L of malic acid was added to commercial formulation, the deposition rate was 1.55 mg/cm^2/h but the alloy was dull and grey. With a mixture of 20.0 g/L of succinic and 15g/L of malic acid, the deposition rate was 2.56 mg /cm^2/hr. The coated test-plate was duller and whiter than with malic acid alone. When the bath was added with only 20g/L succinic acid, the deposition rate was 1.43 mg/cm^2/h and the coating was white, clear and bright. Based on this performance, malic acid was not recommended in the industrial bath because the dull and Grey coating cannot be used in jewelry intermediate coating (Barrier coating).

The Amount of Additives, g/ml	Deposition Rate mg/cm^2/h	Appearance
15 g of Malic acid	1.55	Dull and gray
15 g malic acid with 20 g of succinic acid	2.56	Dull and white
20 g of succinic acid	1.43	White, clear and bright

Table 4.2 Comparison between adding malic and succinic acid

4.1.8.2 Lactic acid

Lactic acid was utilized extensively in electroless nickel-plating bath. Addition of 8 ml of lactic acid per liter to our electroless Co-W-P bath solution resulted a deposition rate of 10.6 mg/cm^2/hr. The deposition rate increased 1.43 to 4.98 mg/cm^2/h while using 4.18.1 formulation. The deposition rate increased 4-fold after adding 8 mL/L lactic acid and the coated alloy was shinny in the initial plating. However, after the bath worked for several cycles, the coating became worse. The coating was white but dull and the composition of metal varied with the concentration of lactic acid.

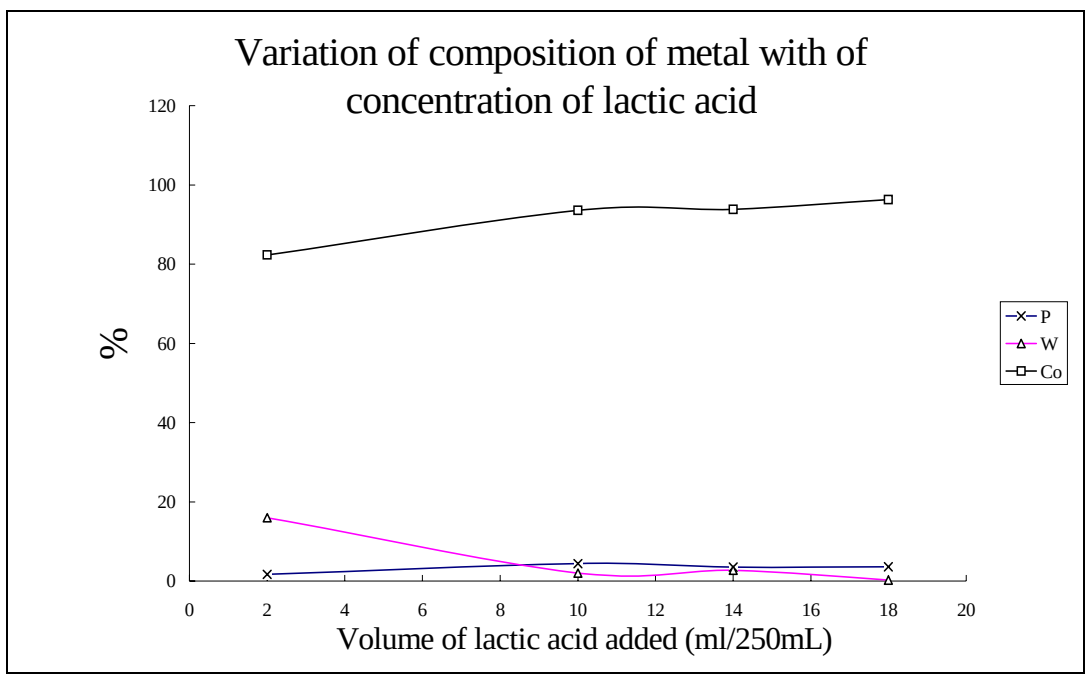

Figure 4.6 Composition of metal in variation of concentration of lactic acid

The metal contents were Co 91.5% P 3.3%, W 5.2% when 32 ml/L lactic acid was used. The phosphorus content was low at the reaction temperature of 95°C. Lactic acid decreased the tungsten concentration in the alloy. Hence, it would not be used in further study.

4.1.9 Addition of wetting agent

The following two images show the action of wetting agent, Y17. 1ml of Y17 was added to a liter of the plating bath. The aim of adding wetting agent was to prevent the formulation of pitting holes.

Figure 4.7, Electromicrogram of Co-W-P without wetting agent

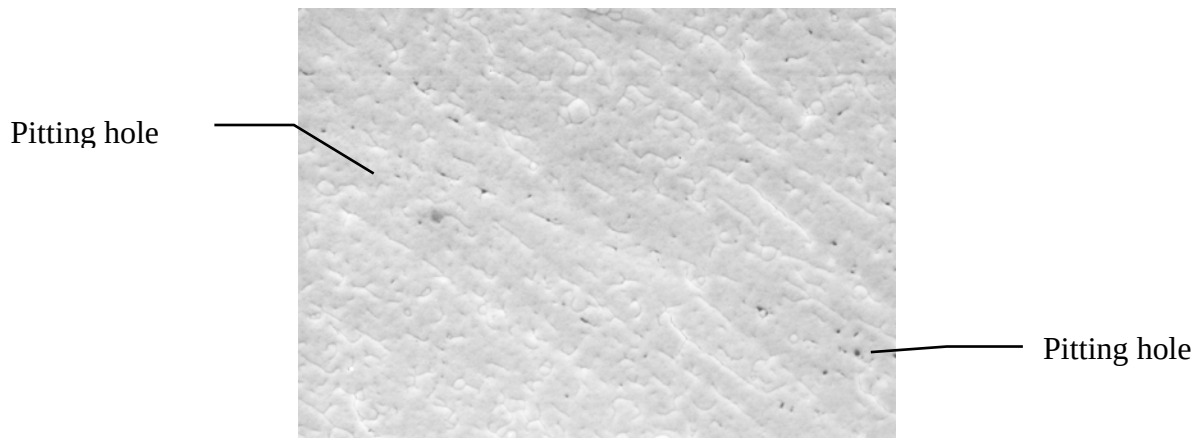

Co90.6%P2.7%W6.7% (1500**X**)

And Figure 4.8, Electromicrogram of Co-W-P with wetting agent

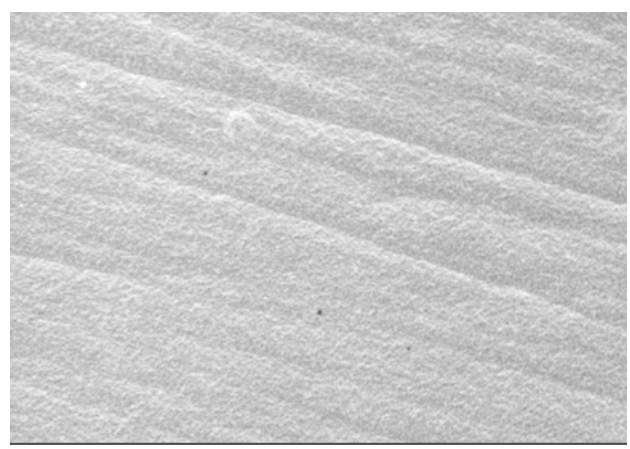

Co86.8%P2.2%W11%(1500**X)**

In conclusion of the proceeding studies, the final formulation for electroless deposition of Co-W-P was Cobalt sulfate 35g/L, Sodium tungstate 33g/L, Sodium hypophosphite, 45g/L, Succinic acid 40g/L, Sodium citrate 65g/L, 1-Phenylthiourea 1mg/L and 1 ml/L of Y-17 wetting agent.

From the result of EDAX, the metal content of the deposited Co-W-P alloy was Co 88%, W 8% and 4% Phosphorus. The Deposition rate for the above formulation is 4.0 mg/cm^2/hr at the reaction temperature of 95^{o}C.

Ingredient	Concentration, (g/L)
Cobalt sulfate	35
Sodium tungstate	33
Sodium hypophosphite	45
Succinic acid	40
Sodium citrate	65
Ammonia	Adjust pH to 10
1-Phenylthiourea	1x 10^{-3} g/L
Y-17 Wetting agent	1 ml/L
Temperature	95^{0}C
The Deposition rate	4.0 mg/cm^2/h.

Table 4.3 the formulation of electroless plating Co-W-P for industrial application

4.20 Optimization of tungsten content using orthogonal experiment design

The Optimization of tungsten content of Electroless Plating of Co-W-P was achieved by orthogonal experiment design.

The L_{25} (5^6) orthogonal table was used. The experiment design was shown as below:

Table: The factors and levels of electroless plating bath of Co-W-P in orthogonal experiment design.

Factor	1 Cobalt Sulphate (mol dm^{-3})	2 Sodium Tungstate (mol dm^{-3})	3 Sodium Hypophosphite (mol dm^{-3})	4 Sodium Citrate (mol dm^{-3})	5 Succinic Acid (mol dm^{-3})	6 Temp (°C)	7 1-Phenylthiourea (mol dm^{-3})
Level 1	0.075	0.05	0.375	0.25	0.30	75	5×10^{-6}
Level 2	0.125	0.10	0.425	0.3	0.35	85	8.5×10^{-6}
Level 3	0.175	0.15	0.475	0.35	0.45	95	1.2×10^{-5}

Table 4.4 Effect of factors affecting the on Tungsten and Phosphorus content in coating for electroless plating bath.

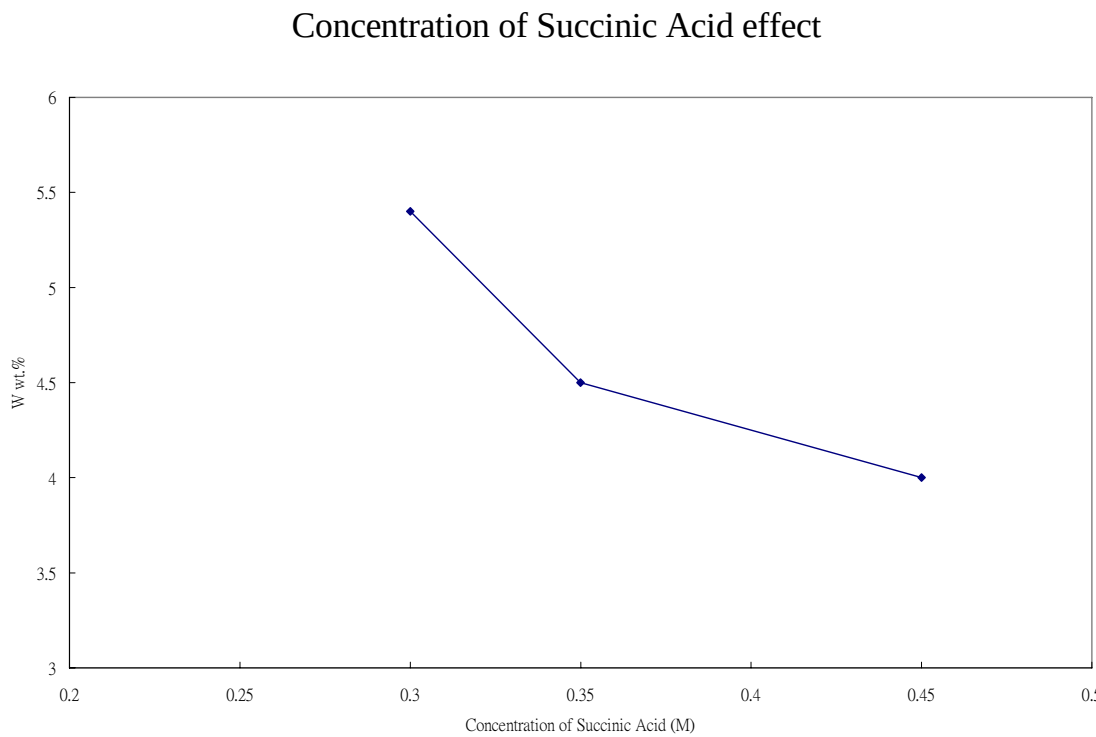

Fig 4.9 Concentration of Succinic acid effect

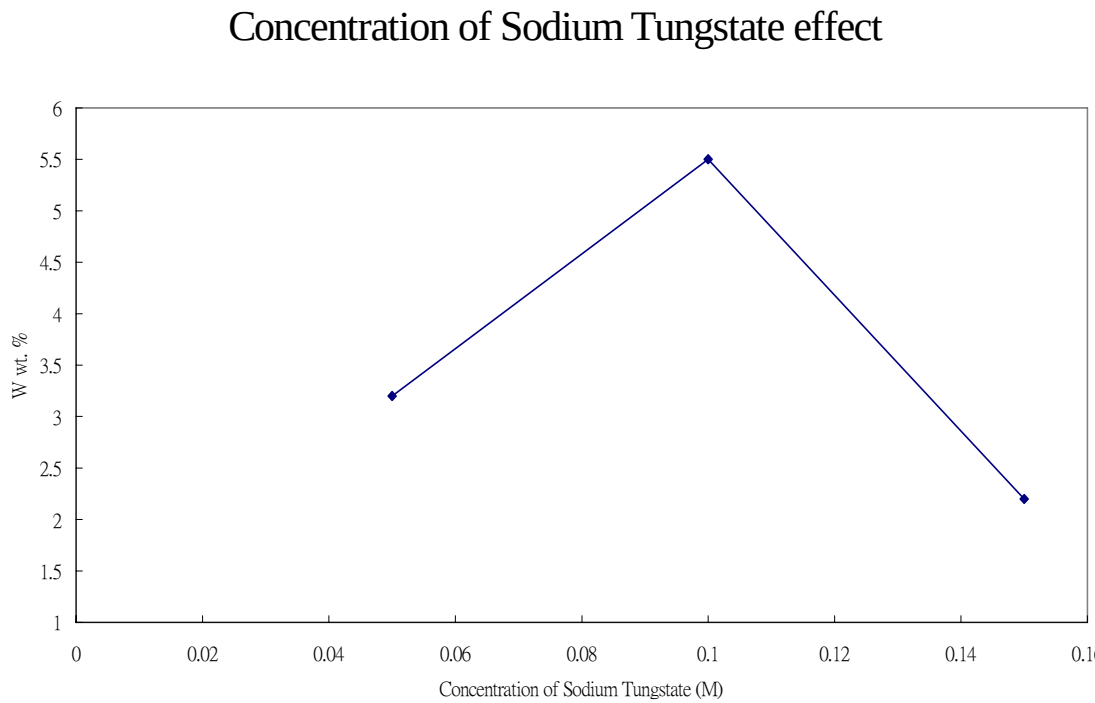

Fig 4.10 Concentration of Sodium Tungstate [15] effect

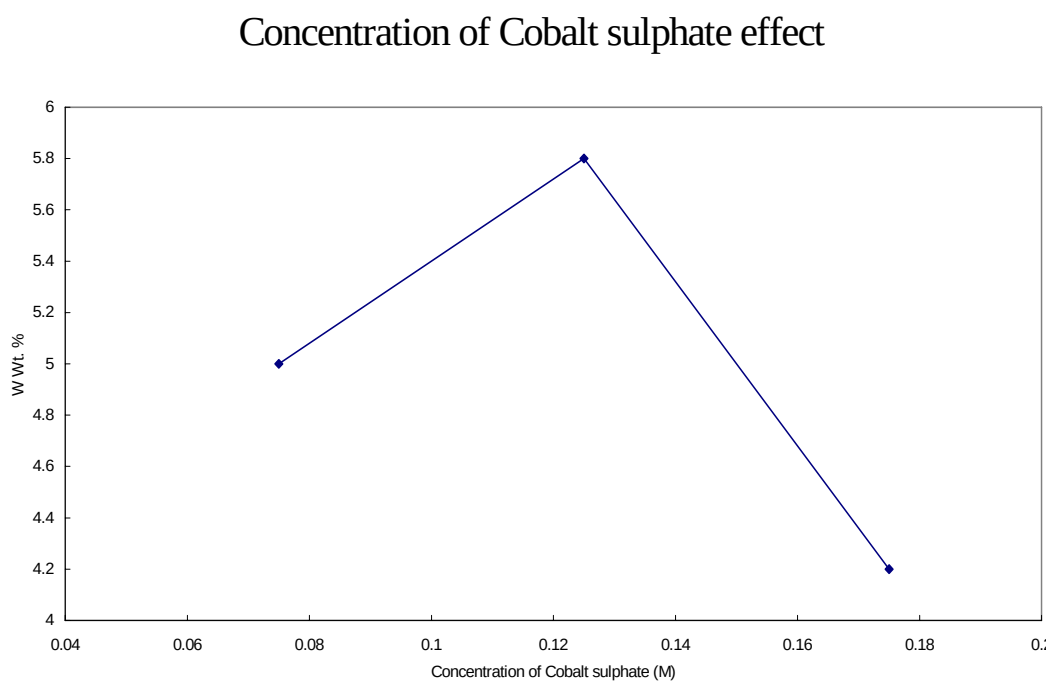

Fig 4.11 Concentration of Cobalt Sulphate effect

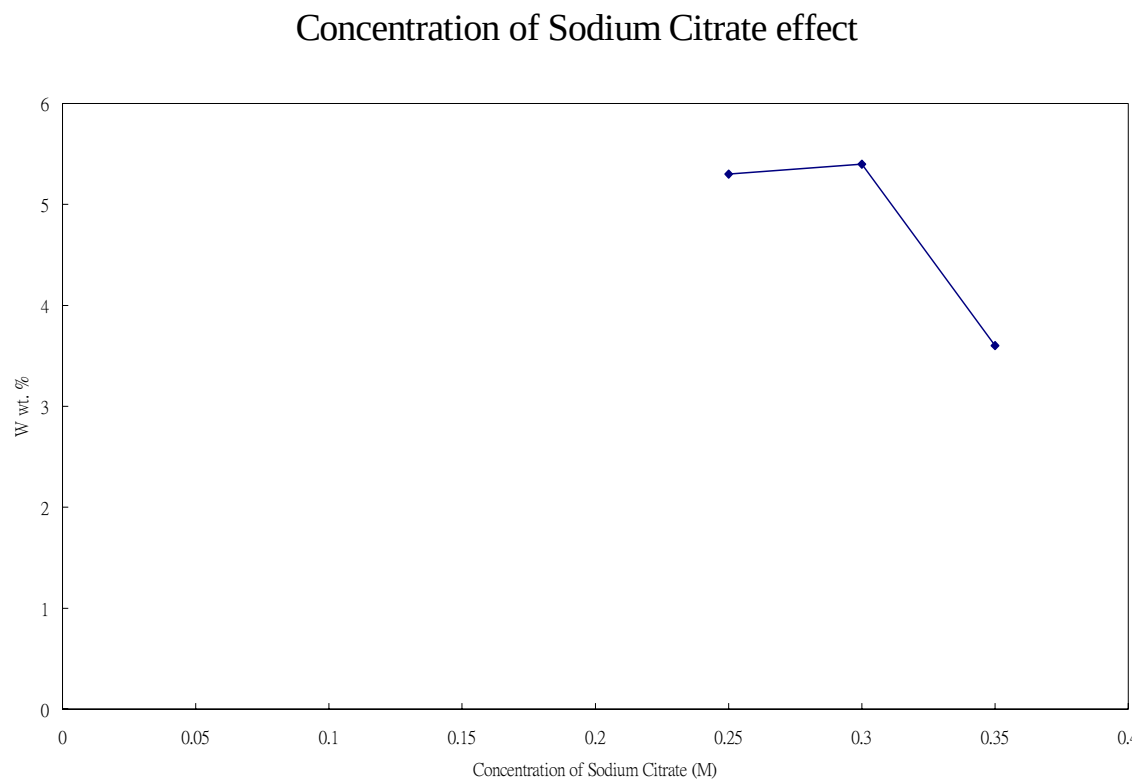

Fig 4.12 Concentration of Sodium Citrate effect

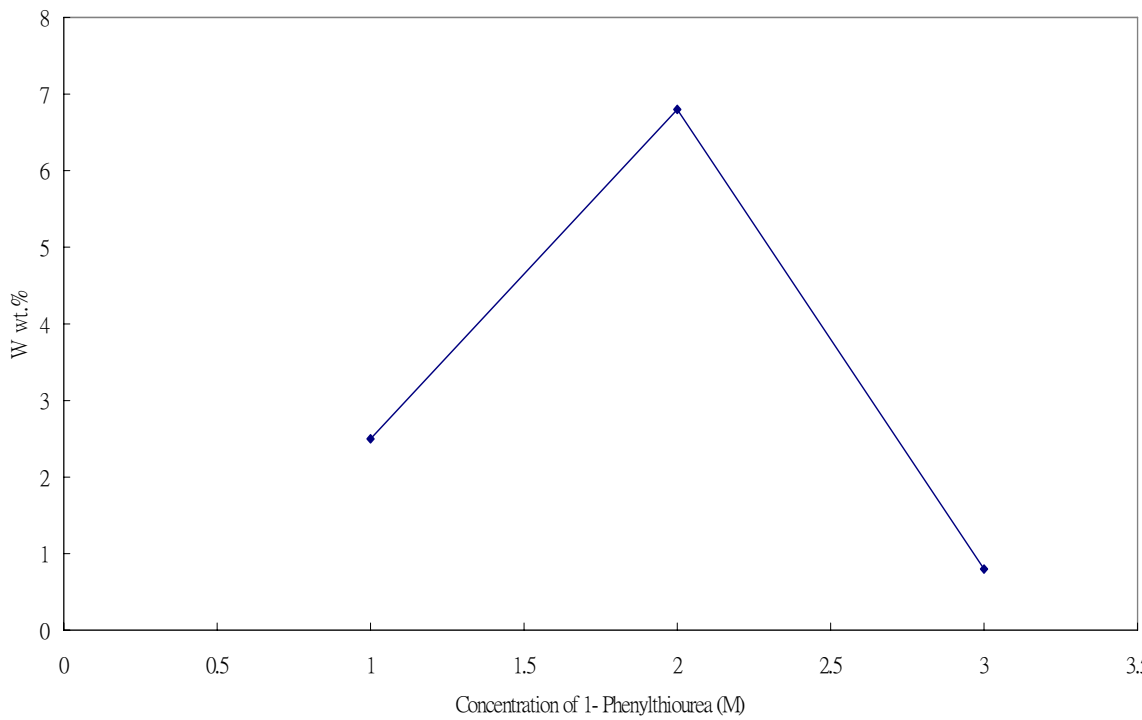

Fig 4.13 Concentration of 1- Phenylthiourea effect

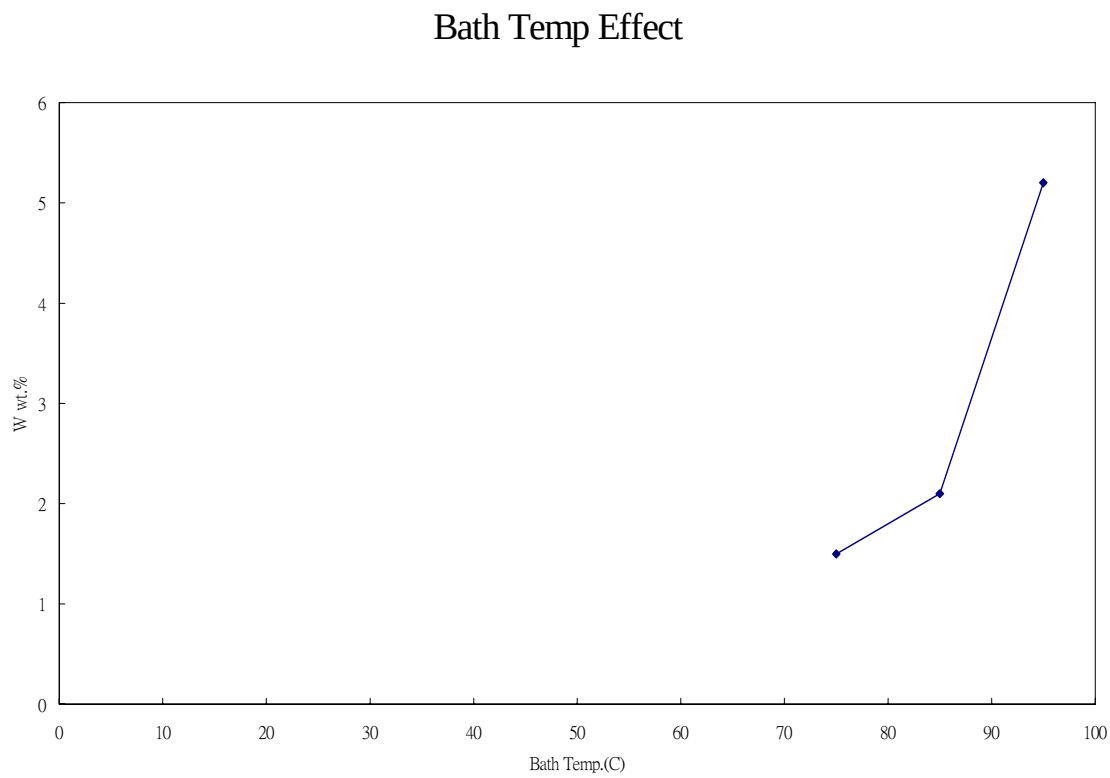

Fig 4.14 Concentration of Temperature effect

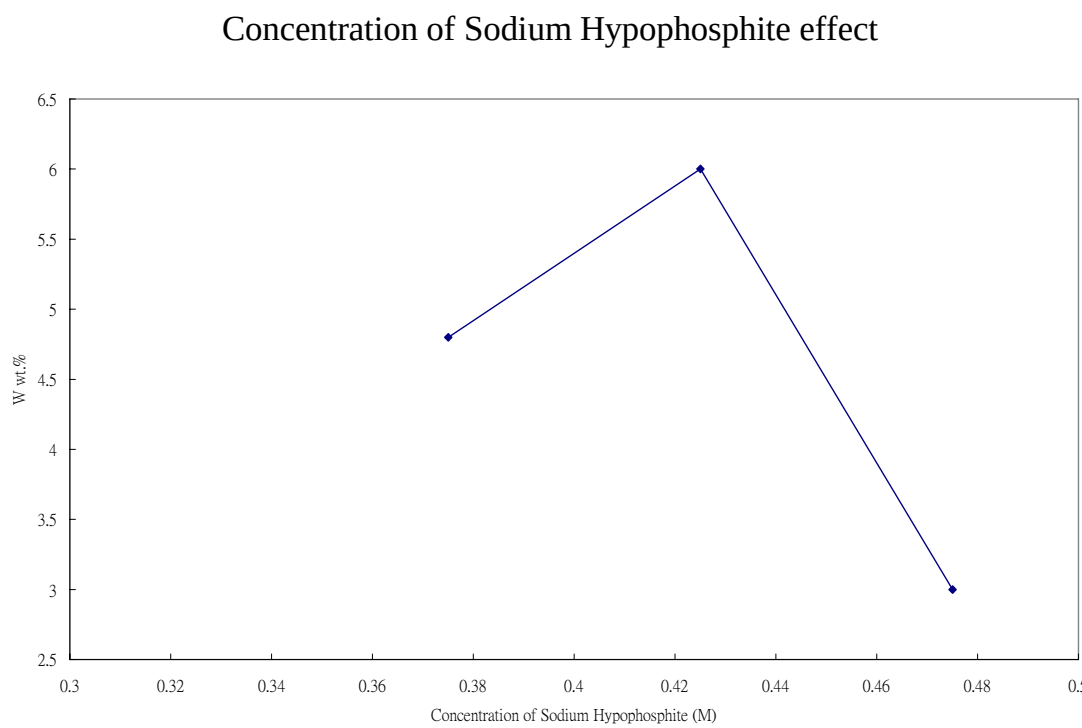

Fig 4.15 Concentration of Sodium Hypophosphite effect

After eighteen experiments, the best combination of each factor is shown below:

Cobalt (II) Sulphate	0.125 M
Sodium Tungstate	0.100 M
Sodium Hypophosphite	0.425 M
Sodium Citrate	0.300 M
Succinic Acid	0.300 M
1-Phenylthiourea	8.5×10^{-6} M
Temperature	95°C

Table 4.5 Result of the Orthogonal Experiment Design

Using the optimized formulation, a Co-W-P with 8.0 wt.% W, 4.0 wt.% P was produced. The test-plate in the experiments had bright and smooth coating. The deposition rate of this bath was 5.8 mg/cm^2/hr. This deposition rate was lower than the one with other accelerators added, which was 10.57 mg/cm^2/hr. However, this bath with higher deposition rate was not as stable as the optimized formulation. This formulation was used for producing test-plates for subsequent diffusion studies.

4.2 Investigation of electroplating of Co-W alloy

The electroless plating process has a better throwing power than electroplating. However, the deposition rate is too slow for industrial mass production. As a result, the method had to be modified. Electroplating is a good method for improving the deposition rate because it does not require a reducing agent and uses a lower temperature than electroless plating. We will use Hull cell experiments to achieve an optimized bath solution. For the hull cell setup, please refer to chapter 2.4 and 3.3

4.2.1 Variation of cobalt sulfate concentration

The starting formulation was $CoSO_4$ (10g/L), sodium tungstate (68g/L), citrate acid (65g/L), and EDTA (30 g/L), and the pH was adjusted to 7 with ammonia. The concentration of cobalt sulfate was varied from 10 to 50 g/L. From result of the hull cell test, the lower limit of current density was 1A/dm^2in the range of 10g/L to 30 g/L cobalt sulfate. For 40g/L and 50g/L, the plating range was wider and the whole test-plate was coated in the hull cell experiment.

The range of cobalt sulfate in the Co-W alloy electroplating formulation requires further studies because we have not yet found the optimal concentration.

4.2.2 Variation of EDTA concentration

The concentration of EDTA added to the solution ranged from 10g/L to 50g/L. Based on the EDAX result, the tungsten and cobalt content in the plated layer against EDTA content in bath was shown as below,

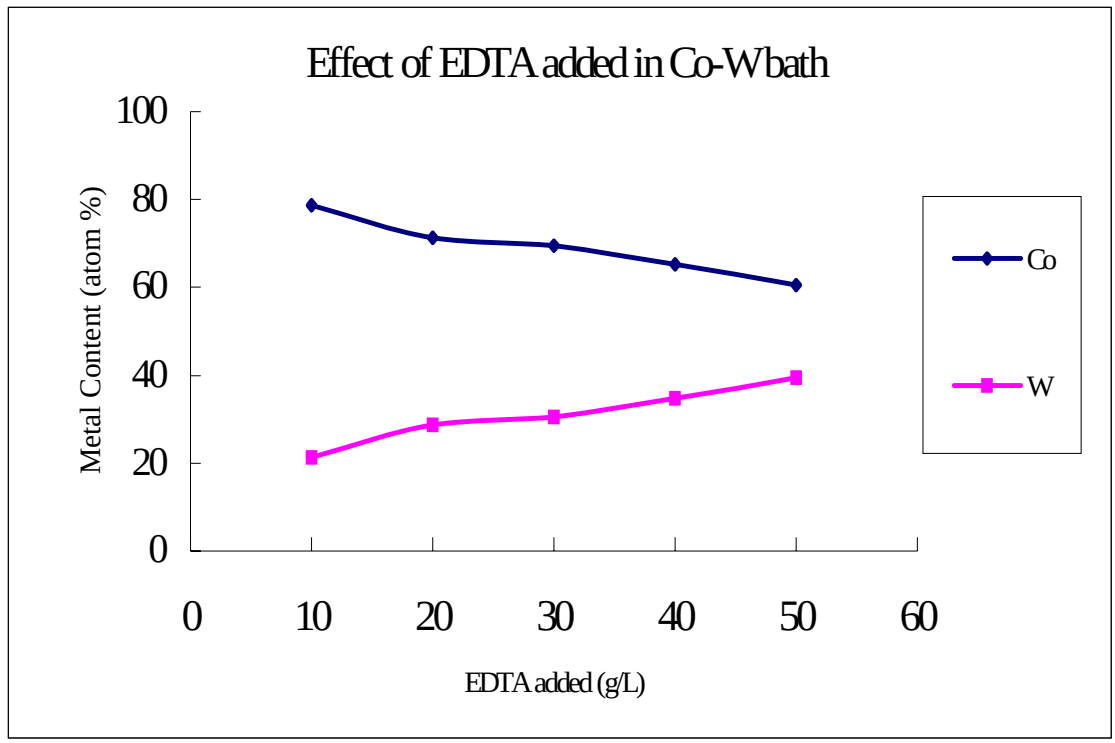

Fig 4.16 The effect of EDTA content in Co-W bath

The result indicated that as the EDTA content increased, the tungsten content in the coating also increased.

4.2.3 The surface morphology of alloy coating.

The coating surface was different for high current density and low current density. It is shown below,

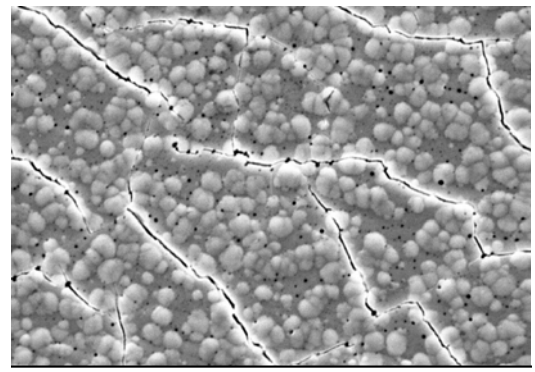

Fig. 4.17 High Current Density (6A/dm^2), Co 65.0%, W35.0%, 5000x

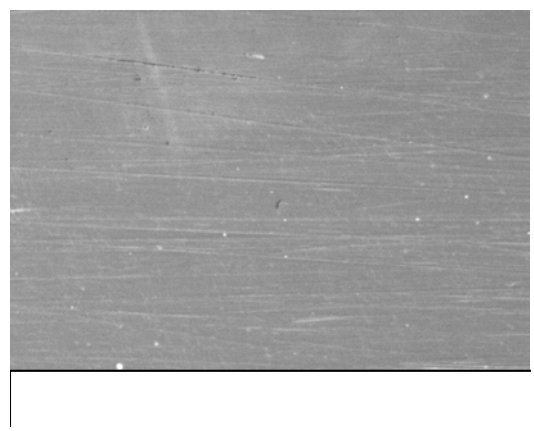

Fig. 4.18 Low Current Density (1A/dm^2), Co 68.2%, W31.8%, 5000x

Many cracks and white ball were seen in figure 4.17 and fig 4.18 showed a smooth surface. The cracks may be caused by the internal stress of the coating. And the 'white ball' was the combination of crystalline and non-crystalline structure. There were many gaps and roughs.

The following two figures, fig. 4.19 and 4.20, showed the different on plate surface before and after exposure to atmosphere for 3 months.

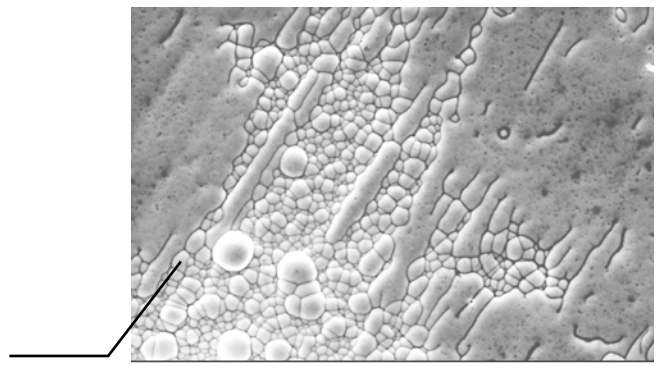

Fig. 4.19 Electromicrogram of fresh plated surface (1500X), Co93.2%P3.2%W3.6%(1500**X**)

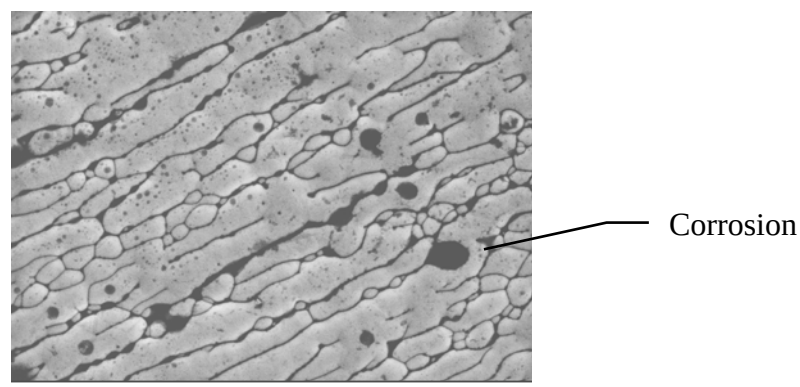

Fig 4.20 Electromicrogram of plated surface after exposing to atmosphere for 3 months Co93.2%P3.2%W3.6%(1500**X**)

Cracks appeared in the electroplated layer and gap appeared in electroless plating. If a passive layer can be formed on the surface [46], the coating can be protected. In this case, the passive film cannot be formed perfectly on the surface to resist corrosion and the surface corroded. The electroplated Co-W layer was deposited at 0.2μm/ mins at $2A/dm^2$.

4.3 Investigation of electroplating of Co-W-P Alloy

The electroplating of Co-W-P was studied and the base formulation for electroplating Co-W-P was cobalt sulfate 20g/L, Sodium tungstate 20 g/L, $Na_2H_2PO_2$ 25g/L, Sodium citrate 41 g/L, Succinic acid 20g/L and Temperature 60°C. The content of each ingredient would be modified to study the effect of the coating.

4.3.1 Change in Sodium citrate content

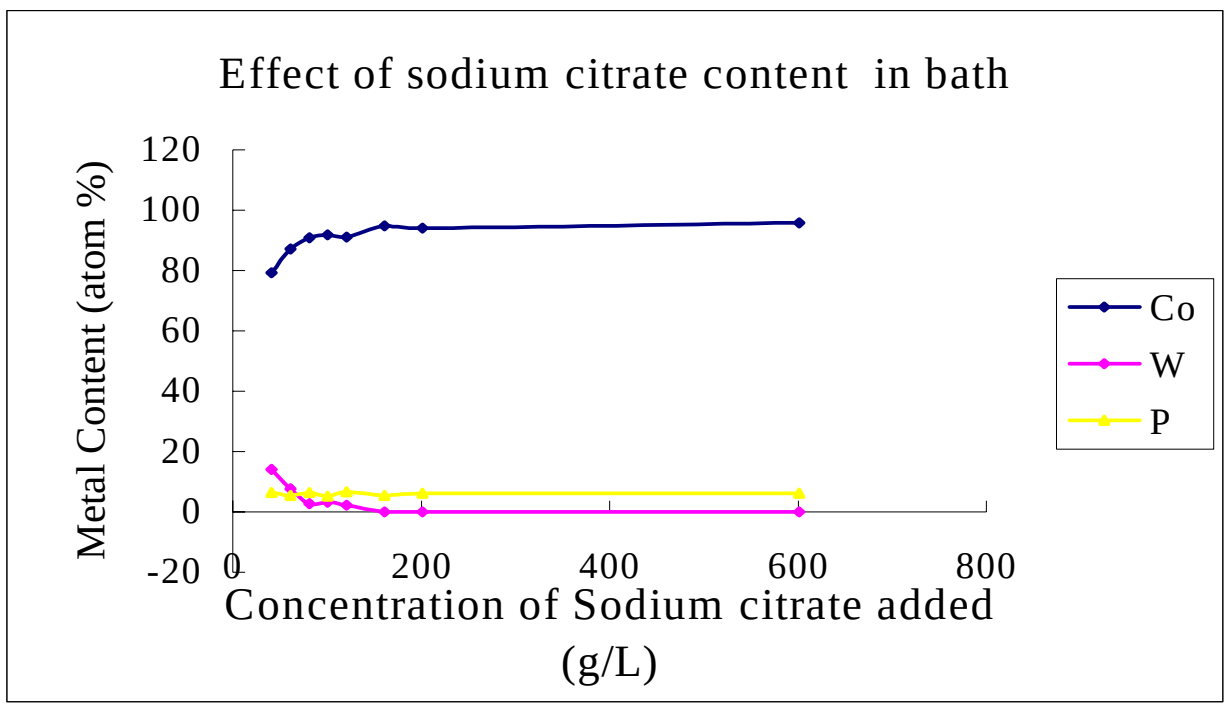

Fig 4.21 The effect of sodium citrate content in the bath.

Form figure 4.21, it can be seen that the tungsten content in coating decreased when the sodium citrate content increased. Sodium citrate can form complex with tungstate ion (WO_2^-) tightly and prevent the absorption of WO_2^- onto the surface of anode. As a result, tungsten was not found in the coating.

4.4 The Diffusion Experiments

The procedure refer to chapter 3.5

4.4.1 Copper/Barrier System

4.4.1.1The Cu/Ni System

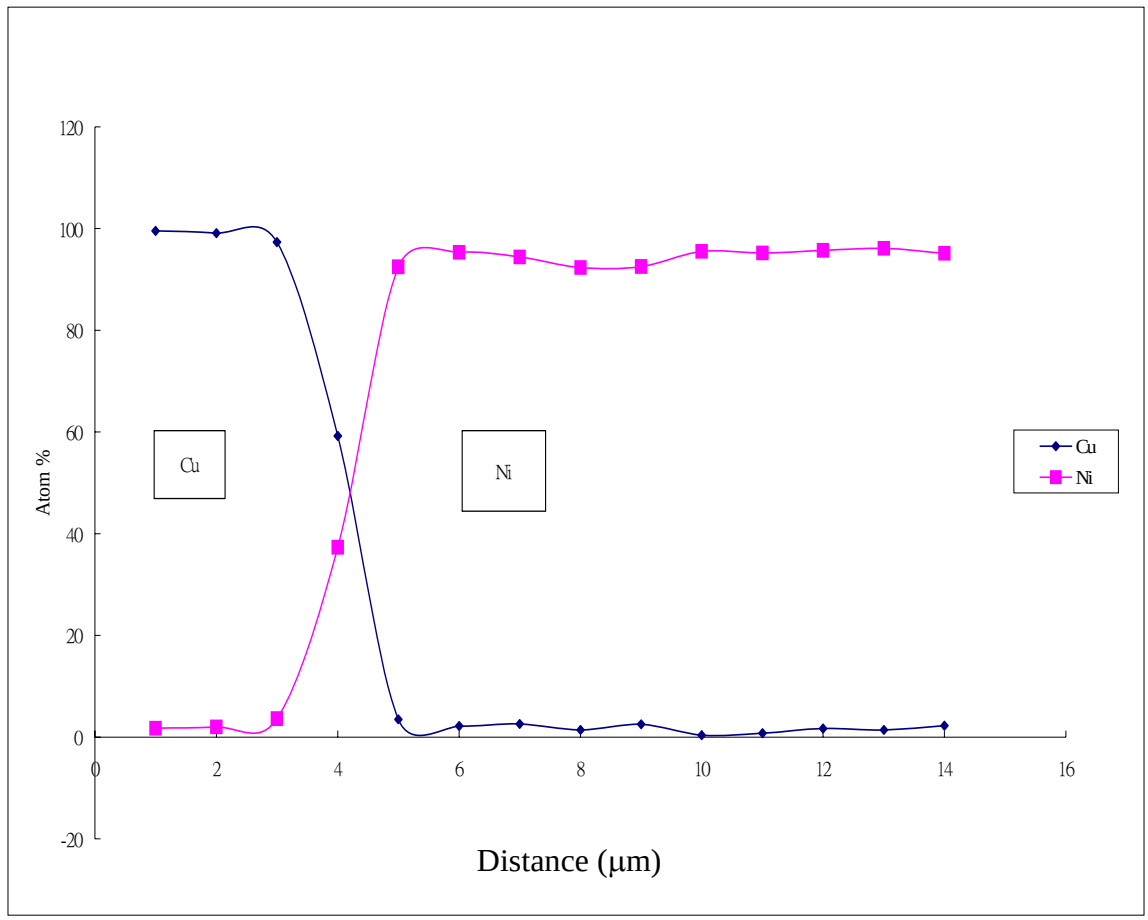

Figure 4.22 Concentration- Distance Profile of Cu/Ni system after heat treatment at 400^{o}C for 168hrs.

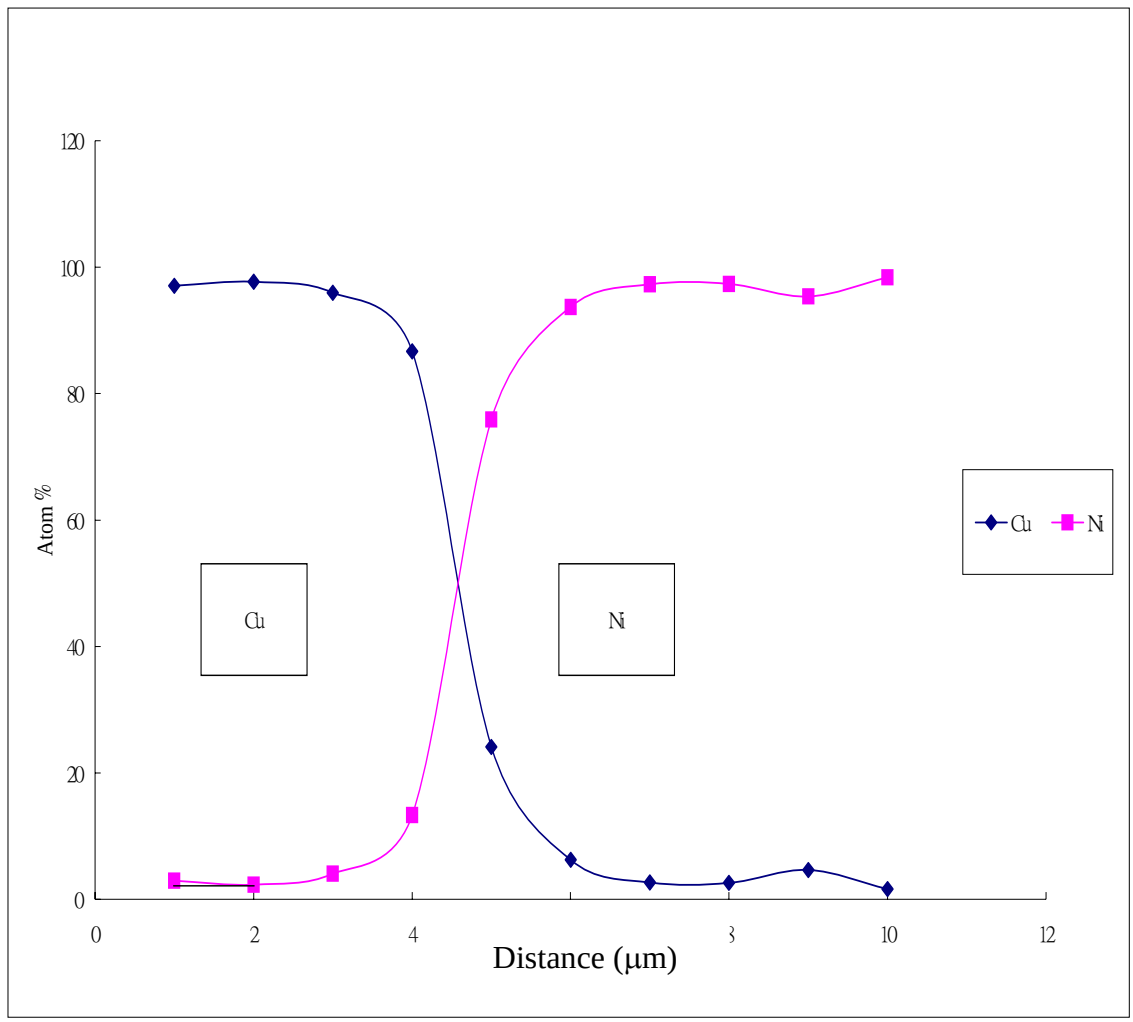

Figure 4.23 Concentration- Distance Profile of Cu/Ni system after heat treatment at 500^{o}C for 72hrs.

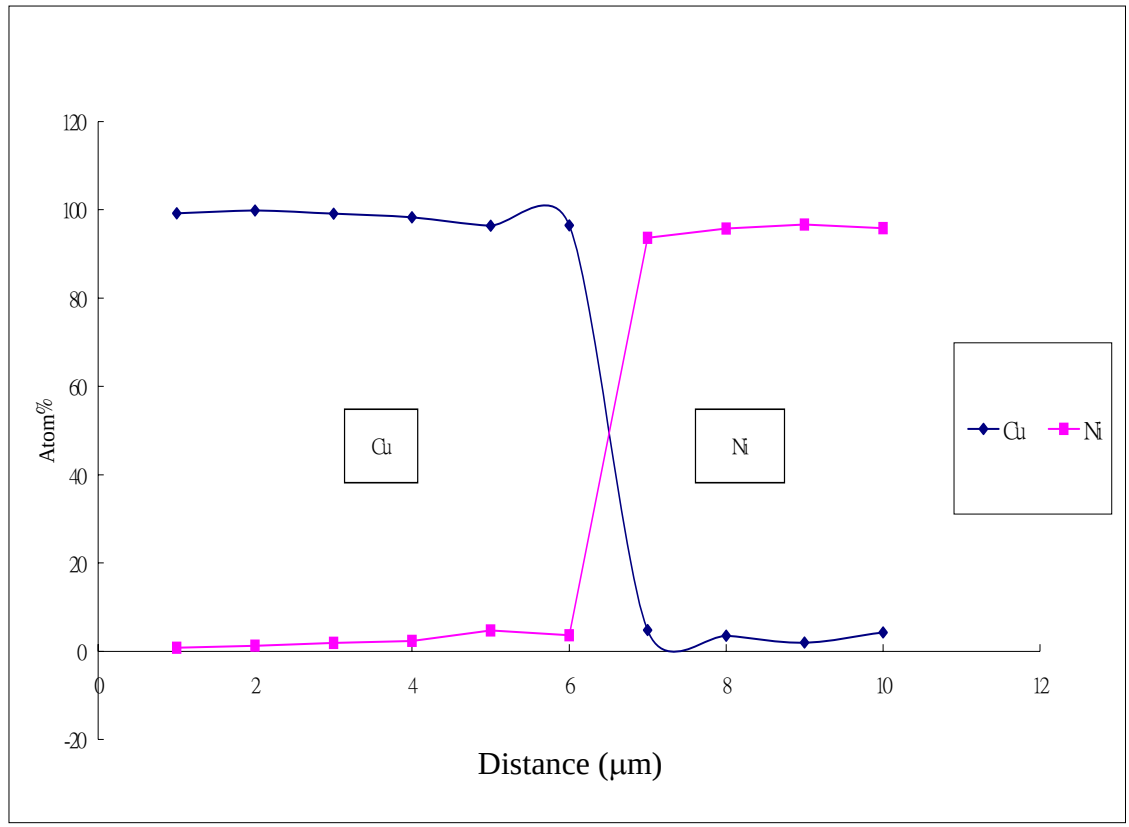

Figure 4.24 Concentration- Distance Profile of Cu/Ni system after heat treatment at 600^{o}C for 24hrs.

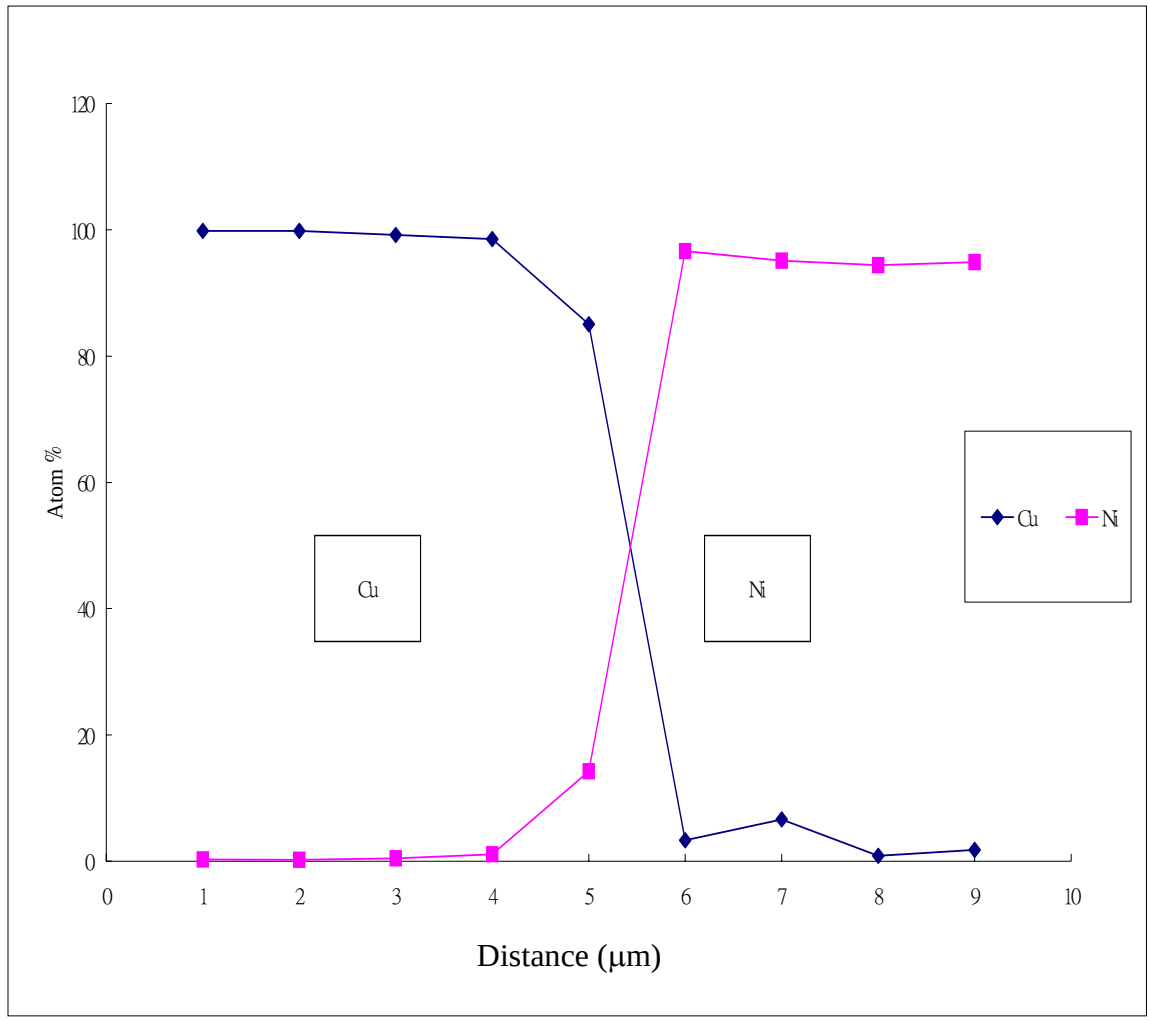

Figure 4.25 Concentration- Distance Profile of Cu/Co-W system after heat treatment at 700^{o}C for 3hrs.

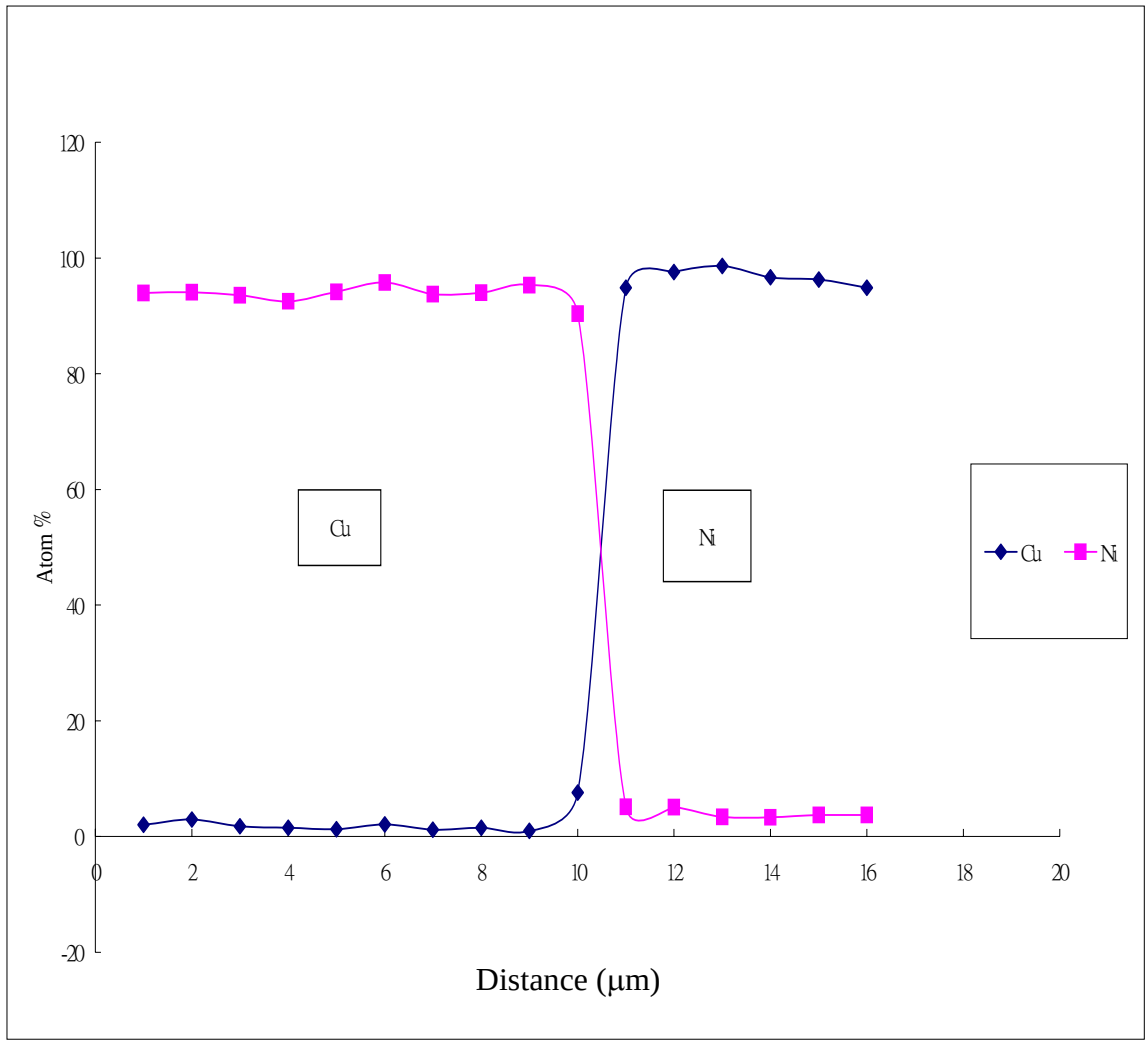

Figure 4.26 Concentration- Distance Profile of Cu/Ni system after heat treatment at 800^{o}C for 0.75hrs.

Temperature of Heat Treatment	Heating Time (hr)	D (cm2/s)			
		20% Cu	40% Cu	60% Cu	80% Cu
400	168	6.253×10^{-15}	8.522×10^{-15}	9.533×10^{-15}	1.086×10^{-15}
500	72	9.523×10^{-14}	8.996×10^{-14}	9.231×10^{-14}	1.032×10^{-14}
600	24	2.322×10^{-13}	2.536×10^{-13}	3.230×10^{-13}	3.865×10^{-13}
700	5	1.935×10^{-13}	2.236×10^{-13}	3.339×10^{-13}	7.562×10^{-13}
800	0.75	9.902×10^{-12}	9.223×10^{-12}	9.563×10^{-12}	9.755×10^{-12}

Table 4.6 Interdiffusion Coefficients of Cu/Ni System at Different Temperature and copper concentration calculated by Boltzmann-Matano Method

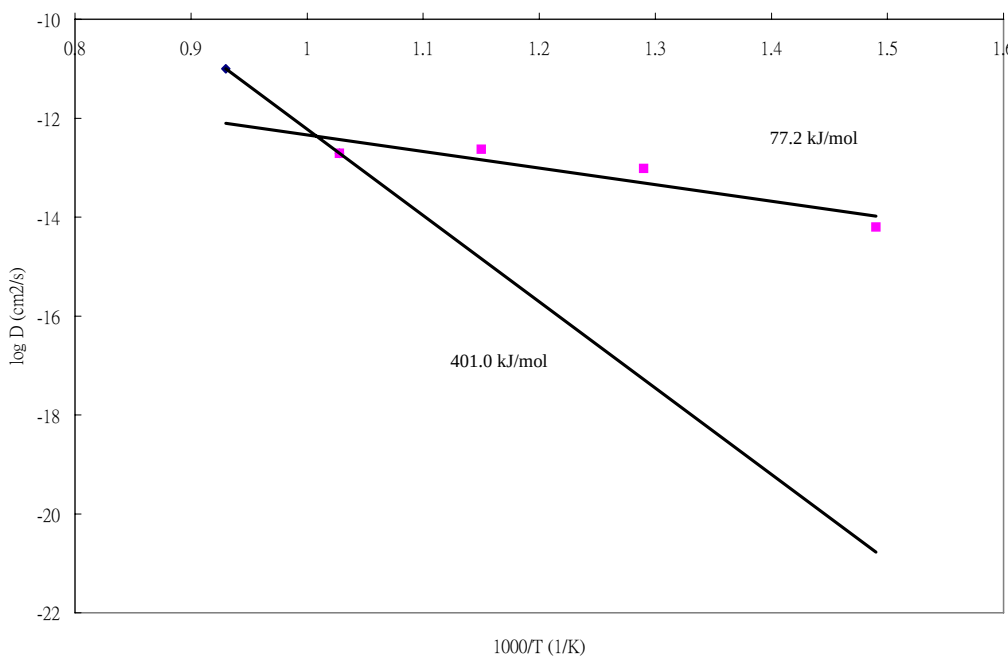

Fig 4.27 The Arrhenius plot of diffusivities at 20 % copper in Cu/Ni system

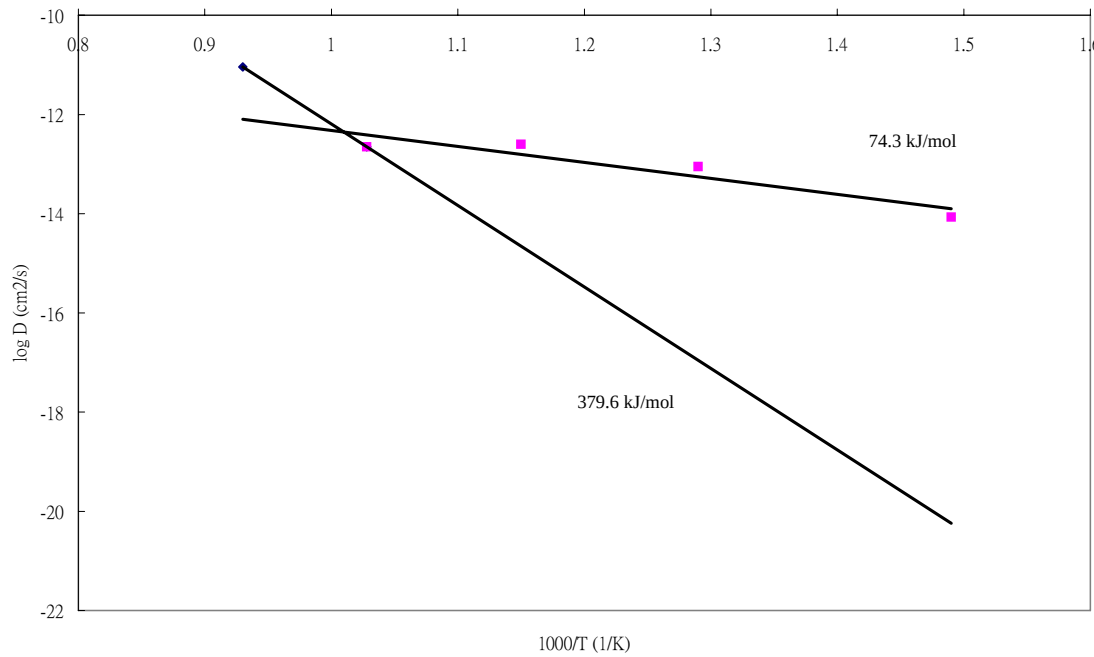

Fig 4.28 The Arrhenius plot of diffusivities at 40 % copper in Cu/Ni system

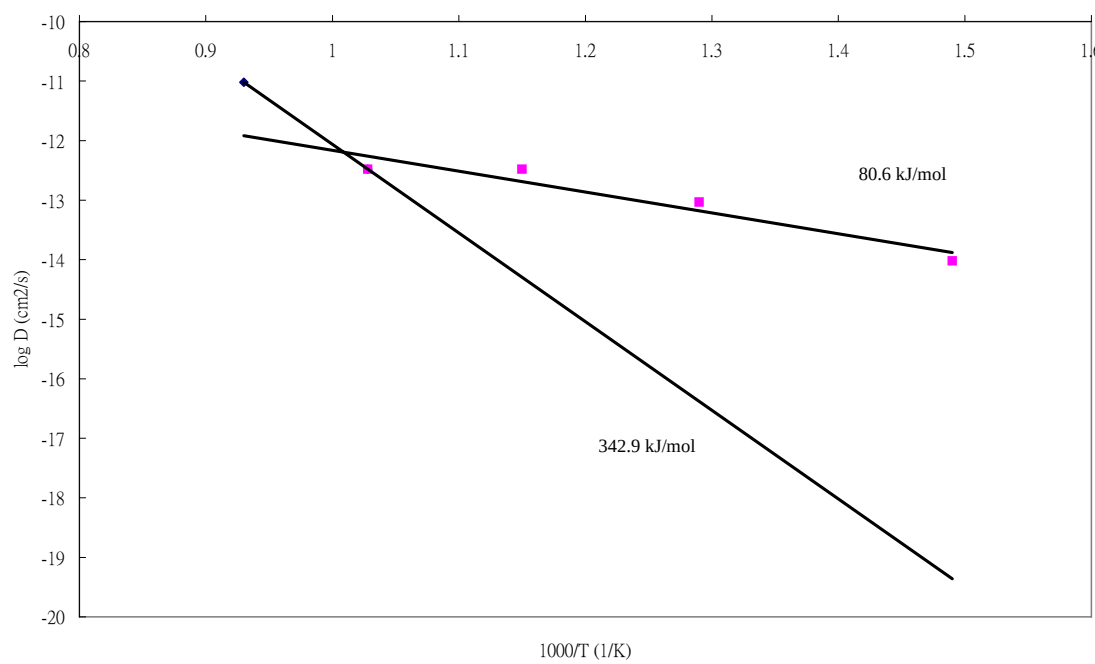

Fig 4.29 The Arrhenius plot of diffusivities at 60 % copper in Cu/Ni system

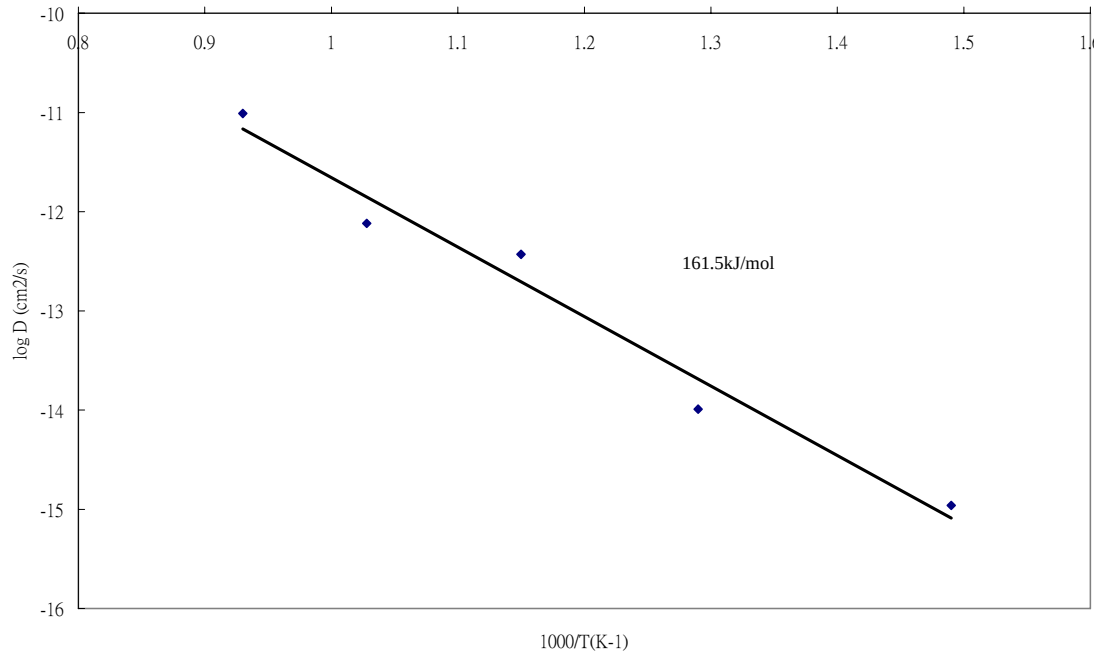

Fig 4.30 The Arrhenius plot of diffusivities at 80 % copper in Cu/Ni system

The above data were collected at four different percentages of copper atoms. Fig 4.27 to 4.29 showed similar results and Fig 4.30 was a straight line. It was observed that there was a transition region in Fig 4.27-4.29 that represented two different forms of diffusion occurring in the three environment. Diffusion was divided into two paths, lattice diffusion and volume diffusion. At low temperature, the lattice diffusion was usually dominant and the activation energy was lower. On the contrary, volume diffusion is predominant at high temperature and measured a higher energy value.

The data was calculated using Arrhenius equation $D = D_o exp(-Q/RT)$, where Do was the frequency factor, Q, the apparent activation energy for diffusion and R, the gas constant 8.32

$Jmol^{-1}K^{-1}$. In mid temperature range of 400 ^{o}C to 700 ^{o}C, all data was found to have decrease a lot from the higher temperature (800^{o}C), indicating that low temperature diffusion mechanism predominated.

Apparent activation energy for diffusion were calculated for Fig 4.26 to Fig 4.29. Referring to chapter 2.7.and 3.5, the value of Q decreases from 401.0 to 161.5 $kJmol^{-1}$ when the copper concentration increased from 20 to 60% in high temperature range. In mid temperature range, the value was similar except in 80 %, which should no transition region in the temperature range.

4.4.1.2 Copper /Co-W-P

The Figure below showed the concentration-distance profile at the diffusion zone of Cu/Co-W-P system under a heat treatment temperature range from 400°C to 800°C. The interdiffusion coefficients of Cu/Co-W-P were listed in Table 4.6

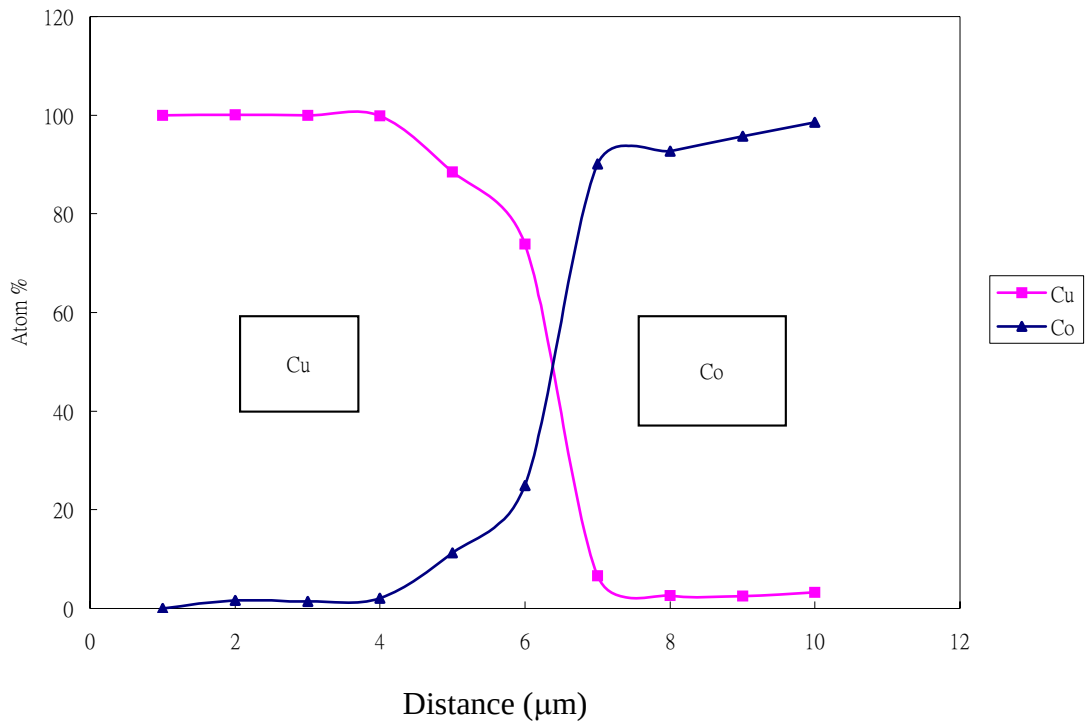

Figure 4.31 Concentration- Distance Profile of Cu/Co-W-P system after heat treatment at 400°C for 168hr.

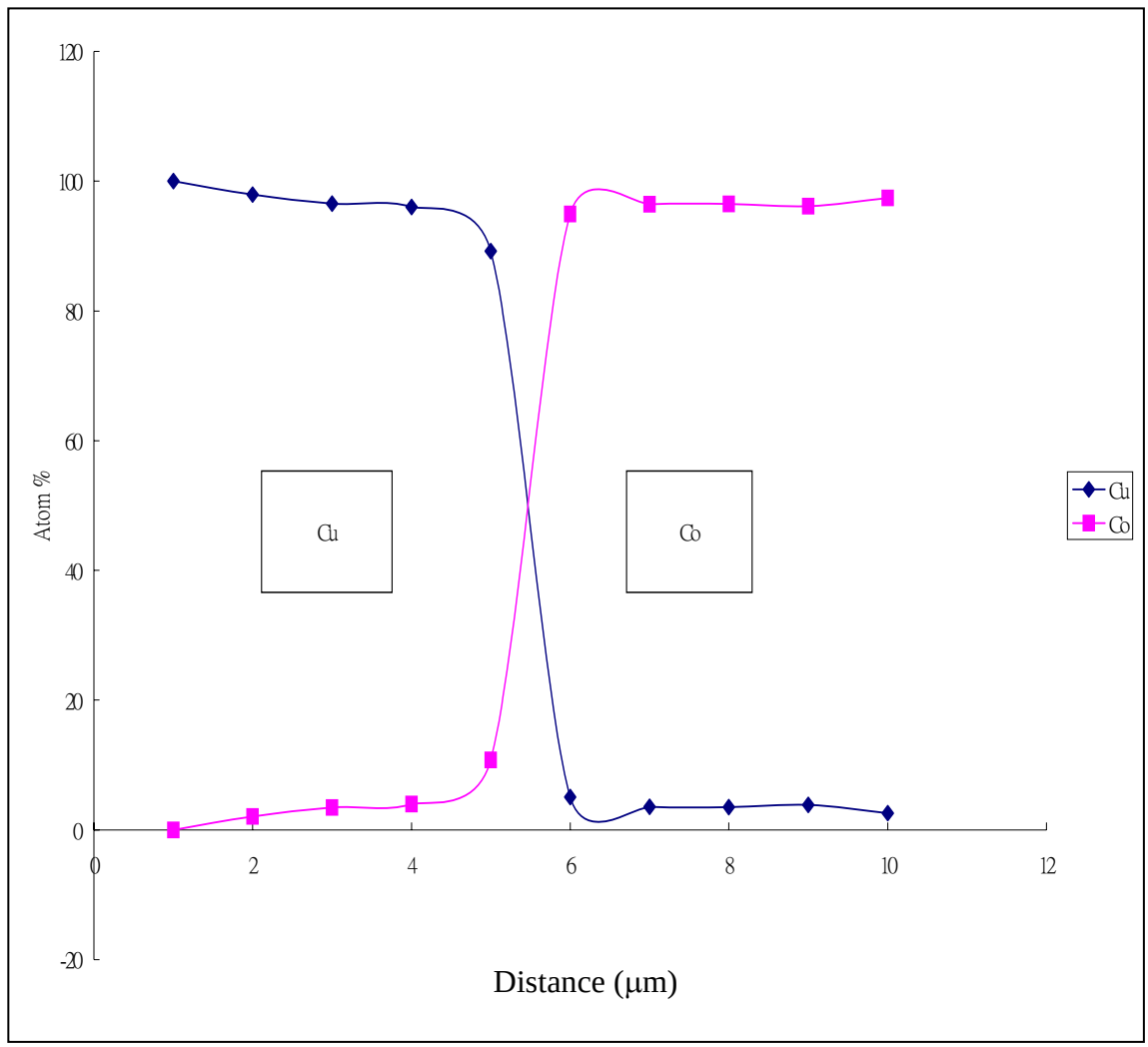

Figure 4.32 Concentration- Distance Profile of Cu/Co-W-P system after heat treatment at 500^{o}C for 72hr.

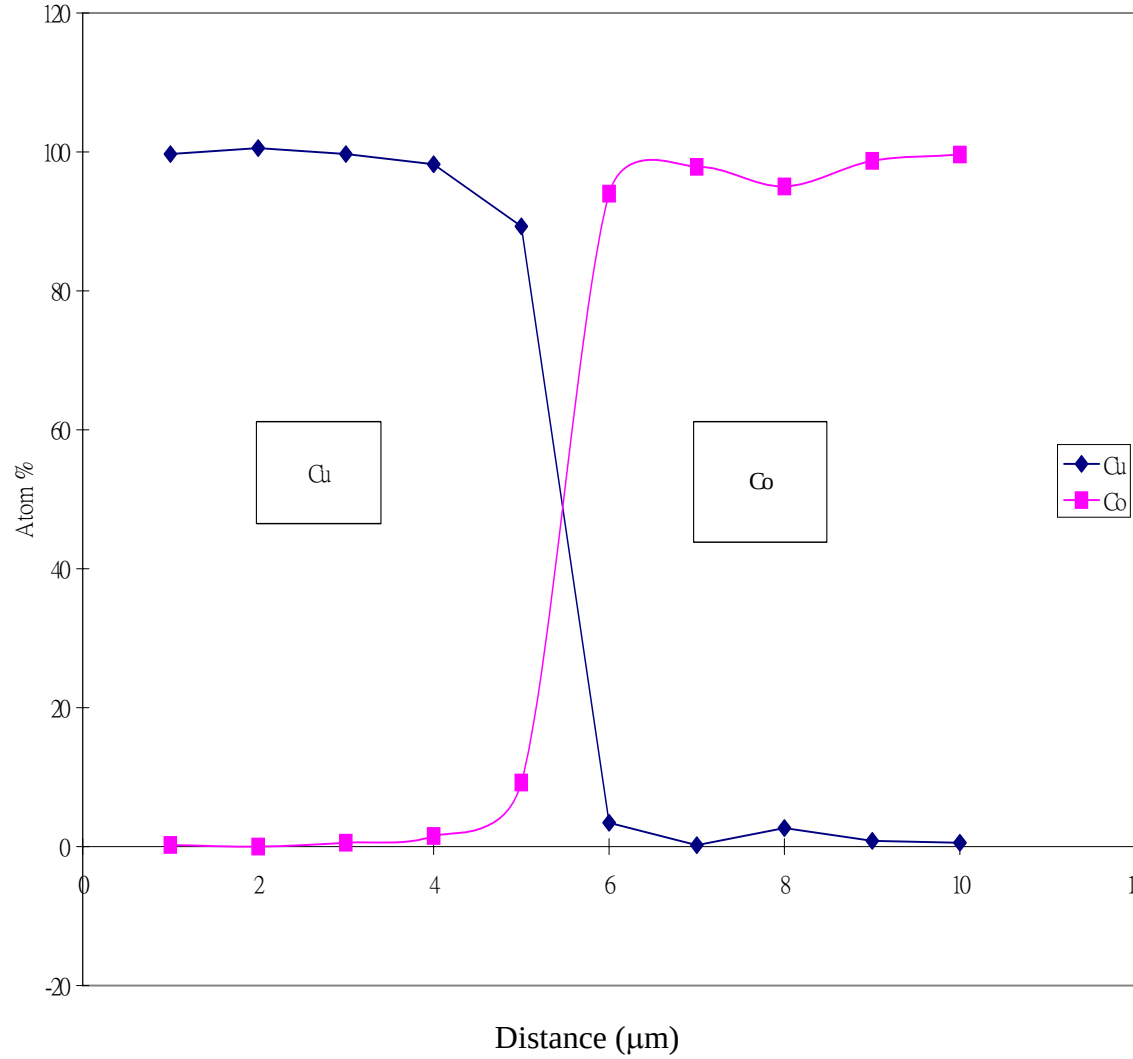

Figure 4.33 Concentration- Distance Profile of Cu/Co-W-P system after heat treatment at 600^{o}C for 24hrs.

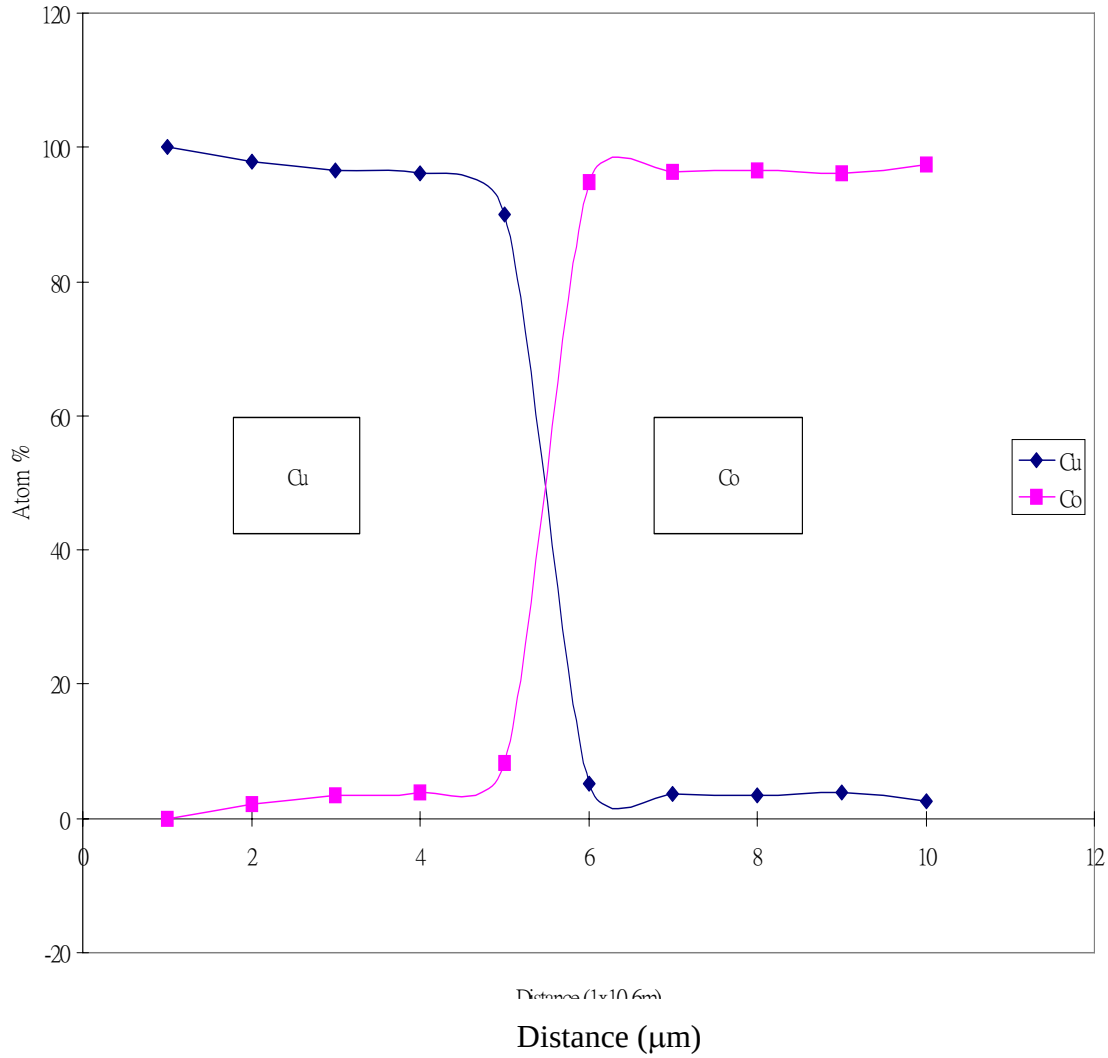

Figure 4.34 Concentration- Distance Profile of Cu/Co-W-P system after heat treatment at 700^{o}C for 3hrs.

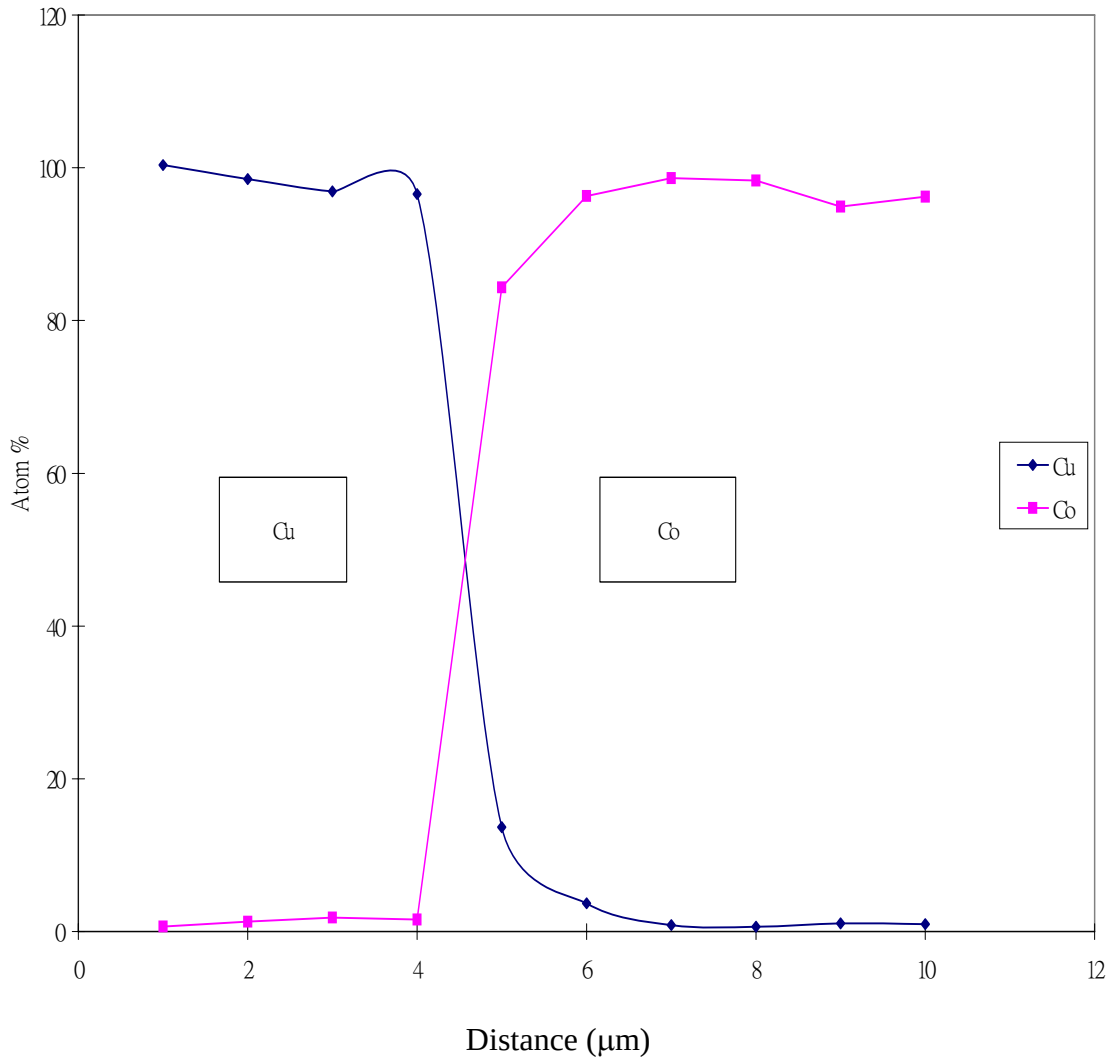

Figure 4.35 Concentration- Distance Profile of Cu/Co-W-P system after heat treatment at 800^{o}C for 0.75hr.

Temperature of Heat Treatment	Heating Time (hr)	D (cm^2/s)			
		20% Cu	40% Cu	60% Cu	80% Cu
400	168	3.881×10^{-15}	4.326×10^{-15}	5.411×10^{-15}	7.653 × 10-15
500	72	1.689×10^{-15}	1.925×10^{-15}	4.058×10^{-15}	5.522 ×10-15
600	24	4.522×10^{-15}	8.935×10^{-15}	1.235×10^{-14}	1.563 ×10-14
700	5	4.432×10^{-14}	4.233×10^{-14}	4.425×10^{-14}	4.386 ×10-14
800	0.75	$7.432 \times^{-13}$	8.935×10^{-13}	8.991×10^{-13}	9.863 ×10-13

Table 4.7 Diffusion Coefficient of Cu/Co-W-P system at different temperature and copper concentration calculated by Boltzmann-Matano Method

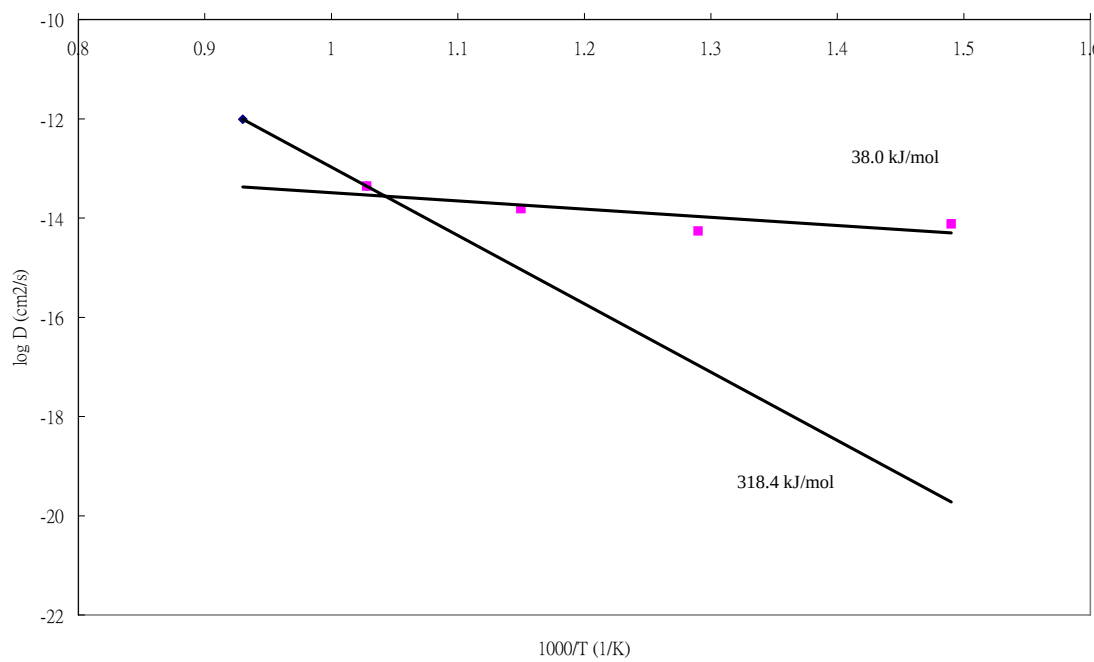

Fig 4.36 the Arrhenius plot of diffusivities at 20 % copper in Cu/Co-W-P system

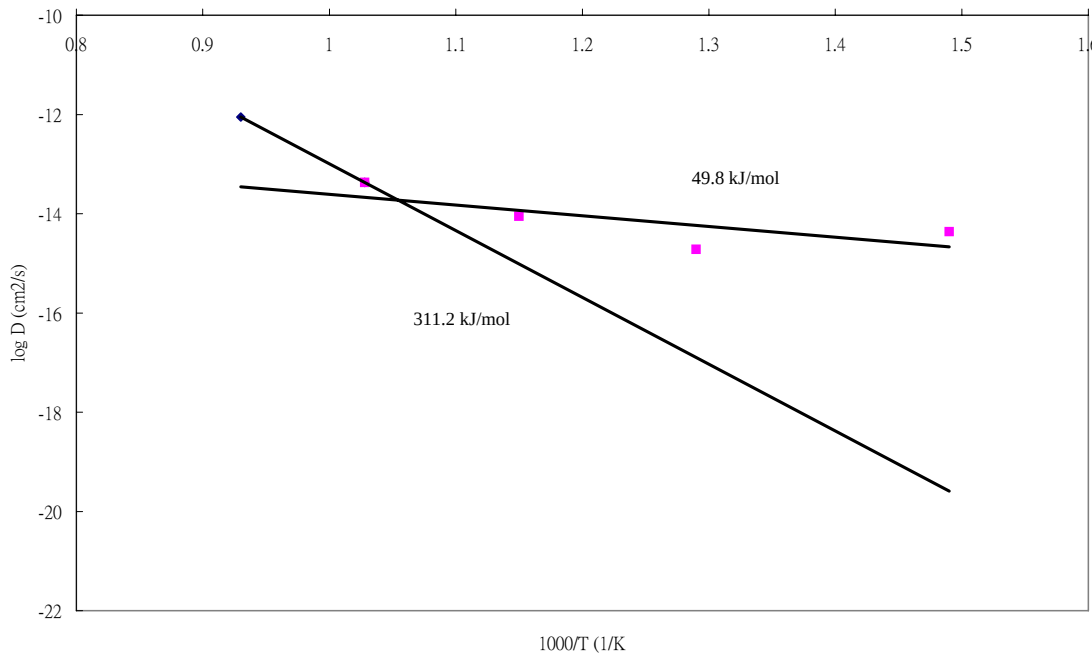

Fig 4.37 The Arrhenius plot of diffusivities at 40 % copper in Cu/o-W-P system

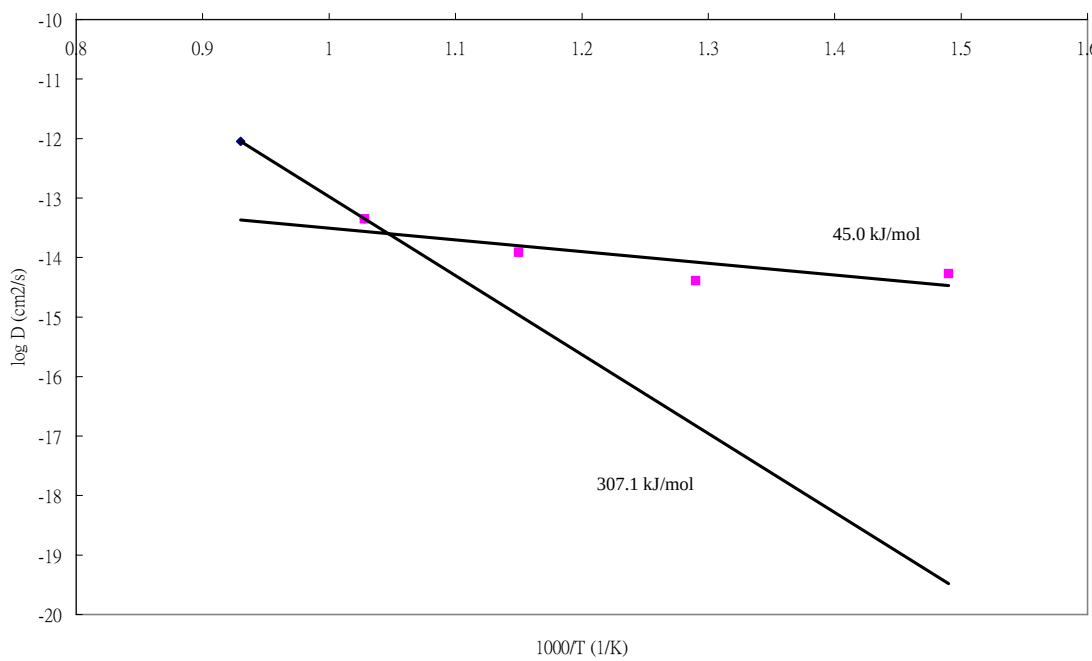

Fig 4.38 The Arrhenius plot of diffusivities at 60 % copper in Cu/Co-W-P system

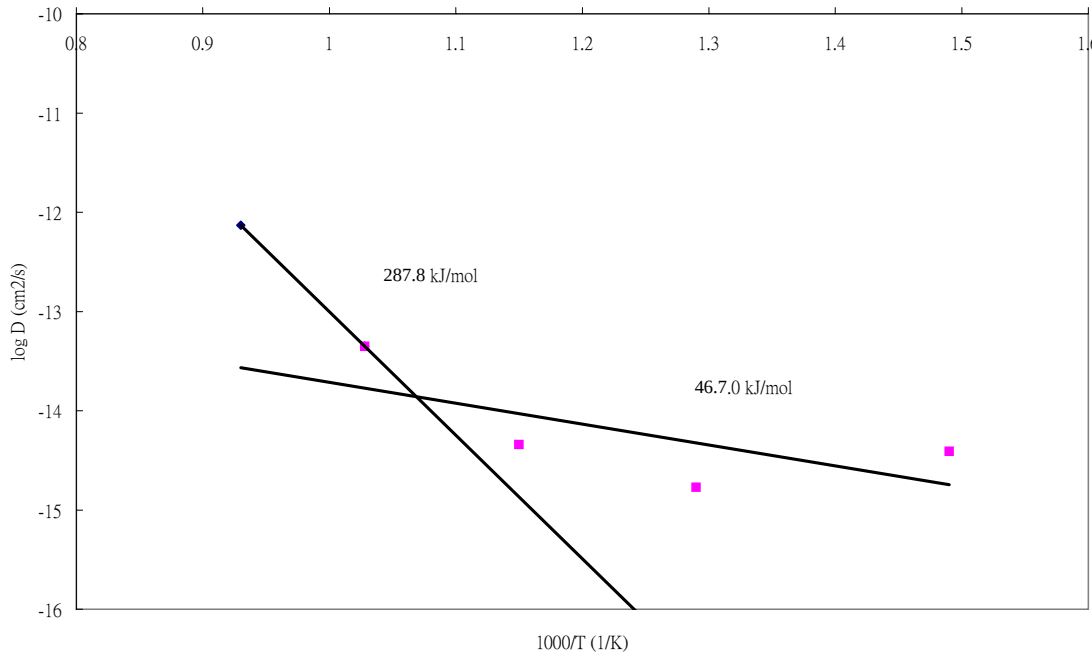

Fig 4.39 The Arrhenius plot of diffusivities at 80 % copper in Cu/Co-W-P system

The Apparent activation energy for diffusion Q increased from 318.4 kJ/mol to 287.8kJ/mol as the copper concentration increased from 20% to 80%.

4.4.1.3 Copper/Co-W

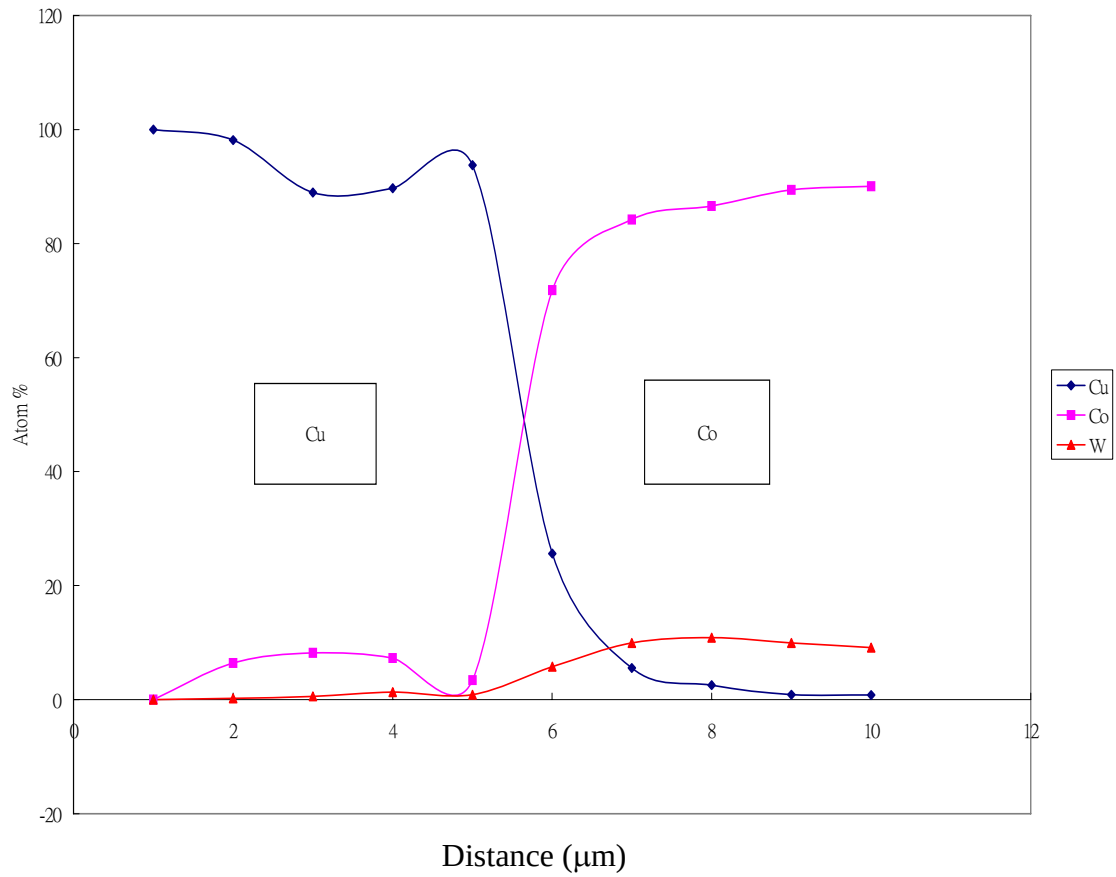

Figure 4.40 Concentration- Distance Profile of Cu/Co-W system after heat treatment at 400^{o}C for 168hrs.

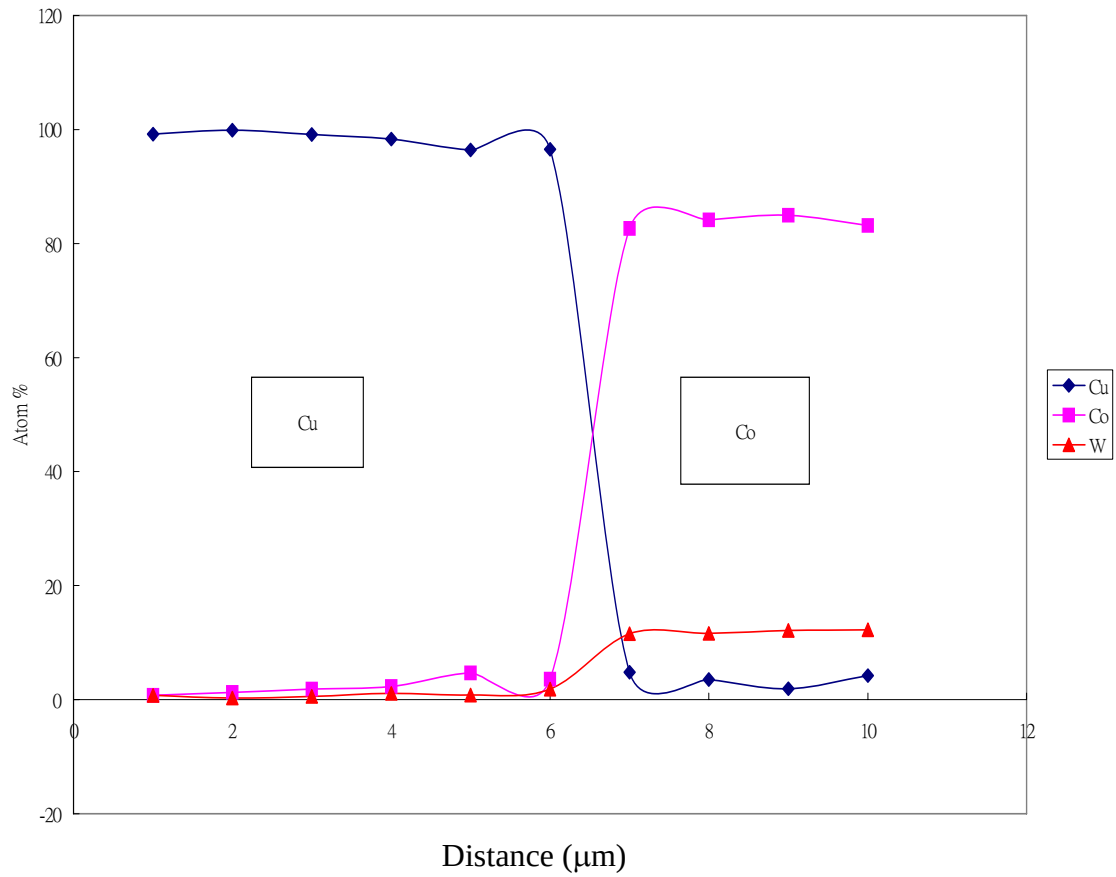

Figure 4.41 Concentration- Distance Profile of Cu/Co-W system after heat treatment at 500^{o}C for 72hrs.

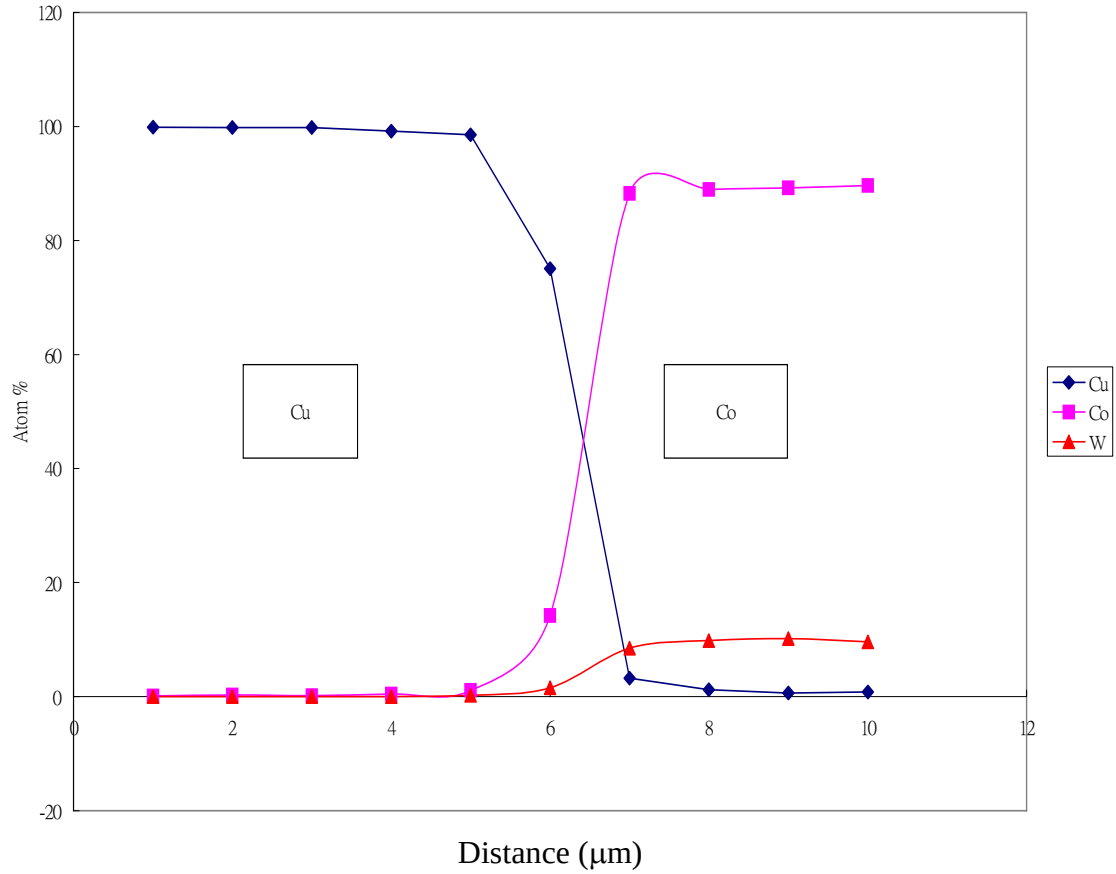

Figure 4.42 Concentration- Distance Profile of Cu/Co-W system after heat treatment at 600^{o}C for 24hrs.

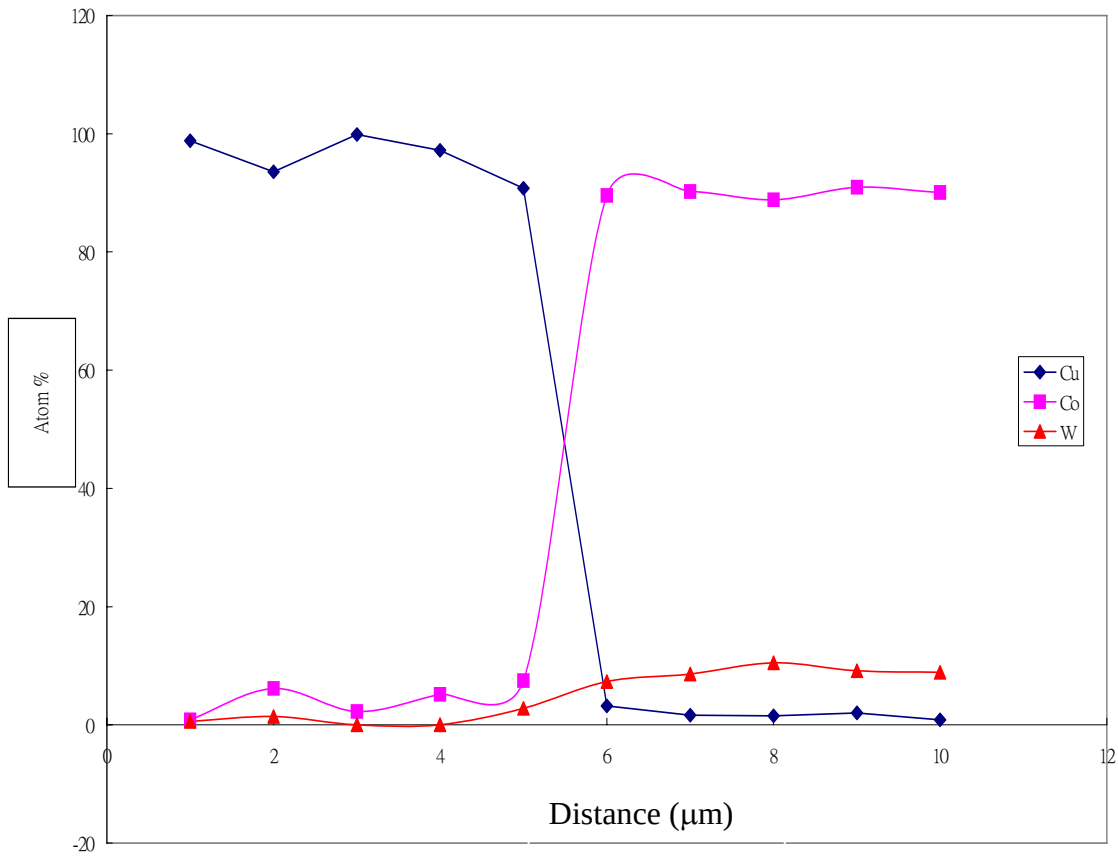

Figure 4.43 Concentration- Distance Profile of Cu/Co-W system after heat treatment at 700^{o}C for 5hrs.

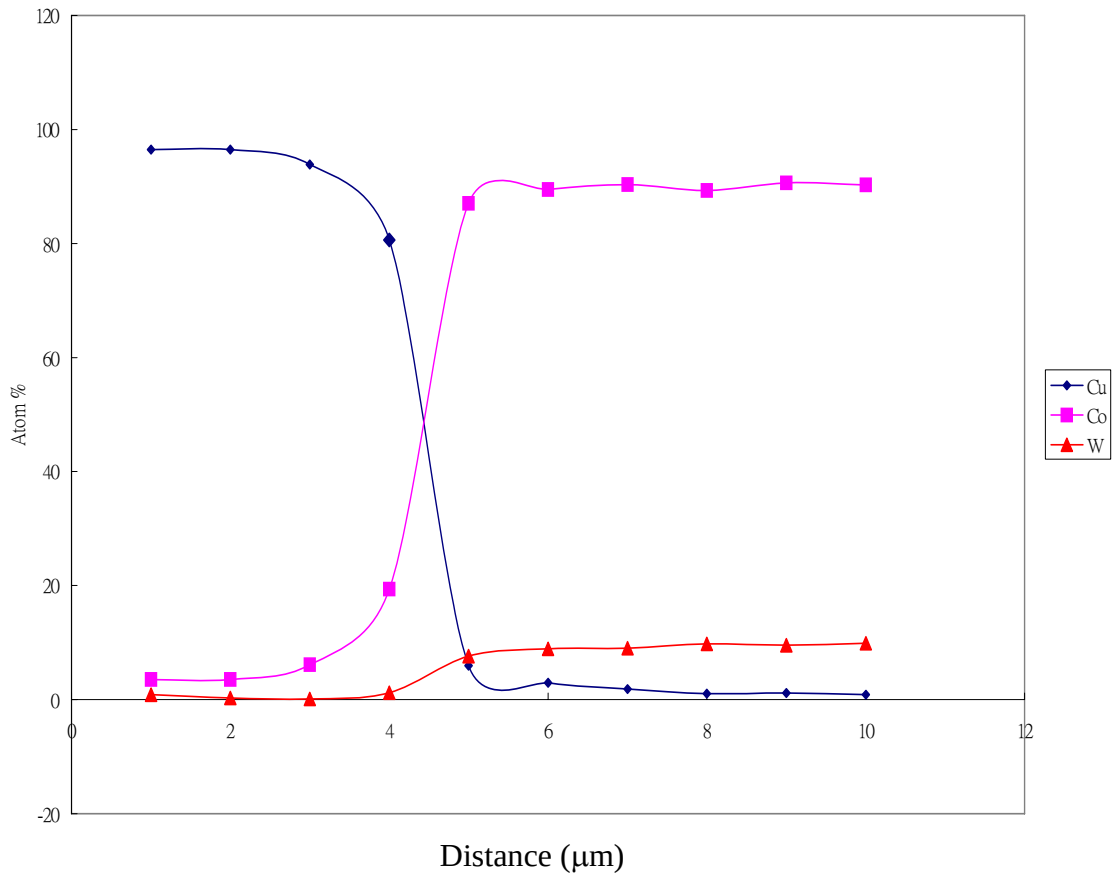

Figure 4.44 Concentration- Distance Profile of Cu/Co-W system after heat treatment at 800^{o}C for 0.75hrs.

Temperature of Heat Treatment	Heating Time (hr)	D (cm^2/s)			
		20% Cu	40% Cu	60% Cu	80% Cu
400	168	4.855×10^{-16}	4.961×10^{-16}	6.123×10^{-16}	8.556×10^{-16}
500	72	9.856×10^{-16}	1.569×10^{-15}	1.993×10^{-15}	3.558×10^{-15}
600	24	5.689×10^{-15}	5.026×10^{-15}	5.432×10^{-15}	8.102×10^{-15}
700	5	9.863×10^{-15}	2.326×10^{-14}	3.091×10^{-14}	7.852×10^{-14}
800	0.75	9.268×10^{-13}	1.325×10^{-12}	3.215×10^{-12}	5.336×10^{-12}

Table 4.8 Interdiffusion Coefficients of Cu/Co-W system at Different Temperature and copper concentration calculated by Boltzmann-Matano Method

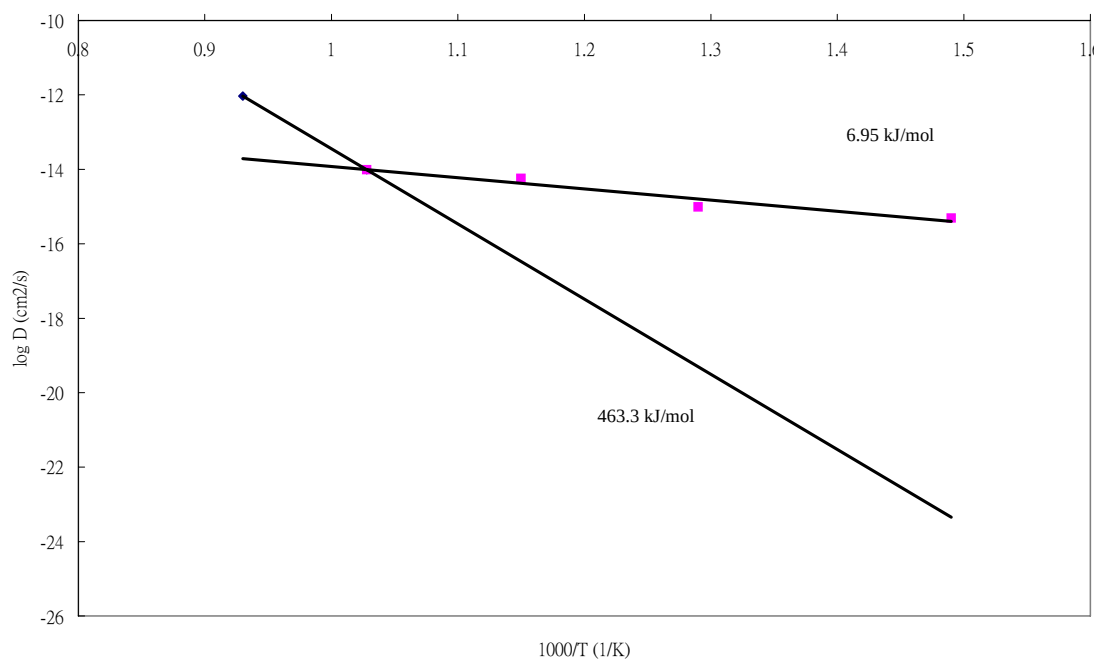

Fig 4.45 The Arrhenius plot of diffusivities at 20 % copper in Cu/Co system

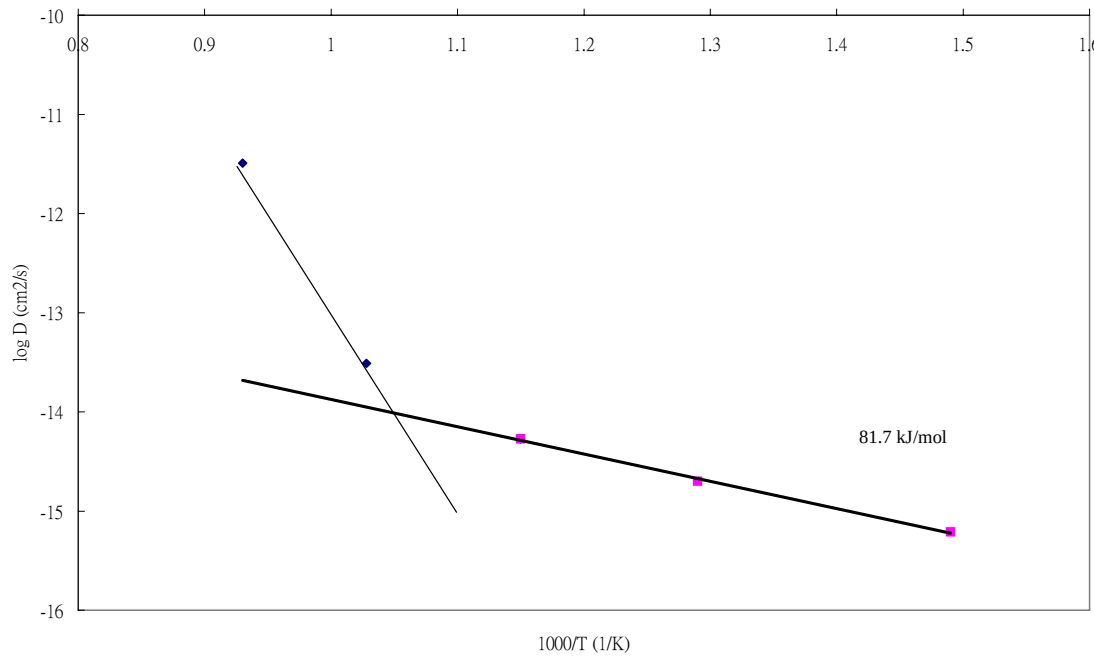

Fig 4.46 The Arrhenius plot of diffusivities at 40 % copper in Cu/Co system

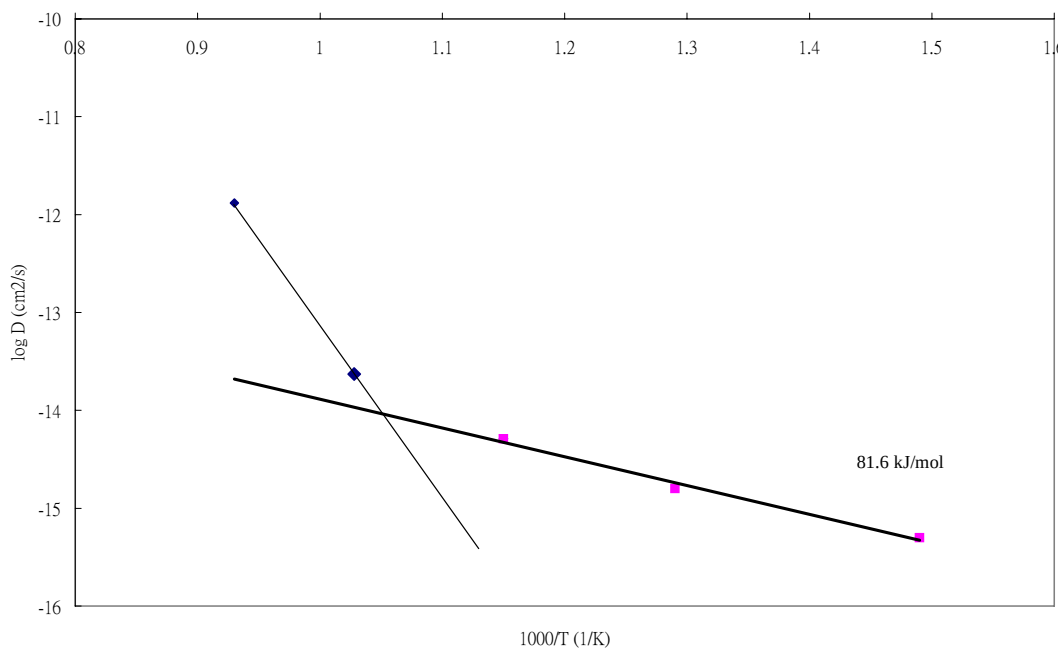

Fig 4.47 The Arrhenius plot of diffusivities at 60 % copper in Cu/Co system

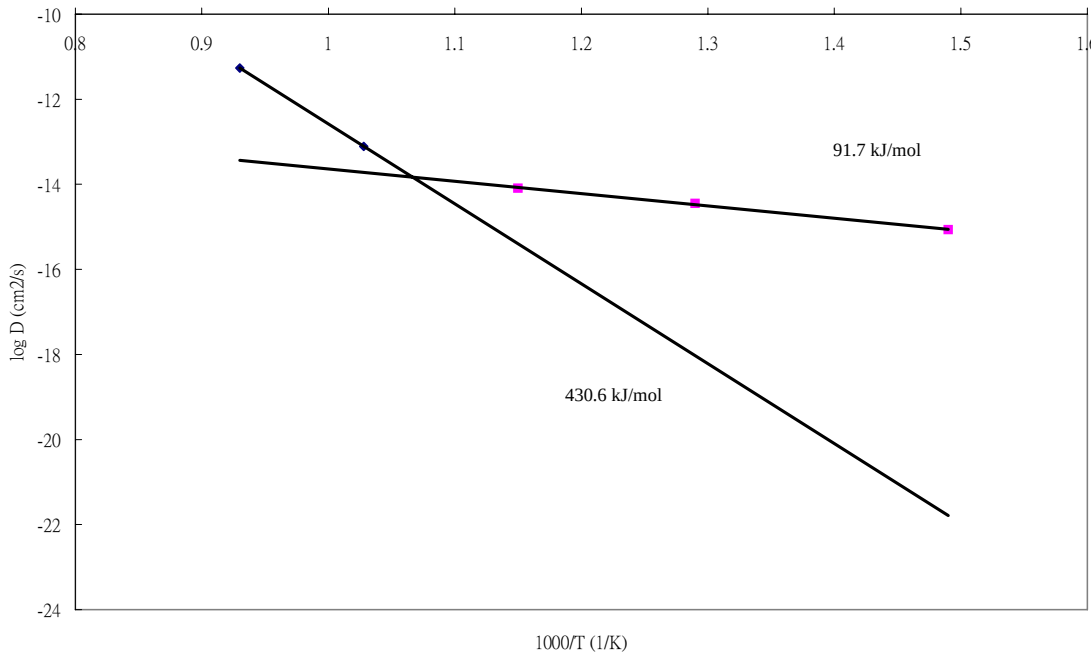

Fig 4.48 The Arrhenius plot of diffusivities at 80 % copper in Cu/Co system

The Apparent activation energy for diffusion Q increased from 474.5 kJ/mol to 430.6 kJ/mol as the copper concentration increased from 20% to 80%.

4.4.2 Comments on Diffusion Experiments of Copper and different barrier systems.

There were three different barriers with different copper diffusion barrier property. The interdiffusion coefficient D represented the velocity of diffusion in barrier.

	400°C	500°C	600°C	700°C	800°C
Cu/Ni	6.253×10^{-15}	9.532×10^{-14}	2.322×10^{-13}	1.935×10^{-13}	9.902×10^{-12}
Cu/Co-W-P	3.881×10^{-15}	1.689×10^{-15}	4.522×10^{-15}	4.432×10^{-14}	7.432×10^{-13}
Cu/Co-W	4.855×10^{-16}	9.856×10^{-16}	5.689×10^{-15}	9.863×10^{-15}	9.268×10^{-13}

Table 4.9 The comparison of the diffusivities at 20 % copper in 3 different barrier

	400°C	500°C	600°C	700°C	800°C
Cu/Ni	8.522×10^{-15}	8.996×10^{-14}	2.322×10^{-13}	2.236×10^{-13}	9.223×10^{-12}
Cu/Co-W-P	4.326×10^{-15}	1.925×10^{-15}	8.935×10^{-15}	4.233×10^{-14}	8.935×10^{-13}
Cu/Co-W	4.961×10^{-15}	1.569×10^{-15}	5.026×10^{-15}	2.326×10^{-14}	1.325×10^{-12}

Table 4.10 The comparison of the diffusivities at 40 % copper in 3 different barrier

	400°C	500°C	600°C	700°C	800°C
Cu/Ni	9.533×10^{-15}	9.231×10^{-14}	3.23×10^{-13}	3.339×10^{-13}	9.563×10^{-12}
Cu/Co-W-P	5.411×10^{-15}	4.058×10^{-15}	1.235×10^{-14}	4.425×10^{-14}	8.991×10^{-13}
Cu/Co-W	6.123×10^{-16}	1.993×10^{-15}	5.432×10^{-15}	3.091×10^{-14}	3.215×10^{-13}

Table 4.11 The comparison of the diffusivities at 60 % copper in 3 different barrier

	400°C	500°C	600°C	700°C	800°C
Cu/Ni	1.086×10^{-15}	1.032×10^{-14}	3.865×10^{-13}	7.562×10^{-13}	9.755×10^{-12}
Cu/Co-W-P	7.653×10^{-15}	5.522×10^{-15}	1.563×10^{-14}	4.386×10^{-14}	9.863×10^{-13}
Cu/Co-W	8.556×10^{-16}	3.558×10^{-15}	8.102×10^{-15}	7.852×10^{-14}	5.336×10^{-12}

Table 4.12 The comparison of the diffusivities at 80 % copper in 3 different barrier

Temperature	Copper Diffusion
400°C	Co-W < Co-W-P ≈ Ni
500°C	Co-W ≈ Co-W-P < Ni
600°C	Co-W < Co-W-P < Ni
700°C	Co-W ≈ Co-W-P < Ni
800°C	Co-W-P < Co-W ≈ Ni

Table 4.13 A summery of comparison of the diffusion barrier property of Ni, Co-W-P and Co-W.

Cu /Ni system	High temperature (800^{o}C) (kJ/Mol)	Mid Range temperature (400^{o}C- 700^{o}C), (kJ/Mol)
20%	401.0	77.2
40%	379.6	74.3
60%	379.6	780.6
80%	161.5	
Cu/Co-W-P system	High temperature (800^{o}C) (kJ/Mol)	Mid Range temperature (400^{o}C- 700^{o}C), (kJ/Mol)
20%	318.4	38.0
40%	311.2	49.8
60%	307.1	45.0
80%	287.8	46.7
Cu/Co-W system	High temperature (800^{o}C) (kJ/Mol)	Mid Range temperature (400^{o}C- 700^{o}C), (kJ/Mol)
20%	474.5	81.7
40%	412.2	81.6
60%	474.5	81.7
80%	430.6	91.7

Table 4.14 The Trend of change in different diffusion Mode at different temperature.

From the result of Arrhenius plot of these systems, the diffusion mechanisms can be indicated. In the Cu/Co-W-P system and Cu/Co-W system, a transition region was found. The higher temperature regions involved volume diffusion and after the transition region, grain boundary diffusion occurred. For system Cu/Ni, there was no transition region at 800 ^{o}C while between 400 ^{o}C to 700^{o}C, a transition region appeared and it was similar to that is Cu/Co-W and Cu/Co-W-P systems.

4.5 Internal stress Studies

The internal stress of cobalt, Cobalt-tungsten-phosphorus (electroless plating), Cobalt tungsten [49] and Cobalt Phosphorus were determined by the spiral contractometer, refer to chapter 3.8

The internal stress data of Co, Co-W-P(electroless plating), electroplating Co-W and Co-P.

Coating	Alloy composition	Internal stress (kg/mm^2)
Electroplating Co	100 % Co	+6.2 - 8.7
Electroless plating Co-W-P	86.8% Co, 9.2% W, 4% P	+7.5 - 8.3
Electroplating Co-W	65 % Co, 35 % W	+8.2 –8.9

Table 4.15 The result of internal stress in different coating.

In nickel coating, there are positive and negative values. This plating method is a newly developed formulation for a new coating alloy and we hope these data can provide reference for further experiment.

For the testing of adhesive power, there is a simple method for industrial use which is the tape test (Using 3M tape to stick on the sample coating). The result is nothing has peeled peer off throughout the test.

4.6 X-Ray diffraction

Two different coatings were analyzed by X-ray diffraction.

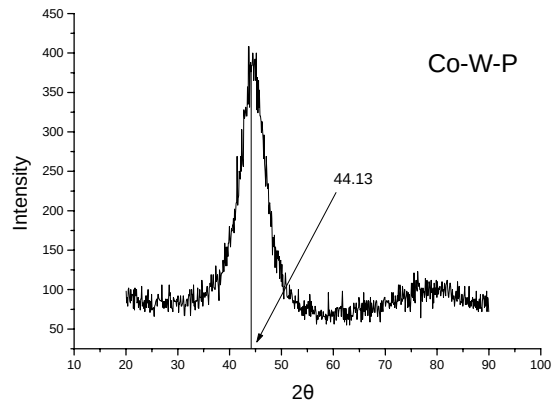

Fig 4.49 XRD diffractogram of Co-W-P(Co88%W8%P4%) deposited by electroless plating bath

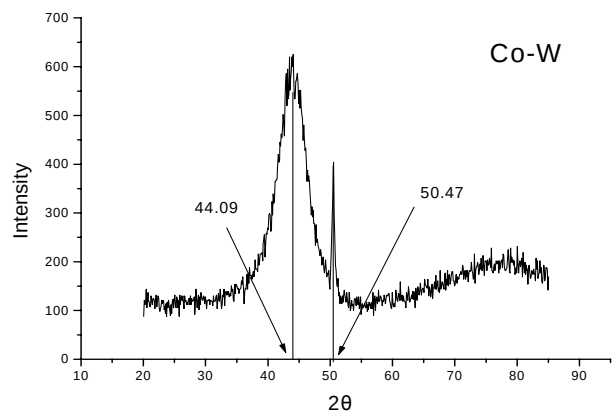

Fig 4.50 XRD diffractogram of electroplated Co-W(Co 65%W35%) film

Comparing the two diffractograms, both Fig. 4.49 and 4.50 showed a board peak at about 44 degree. The peaks were not sharp and this suggested that the structure was not crystalline. Only an amorphous or crystal/amorphous mixed form was present. In Fig 4.50, there was a sharp peak at 2θ =50.47°, this should be the copper peak arising from the copper substrate of the test-plate

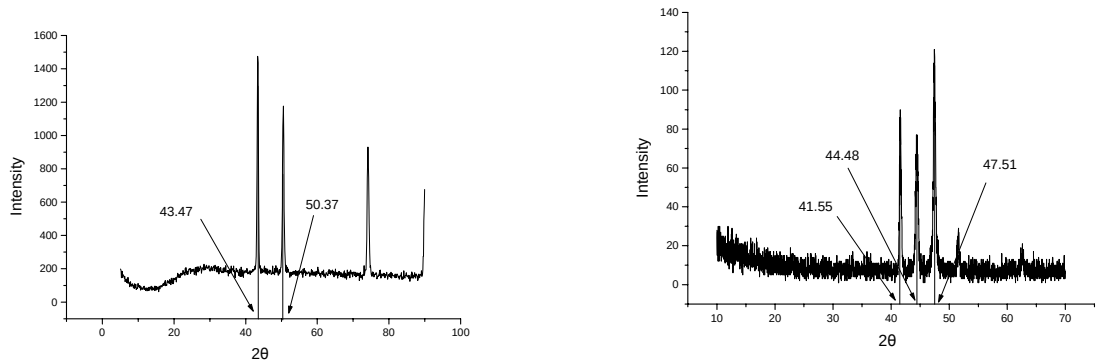

Fig. 4.51 XRD diffractogram of Copper (left) and Cobalt (right)

Fig 4.51 was the reference XRD patterns for crystalline form of copper and cobalt. The sharp peak of copper in figure 4.49 was from the crystalline base plate. It suggested that the X-ray beam may be too strong and the overcoat layer was too thin. It was illustrated below, Fig 4.52.

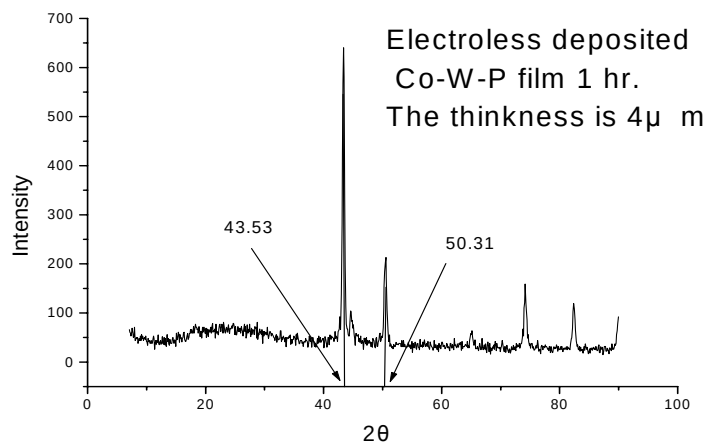

Fig 4.52 XRD diffratogram of Copper

The sharp peak of this Fig 4.52 was similar to that of the reference copper sample.

4.7 Corrosion Test

4.7.1 DC polarization

Three sets of data were compared, passivation were observed in Fig 4.18 and 4.19, but not in Fig 4.53

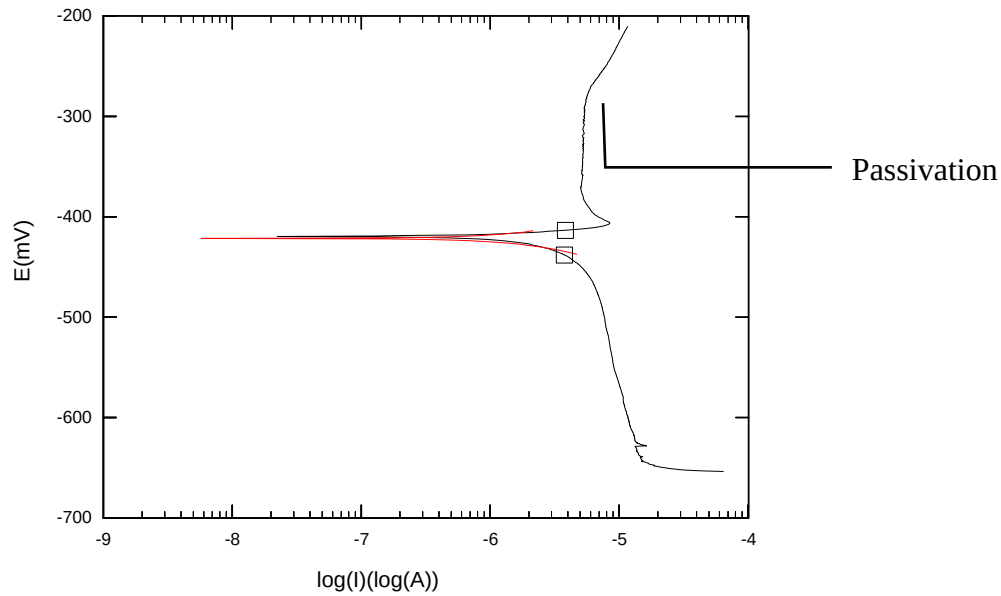

Fig 4.53 A Potential scan of the electroplated Co-W (Co 65%W35%)

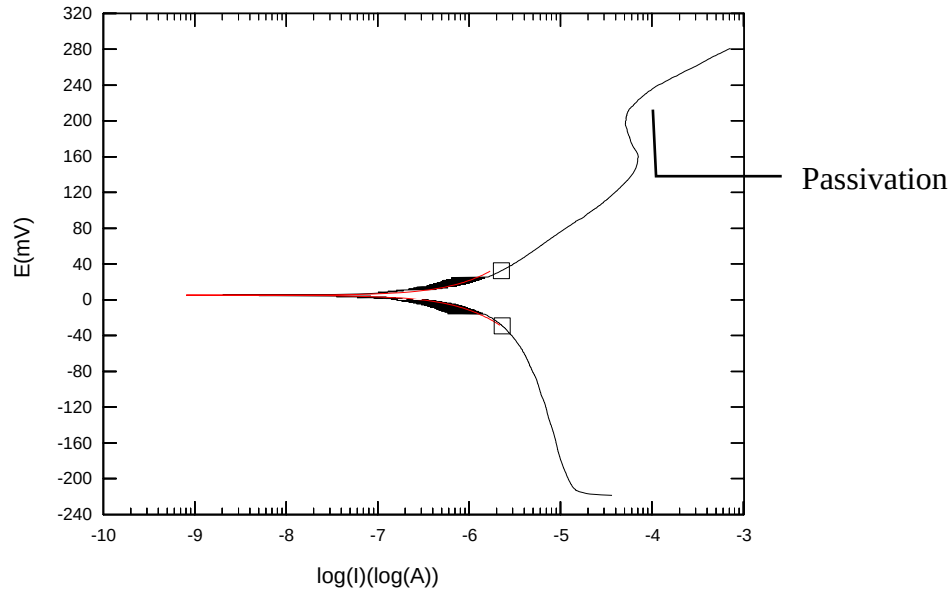

Fig 4.54 A potential scan of Electroless Co-W-P(Co88%W8%P4%)

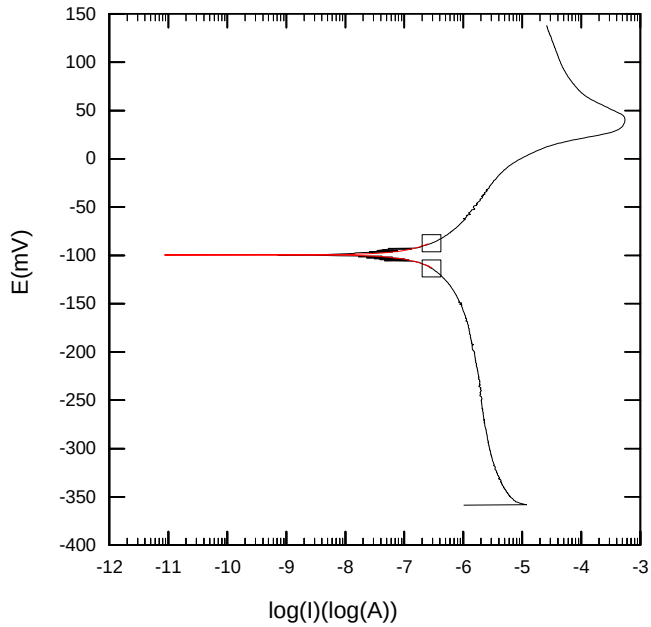

Fig 4.55 A potential scan of the Electroplating Co-P(Co94%P6%)

Sample	Composition	Ecorr(mV)	Icorr(nA/cm^2)
Electroless Co-W-P	Co88%W8%P4%	-428.2	1266
Electroplating Co-W	Co65%W35%	+5.30	6857
Electroplating Co-P	Co94%P6%	-105.6	727.7

Table 4.16 the result of a potential scan of the coating

Comparing Fig. 4.53, 4.54 and 4.55, it can be seen that there were passivations only in Fig 4.53 and 4.54 The compositions of the coatings were different. If the layer had more tungsten, the corrosion resistance was better. And if the phosphorus content in the coating increased, Ecorr also increased. The significance was that if the tungsten and phosphorus content increased, the anti-corrosion property would be better.

4.7.2 Analysis of corrosion resistance

The corrosion resistance of cobalt-tungsten-phosphorus is compared with that of cobalt-phosphorus.

Sample	Co %	W %	P %	Lose weight of Co $\mu g/cm^2$/week
Co-P	88	-----	12	5570
Co-W-P	86.8	11.0	2.2	1170

Table 4.17 Corrosion rate in different composition of alloy

The average corrosion rate of electroless Co-W-P was 4 times lower than electroless Co-P. This suggested that Co-W-P. It may be a good corrosion resisting and anti-diffusion material. Since copper metal dissolved lightly in electroless Co-W-P at room temperature. Electroless Co-W-P was a good intermediate material in jewelry treatment.

Accelerator such as 1-phenylthiourea not only increased the deposition rate, but could also behave as brightener and reducing agent. Sodium citrate could also act as stabilizer for the bath. It could avoid the formation of $Co(OH)_2$ and $Co(HPO_3)$. Lactic acid and succinic acid could increase the deposition rate because it was involved in decomposition of hydrogen atom from sodium hypophosphite.

4.8 Soldering Result

Refer to Chapter 2.17 and 3.9 for the procedure

Temperature ^{o}C	Electroless Ni	Electroless Co-W-P	Electroplating Co-W
250	35%	80%	50%
300	65%	100%	70%
350	80%	100%	70%
400	90%	100%	70%

Table 4.18 the performance of soldering in different coating at aging 3 months

Temperature ^{o}C	Electroless Ni	Electroless Co-W-P	Electroplating Co-W
250	65%	90%	50%
300	80%	100%	70%
350	95%	100%	80%
400	95%	100%	80%

Table 4.19 the performance of soldering in different coating at aging 3 months(Resin Flux before dip into molten solder)

Temperature ^{o}C	Electroless Ni	Electroless Co-W-P	Electroplating Co-W
250	95	95%	95%
300	100%	100%	100%
350	100%	100%	100%
400	100%	100%	100%

Table 4.20 the performance of soldering in fresh plate sample

Performance of Electroless Nickel, Electroless Co-W-P alloy and Electroplated Co-W alloy in different cases were compared. In the fresh plated case, all the three of the coatings had similar performance. In the case of 3-months aging, electroless Co-W-P alloy was better than electroless Nickel and the electroplated Co-W was the worst.

After resinflux, it was found that performance of Electroless Co-W-P alloy coating was better than electroless Nickel and electroplated Co-W was the worst.

From this observation, we found that electroless Co-W-P had great potential in replacing the electroless Nickel in soldering aspect.

CHAPTER 5 CONCLUSION

5.1 General Comments

Processes for the electroless plating of Cobalt-Tungsten-Phosphorus and electroplating of Cobalt-tungsten alloys coatings were developed. Complexing agent, sodium citrate, was the main component for both of the plating bath. The deposition rate of electroless plated Cobalt-Tungsten-Phosphorus is 5.8mg/cm^2/hr after optimization. The higher corrosion resistance may be accounted for the higher tungsten or phosphorus content in the coating. The coating contained 8.0 wt.% of tungsten and 4.0 wt.% of Phosphorus. We found that if the phosphorus content increased, the corrosion resistance would also increase.

The concentration of EDTA determined the content of tungsten that could be varied between 20-35wt.% in electroplated Co-W coating. The solderability of electroplated Cobalt-Tungsten alloy was very good and the whole hull cell plate could be covered by solder.

From this study, it was known that the internal stress of the plated coatings was positive and this meant that the cobalt alloys obtained from electroplating and electroless plating had tensile stress.

Cu/Barrier diffusion was determinated by copper concentration profiling and calculated using the Boltzmann-Matano method. The interdiffusion coefficient indicated that the interdiffusion coefficients of Cobalt alloys were less than that of Nickel alloys. The results indicated that the barrier property of these two cobalt alloys was as effective as and less costly than nickel alloys

barrier. The diffusion study was limited to the temperature range between 400^{o}C to 800^{o}C. We observed a transition region between volume diffusion and grain boundary diffusion. This result meant that the cobalt alloys barriers were good replacements for nickel alloys in this range of temperature.

5.2 Main Findings.

1. The deposition rate was relatively low in electroless plating and 1-Phenylthioura could accelerate the deposition.
2. The orthogonal experiments helped to optimize the formulation. We used the method to optimize a Co-W-P electroless deposited coating which gave it higher corrosion resistance. The metal content of the coating was also adjusted to result a higher content of tungsten. This was to reach a higher corrosion resistance of the coating. The content of coating is 88.0 wt.% Co, 8.0 wt.% W and 4 wt.% P
3. The electroplated Cobalt-Tungsten alloy had a very good coverage even in the lower current density region(0.2 A/M^{2})
4. The Tungsten content of electroplated Cobalt-Tungsten alloy could be controlled by the concentration of EDTA in the electroplating bath. The percentage of tungsten could be varied between 20-35 wt.%.
5. The interdiffusion coefficient of electroless plated Cobalt-Tungsten-Phosphorus alloy and

electroplated Cobalt-Tungsten alloy was less than that of nickel alloys. This meant that both of these cobalt alloys had the potential to replace Nickel alloys.

6. From the Arrhenius plots of Cu/Ni, Cu/Co-W-P and Cu/Co-W systems, based on the activation energy, a transition region was observed and this indicated there was a change in the diffusion mechanism.

7. Both of the cobalt alloy coatings had tensile stress (positive value in internal stress)

5.3 Suggestion and Further work

The objective of the project is to investigate the technology of ternary Co-W-P coating and the application of the cobalt alloys coating. Our experimental results only provide basic information on the coatings and the author hopes that the following suggestions can help achieve better understanding of the deposition process, formulation and diffusion mechanism.

1. The interdiffusion coefficients of the Cu/Co-W-P and Cu/Co/W systems were measured in the range 400^{o}C to 800^{o}C. If time allows, we suggest coating an outer gold layer and estimate the diffusion between Cu/Barrier/Outer coating system.

2. The formulation and condition developed were tested in laboratory scale. We suggest performing trial runs at industrial scale as this barrier is intended for industrial usage and different problems may arise in industrial environment.

3. A study in the prevention of oxidation of the bath solution is useful to extend the bath life.

The possible method is using ion-exchange membranes [53] to separate reducing chemicals or side reactants that may harm the bath.

4. Although the EDAX experiment is 2-5% error within the result, there is only in our university.. If we need to have further study, we can use a more accurate equipment like X-ray photon spectroscopy.

REFERENCE

1. D.A. Basketter, E.G. Barnes and C.F.Allenby. In The Environmental Threat to the skin, R. Mark and G. Plewig(ed.) London:Martin Dunitz,1992: p215-217
2. Common Position (EC) No. 12/94, *Official Journal of the European Communities*, No.C137/60-64, 19 May (1994).
3. Nishizawa, T. and Ishada, T. in "*Handbook of Binary Phase Diagrams"*, Vol. 2, Moffalt, W.G. (Ed.), Genium Pub. Cop., Schenectady, NY, 1984.
4. Beck, R. P., Metalloberflache, 1993, **47**, 20.
5. Lim, J. K., Russo, J.S. and Antonier, E., *Plat. Surf. Finish.*, 1996, **83**(3), 64.
6. 趙文軫, 金屬材料表面新技術, 西安交通大學出版社, p6-p13, p15-p20, p111-p113, p124-p134.
7. Wu Yong-xin, Wen Xiao-zhong Yang Zhi-xiong, Li Zhi-yong and Xiao Zu-long, Barrier Properties of Cobalt-Tungsten Alloy for Copper Diffusion, Plating and Finishing. 2002
8. Ng Wing Yan. Cheung Ka Lok, A Study on the Chemical Deposition of Co-W-P Ternary Alloy, The Hong Kong Polytechnic University, 1997
9. Liu Shulan, Qin Qixian, Yang Xiumin, Yu Delong, Investigation on the Wear resistant Characteristics of Chemical Plated Ni-W-P Plating and Finishing 1994, Sep, Vol 16, No,5, p4-p7.
10. 神戶德藏 著, 莊曾發 復漢, 無電解鍍金, p57-p92.

11. CHEN Lijia, WANG Heying, ZHAO Zhang Zhongjian, Xiuting(1997), A Study of Kinetic of Electroless Ni-P Alloy Deposition, 電鍍與精飾 1997 年 6 月, 第 16 卷 第 2 期, p9-p12.

12. Qin Qixian, Luan Benli and Yang Xiumin(1993), A Study on Chemical Plating Nickel-tungsten-Phosphorus Ternary Alloy
電鍍與精飾 1993 年 5 月, 第 15 卷 第 3 期(總 90 期), p7-p10.

13. K. Aoki and O. Takano,1986, Corrosion Characteristics of Crystalline And Amorphous Electroless Ni-W-P Deposits. Plating and Surface Finishing, May,1986, p136-p141.

14. Koji Aoki and Osamu Takano 1990, Electrical Resistance of Electroless Ni-W-P Alloy Deposits, March,1990, p48-p52.

15. Zhang Bangwei, Hu Wangyu, Qu Xuanyuan, Zhang Qinglong, Zhang Heng and Tan Zhaosheng.Trans. Preparation, Formation and Corrosion for Ni-W-P Amorphous Alloy by Electroless Plating. IMF, 1996, **74**(2), 69

16. Izumi Ohno, Electrochemistry of electroless plating, Materials Science and Engineering, A146(1991) 33-49

17. Milan Paunovic, Mordechay Schlesinger, Fundamentals of electrochemical deposition, p1

18. E.J.Podlaha and D.Landolt, J. electrochem. Soc., Vol 143, No. 3, March 1996. p885-892

19. E.J.Podlaha and D.Landolt, Jelectrochem. Soc., Vol 143, no. 3, March 1996, p893-899

20. Induced Codeposition Molybdenum alloys with nickel, cobalt and iron, E.J.Podlaha and D.Landolt

21. Anon., Metal finishing, 1994,June,77

22. Barrier Properties of Cobalt-Tungsten alloy for Copper diffusion, Wu Yong-xin, Wen Xiao-zhong, Yang Zhi-Xiong, Xiao Zu-long and Li Zhi-yong, Hong Kong Polytechnic University, Hong Kong

23. Study on Electrodeposition of Noncrystalline Fe-Cr-P Alloy, Li Songlin, Zhou Haihui, Guo Hetong, Yao Suwei, the world of chemistry Vol. 9

24. Study on Electrodeposition of Noncrystalline Fe-Cr-P Alloy, Li Songlin, Zhou Haihui, Guo Hetong, Yao Suwei, the world of chemistry Vol. 9

25. Electrochemical and chemical reactions in bath for plating amorphous alloys. M.Donten, J.OsterYoung, Dept of Chemistry, State University of New York at Buffalo, New York 14214, USA

26. Formation and performance of Ni-W Amorphous alloy deposit, Zhou Wanqiu, Electroplating & finishing, Vol 15 No.4

27. Pulse electroplating of rich-in-tungsten thin layers of amorphous Co-W alloys M.Donten, Z.Stojek, dept of chemistry, University of Warsaw, ul. Pasteural, 02-093 Warsaw, Poland

28. 1 of Research on amorphous electroplating Fe-W-P alloy

29. 2 of Research on amorphous electroplating Fe-W-P alloy

30. Voltammetic, Optical, and Spectroscopic Examination of Anodically Forced Passication of Cobalt-Tungsten Amorphous Alloys, Mikolaj Donten, Zbigniew and Janet G. Osteryoung,

Dept of Chemistry, University of Warsaw, ul. Pasteura 1, 02-093 Warsaw, Poland, Dept of Chemistry, North Carolina State University, Raleigh, North Carolin 27695-820

31. Formation and performance of Ni-W Amorphous alloy deposit, Zhou Wanqiu, Electroplating & Finishing, Vol 15 No. 4) (M.D. Archer and C.C.Corke, Electrochim, Acta 32(1987), 13)

32. (H.Matyja and P. Zielinski(eds),'Amorphous metals', World Scientific, Singapore and Philadelphia (1986).)

33. Zhang Bangwei, Hu Wanyu, Qu Xuanyuan, Zhang Qinglong, zhang Heng and Tan Zhaosheng. Trans. Preparation, Formation and Corrosion for Ni-W-P Amorphous Alloy by Electroless Plating. IMF, 1996, 74(2),69

34. Ng Wing Yan, Lee Chi Yung, Accelerator for Electroless Cobalt-Tungsten-Phosphorus, The Hong Kong Polytechnic University, 1998

35. The Fundamentals of Electrochemistry and Electrodeposition, Samuel Glasstone, Frankin Publishing Company, 1960. p86-90

36. Brenner A, Riddell G E. Proc Amer Electropl Soc, 1946;33:16

37. Lau Yin Ming, A New viewpoint of the mechanism of electroless nickel, Electroplating & Pollution Control, Vol 19 No. 2, page 12-14, Mar 1999

38. A study on Stabilizers for electroless nickel electrolyte, Electroplating & Pollution Control; Vol 19 No. 1, page 22-24, Jan 1999

39 Effect of plating process parameters on electroless deposition rate, Electroplating & Pollution Control; Vol 19 no 5, page 15-22, Sept 1999

40 Jackson B, Macary M, Shantan G. Trans Inst Met Fini, 1990;68(8): 75

41 張維, 表面工業染誌, , 1996:56:35

42 無電解鍍金, p167-183 復漢出版社, 神戶德蔵

43 M. Donten, J Oster Young, Electrochemical and chemical reactions in baths for Plating amorphous alloys, Journal of Applied Electrochemistry 21 (1991) 496-503

44 Milan Paunovic, Philip J. Bailey, and Robert G. Schad, Electrochemically Deposited Diffusion Barriers, J. Electrochem Soc, Vol. 141 No. 7, July 1994

45 Shinichi Wakabayashi, Takahiro Iijima, Masao Nakazawa, Norio Kaneko and Hiroyuki Nezu, Diffusion Behavior of Copper Through Electroplated Silver Leadframes, Plating and Surface Finishing, p63-67, March 1996

46 T.E. Mitchell, Ivan E. Locci, and Augusto A. Ruiz, J. Mater. Res. ‘Vol 4, No. 2, Mar/Apr 1989

47 J.S. Sallo and R.D. Fisher, Journal of The Electrochemical Society, page 277-280, Apr 1960

48 Lin Wenxiu, Ruan Liqin, Lin Ping, Plating and Finishing, Vol. 21 No. 3, May 1999

49 Albertine kroho and Theodore M. Brown, Journal of the Electrochemical Society, p60-64, Jan 1961

50 Wing-Yan Ng, Hau- Chung Man, Chi-Hung Yeung Cho-lung Siu and Chi-yung Lee,

Determination of Diffusion Coefficient of Basis Metal in Plated Coating, Plating and Finishing

51 Izumi Ohno, Electrochemistry of Electroless plating, Materials Science and Engineering, A146(1991) 33-49

52 E.J. O'Sullivan, A.G. Schrott, M. Paunovic, C.J. Sambucetti, H.R. Marino, P.J. Bailey, S.Kaja, and K.W. Semkow,Vol 42, No. 5, Electrochemical Mircofabrication, Journal of Research & Development

53 Malcolm T. Hepworth, M.Laferty, Membrane Process for Separating Contaminant Anions from Aqueous Solutions of Valuable Metal Anions, United States Patent, 4,234,393, Nov 18, 1980

54 Wing-Yan Ng, Hau- Chung Man, Chi-Hung Yeung Cho-lung Siu and Chi-yung Lee, Cobalt-Tungsten-Phosphorus alloy diffusion barier coatings, Method for their preparation, and their use in plated articles, United States Patent. US 6,528,185 B2, Mar 4, 2003

55 Zhou Hong, hu Yingning, Liao Xiaping, Chemical World, Vol. 7, 1999

56 Tatauya Horikawa, Atsuko Adachi, Susumu Harada, Masamitsu Ichihashi, Case report, Environ Dermatol 6:83-87 1999

57 Jean-Paul Radin, journal of biomedical Materials Research, Vol. 22, 649-666 (1988)

58 Huang Qing-an, Zhang Lin, Electroplating & Finishing, Vol. 13, no. 2, Jun 1994

59 T. Watanabe, New Materials & New Processes, Vol. 3(1985)

60 Wing-Yan Ng, Hau- Chung Man, Chi-Hung Yeung Cho-lung Siu and Chi-yung Lee, Electroplating & Finishing. Vol 19 No.4, Aug 2000

61 Walter J. Wieczerniak;Sylva Martin., United States patent, US 5,525,206, Jun 11, 1996

62 Francine Popescu, United States Patent, 4,077,855, Mar. 7, 1978